RELIABILITY-BASED DESIGN AND LOAD TOLERANCE EVALUATION USING STOCHASTIC RESPONSE SURFACE AND PROBABILISTIC SENSITIVITIES

By

HAOYU WANG

A DISSERTATION PRESENTED TO THE GRADUATE SCHOOL
OF THE UNIVERSITY OF FLORIDA IN PARTIAL FULFILLMENT
OF THE REQUIREMENTS FOR THE DEGREE OF
DOCTOR OF PHILOSOPHY

UNIVERSITY OF FLORIDA

2006

To my family

ACKNOWLEDGMENTS

I would like to express my appreciation to my advisor, Professor Nam-Ho Kim, for his endless encouragement and continuous support during my Ph.D. research. Without his guidance, inspiration, experience and willingness of sharing his knowledge, this work would have never been possible. Dr. Kim made a tremendous contribution to this dissertation, as well as my professional and personal life.

I must express my gratitude to the members of my supervisory committee, Professor Raphael T. Haftka, Professor Stanislav Uryasev, Professor Nagaraj K. Arakere, and Professor Ashok V. Kumar, for their willingness to review my Ph.D. research and provide constructive comments to help me complete this dissertation. Special thanks go to Professor Raphael T. Haftka for not only his guidance with several technical issues during my study, but also comments and suggestions during group meetings which were extremely helpful for improving my work.

Special thanks are also given to Professor Nestor V. Queipo from the University of Zulia at Venezuela, for his interaction in my research and collaboration in publishing papers during his visiting at the University of Florida.

My colleagues in the Structural and Multidisciplinary Optimization Lab at the University of Florida also deserve my gratitude. In particular, I thank Dr. Xueyong Qu, Dr. Amit A. Kale, Dr. Erdem Acar, Tushar Goel, Long Ge, Saad Mukrus for their encourage and help.

My parents deserve my deepest appreciation for their constant love and support.

Lastly, I would like to thank my beautiful and lovely wife, Zhilan, for her love, patience and support during my study.

TABLE OF CONTENTS

LIST OF TABLES

LIST OF FIGURES

Figure page

Abstract of Dissertation Presented to the Graduate School
of the University of Florida in Partial Fulfillment of the
Requirements for the Degree of Doctor of Philosophy

RELIABILITY-BASED DESIGN AND LOAD TOLERANCE EVALUATION USING STOCHASTIC RESPONSE SURFACE AND PROBABILISTIC SENSITIVITIES

By

Haoyu Wang

December 2006

Chair: Nam-Ho Kim
Major: Mechanical Engineering

Uncertainty is inevitable in structural design. This research presents an efficient uncertainty analysis technique based on stochastic response surfaces (SRS). The focus is on calculating uncertainty propagation using fewer number of function evaluations. Due to sensitivity analysis, the gradient information of the performance is efficiently calculated and used in constructing SRS.

Based on SRS, reliability-based design optimization (RBDO) is studied intensively in this research. Probability sensitivity analysis using the sampling technique is also proposed. Since the computational cost of RBDO increases significantly proportional to the increasing number of random variables, global sensitivity analysis is introduced to adaptively reduce unessential random variables. It has been shown that the global sensitivity indices can be calculated analytically because the SRS employs the Hermite polynomials as bases.

Traditional structural design focuses on designing a reliable structure under well characterized random factors (dimensions, shape, material properties, etc). Variations of these parameters are relatively small and well characterized. However, everyday engineering life tends to use the existing structural part in a different applications instead of designing a completely new part. In this research, a reliability-based safety envelope concept for load tolerance is introduced. This shows the capacity of the current design as a future reference for design upgrade, maintenance and control. The safety envelope is applied to estimate the load tolerance of a structural part with respect to the reliability of fatigue life.

Stochastic response surface is also applied on robust design in this research. It is shown that the polynomial chaos expansion with appropriate bases provides an accurate and efficient tool in evaluating the performance variance. In addition, the sensitivity of the output variance, which is critical in the mathematical programming method, is calculated by consistently differentiating the polynomial chaos expansion with respect to the design variables. A reliability-based robust design method that can reduce the variance of the output performance as well as the deviation of the mean value is proposed using SRS and efficient sensitivity analysis. Numerical examples are shown to verify accuracy of the sensitivity information and the convergence of the robust design problem.

CHAPTER 1
INTRODUCTION

Motivation

A typical mechanical design procedure includes two steps: first, a design space is defined and a mathematical model is established, which includes the objective function and required constraints. Second, a proper optimization algorithm is selected properly based on this mathematical model to solve the design problem. In engineering design, the deterministic optimization model has been studied intensively to reduce the objective function by pushing design to the limits of system failure boundaries. However, everything in the real world involves uncertainties, and so does the design of mechanical components. After realizing deterministic design leaves very little or no room for tolerances of the imperfections in design, manufacturing and variety of service conditions, design engineers incorporate a safety factor into the structural design to leave safety margins. Without considering uncertainties and probabilistic quantification, deterministic design with a safety factor may be either unsafe or too conservative.

Motivated by overcoming the bottleneck of the deterministic design, the reliability-based design optimization (RBDO) model has become popular in past two decades since uncertainties exist everywhere in every phase of the structure system, from design and manufacturing to service and maintenance. If elements in the mathematical model are considered to be probabilistic with certain types of random distribution, the design problem becomes a typical RBDO problem. The probabilistic elements can be design variables, material properties, applied loads, etc. One of the most important issues in

RBDO is a good model of uncertainty propagation in mathematical models. Besides RBDO, which only considers the failure mode as a constraint in the probabilistic point of view, robust design will also be considered in this research in order to design a structure ′less sensitive′ to the existing uncertainty factors. In optimization point of view, that means minimization of performance variance.

For a certain design, it is also important to consider the service capability of the system subject to applied loads since engineers tend to use the same design in different applications instead of a completely new design. Another motivation of this research is the load tolerance design. A good estimation of load tolerance shows the capacity of the current design, future reference for design upgrade, maintenance and control. Since static or quasi-static loading is rarely observed in modern engineering practice, the majority of engineering design projects involves machine parts subjected to fluctuating or cyclic loads. Such loads induce fluctuating or cyclic stresses that often result in failure by fatigue. In addition, because service loads are subjective, which means the load characteristic of one operator may be completely different from that of the other, it is necessary to consider the uncertainties while estimating the load tolerance of dynamic systems.

Objective

Uncertainty in the design parameters makes structural optimization a computationally expensive task due to the significant number of structural analyses required by traditional methods. Critical issues for overcoming these difficulties are those related to uncertainty characterization, uncertainty propagation, ranking of design variables, and efficient optimization algorithms. Conventional approaches for these tasks

often fail to meet constraints (computational resources, cost, time, etc.) typically present in industrial environments.

The first objective of this research is to develop a computationally efficient method for uncertainty propagation. Local and global sensitivities can then be used to improve the efficiency of estimating uncertainty propagation. Besides efficiency, the accuracy and applicability of the methods to a wide range of applications need to be addressed.

The second objective of this research is to develop a computationally efficient RBDO and robust design framework based on proposed uncertainty analysis. In the gradient-based algorithm, the sensitivity information is required during the optimization procedure. The computational cost can be significantly saved if the gradient can be obtained analytically, instead of using the finite difference method. The probabilistic sensitivity analysis is utilized to calculate the gradient of the reliability constraints. In the framework of robust design, sensitivity analysis of performance variance is also studied.

Traditional structural design usually makes assumption on randomness of factors involved in modeling a structural system such as design variables, material properties, etc. However, it is also important to consider the capacity of the system subject to uncertain loads. The final objective of this research is to present a reliability-based load design method, which provides the safety envelope, for a structure subject to fatigue failure.

Scope

In the standard framework of RBDO, constraints are provided in terms of the probabilities of failure. The uncertainties involved in the system are modeled by assuming random input variables with a certain type of probabilistic distribution. RBDO achieves the design goal by meeting the requirement of structural reliability constraints.

The RBDO involving a computationally demanding model has been limited by the relatively high number of required analyses for uncertainty propagation during the design process. The scope of this research is to present an efficient uncertainty propagation technique based on stochastic response surfaces (SRS) constructed using model outputs at heuristically selected collocation points. The efficiency of the uncertainty propagation approach is critical since the response surface needs to be reconstructed at each design cycle. In order to improve the efficiency, the performance gradient, calculated from local sensitivity analysis, is used.

Even if the local sensitivity information can reduce the number of required simulations, the dimension of the SRS is still increased according to the number of random variables. If the contribution of a random variable is relatively small to the variance of the model output, it is possible to consider the random variable as a deterministic one. In this research, the global sensitivity index is used for that purpose. The role of the global sensitivity is to quantify the model input's contributions to the output variability, hence establishing which factors influence the model prediction the most so that i) resources can be focused to reduce or account for uncertainty where it is most appropriate, or ii) unessential variables can be fixed without significantly affecting the output variability.

Reliability constraint in RBDO requires probability sensitivity analysis for gradient-based algorithms. In this research, both FORM-based and sampling-based reliability sensitivity analysis are investigated. The analytical expression for probability sensitivity based on SRS is derived and used for RBDO.

Variations in dynamic loads are usually too complicated to be predicted. A simplified uncertainty modeling technique based on the mean and amplitude of the load history is proposed. Using the uncertainty in the load history, a reliability-based safety envelope is constructed that can provide load tolerance of the current design. In addition, the effect of different distribution types is investigated so that the design engineers can choose the conservative distribution type.

This research involves uncertainty modeling and quantification, design sensitivity analysis, fatigue life prediction, reliability-based design optimization (RBDO) and robust design. Methodologies investigated or applied in reliability analysis include moment-based methods such as first- and second-order reliability method (FORM/SORM), approximation methods such as Monte Carlo Simulation (MCS) with stochastic response surface method (SRSM). Furthermore, sensitivity analysis for reliability constraints of RBDO is investigated to improve the computational cost involved in reliability analysis and design. Performance variance and sensitivity are calculated based on SRSM for robust design. Computationally affordable reliability-based optimization and robust design method, and safety envelope for load tolerance are presented in this work.

Outline

A literature survey is presented in chapter 2, which includes all aspects involved in this research such as reliability analysis, reliability-based design optimization, robust design, sensitivity analysis, dimension reduction strategy and fatigue analysis.

Chapter 3 describes the uncertainty modeling and widely used reliability analysis methods. A stochastic response surface method (SRSM) coupled with the sensitivity analysis of performance measure is introduced. It is shown that the local sensitivity information improves computational efficiency significantly by reducing required

number of samples. Convergence and accuracy of the proposed SRSM scheme are also discussed in this chapter.

In Chapter 4, the mathematical model is defined for RBDO. RBDO using either direct probability measure or inverse measure is investigated and compared. The difference of numerical procedures between RBDO and deterministic optimization are also compared. As required by RBDO, probability sensitivity analysis is studied in this chapter.

In Chapter 5, a dimension reduction strategy is proposed by introducing the concept of variance-based global sensitivity analysis, which saves the computational resources further by fixing the unessential design variables.

Chapter 6 demonstrates a fatigue reliability-based load tolerance design by using reliability sensitivity information. A reliability-based safety envelope is constructed by path following continuation method.

Chapter 7 proposes an optimization model for robust design where SRS is used to calculate the performance variance and its sensitivity.

Chapter 8 concludes this research followed by recommendations for future research work.

CHAPTER 2
LITERATURE SURVEY

Uncertainty and Reliability Analysis of Structural Applications

Reliability-based design optimization (RBDO) provides tools for making decision within a feasible domain of design variables with consideration of uncertainties underneath. In the past decades, tremendous amount of work has been carried out in this area and it is still moving forward.

Compared to deterministic optimization, design variables included in RBDO are random and usually modeled with specific distribution types, so do the random parameters such material properties as Young's modulus and Poisson's ratio. Usually random parameters do not change during optimization, but their effects to the probability propagation must be counted due to its uncertainty. Reliability, which is defined as the probability that a system response does not exceed the limit threshold, is often considered as constraints. The system response is a function of design variables and random parameters, which is called a performance function in this research. Performance function is usually implicit and nonlinear prediction of random variables, making probabilistic description of a system response difficult.

Several approximation methods for reliability analysis have been developed in the literatures. Among them, Monte Carlo Simulation (MCS) (Metropolis and Ulam 1949; Rubinstein 1981) has been widely used due to its simplicity and dependability. However, the large sample size required in MCS in order to reduce the noise and to reach a certain level of accuracy makes it practically formidable in computationally intensive

engineering applications, such as Finite Element Analysis (FEA). Even improved version of MCS are developed, such as importance sampling, Latin Hypercube Sampling (Wyss and Jorgensen 1998), Stratified Sampling, etc, they are still expensive in structural reliability analysis.

Moment-based methods (Breitung 1984; Haldar and Mahadevan 2000; Hasofer and Lind 1974) have been developed to provide less expansive calculation of the probability of failure compared to MCS. However, they are limited to a single failure mode. As the most widely used moment-based methods, the development of the theory of First- and Second-Order Reliability Method (FORM/SORM) is claimed to be finished and only technical work left to do (Rackwitz 2000). FORM/SORM are based on the linear/quadratic approximation of the limit state function around most probable point(MPP), which is defined in standard normal space as the closest point from the origin on the response surface.

For highly nonlinear problems, predictions of reliability from FORM/SORM are not accurate enough because they approximate the response using a linear or quadratic function. The response surface method (Khuri and Cornell 1996; Myers and Montgomery 1995) is proposed to resolve this difficulty. This method typically employs polynomials bases to approximate the system performance and facilitate reliability analysis with little extra computational cost by combining with MCS. Since the accuracy of MCS with fixed sample size relies on the seeking level of probability of failure which sometimes is extremely low in structural design, the probability calculated by MCS near optima is too rough to represent the true value of failure probability. Reliability analysis using safety factor (Wu et al. 2001) or probability sufficiency factor (PSF) (Qu and Haftka 2004) is

proposed to ameliorate this effect. With the PSF as the constraints in RBDO, the variation of magnitude of constraints is usually several orders of magnitude lower than that of the probability of failure, and so is the magnitude of the numerical noise caused by MCS.

One of the significant advantages of the moment-based approach is that the sensitivity of the system reliability or probability of failure can be obtained with very little extra computation (Yu et al. 1998). However, moment based approach such as FORM/SORM still has limitations when the performance function is highly nonlinear (Ghanem and Ghiocel 1996). The evaluation of the probabilistic constraints may have large errors in this case. Mahadevan and Shi (Mahadevan and Shi 2001) presented a multipoint linearization method (MPLM) for the reliability analysis of nonlinear limit states, which determines the multiple linearization points through the secant method. It increases the complexity of the problem with limited accuracy improvement.

The response surface method can approximate the system response and with little extra computation for MCS, the probability of failure can easy to be obtained. Compared to the conventional deterministic design response surface, Stochastic Response Surface (SRS) (Isukapalli et al. 1998) has the advantage that it only approximates the function around most probability region which highly improved accuracy.

Another advantage of SRS is the choice of basis function. The monomial bases(Qu et al. 2000) are widely used due to its simplicity. Other polynomial bases are also being studied intensively such as radial basis function (RBF) (Krishmamurthy 2003), orthogonal polynomials (Xiu et al. 2002),etc. Since Ghanem and Spanos proposed the spectral approach of stochastic finite element method (Ghanem and Spanos 1991), the homogeneous Polynomial Chaos Expansion (PCE) has been widely utilized to represent

the uncertainties due to the nature of stochastic process. To make better approximation with less model analyses, sampling methods are studied intensively. Different sampling methods were studied and brought in different applications recent years, such as Latin Hypercube Sampling (LHS) (Choi et al. 2003; Qu et al. 2000) and collocation sampling method (Webster et al. 1996). In the collocation method, Webster and Tatang derived a set of polynomials from the probability density function of each input parameter such that the roots of each polynomial are spread out over the high probability region of the parameter by deriving orthogonal polynomials. Because the uncertainty is usually evaluated by transforming all the random variables and parameters into the Gaussian space, the corresponding orthogonal polynomials are Hermite polynomials. To obtain additional accuracy of SRS, moving least square (MLS) method (Youn 2001, Dec; Youn and Choi 2004) is proposed by introducing weight functions.

The number of simulations can be reduced if the sensitivity information is available. Isukapalli (Isukapalli et al. 2000) used an automatic differentiation program to obtain the sensitivity and utilized it in constructing the response surface. However, the computational cost for automatic differentiation is usually very high(Van Keulen et al. 2004), which reduces the significance of the method. Design sensitivity analysis can provide analytical sensitivity information of response with little extra computation (Kim et al. 2000). Thus, coupling the regression based stochastic response surface method (SRSM) with sensitivity can save large amount of computational cost, especially when the required number of design variables is large (Kim et al. 2004b).

Several methods(Lauridensen et al. 2001; Malkov and Toropov 1991; Rijpkema et al. 2000; Van Keulen et al. 2000) have been proposed to use sensitivity information in

constructing response surface. Vervenne (Vervenne 2005) proposed a gradient-enhanced response surface method based on above mentioned methods. He developed a two-step approach is proposed: first, different response surfaces using function values and derivatives are constructed separately; Second, these response surfaces are combined together to form a single response surface which fits as good as possible for both function value and response surfaces. In his study, several types of response surface and different combination scheme have been compared.

Reliability-Based Design Optimization

As mentioned in the previous section, FORM/SORM performs reliability analysis through linear/quadratic approximation of the performance function at MPP. Thus, searching MPP is the main task for moment-based RBDO. However, most advanced MPP search methods such as two point adaptive nonlinear approximation method (TPA) (Grandhi and L.P. 1998; Wang and Grandhi 1995; Xu and Grandhi 1998) or hybrid mean value (HMV) method(Youn 2001, Dec; Youn et al. 2003) can not make significant improvement of efficiency in the computational cost(Du and Chen 2002b).

In conventional RBDO, the probability constraint is described by the reliability index, which in FORM is the shortest distance from the origin to the limit state in standard normal space. This approach is called reliability index approach (RIA). By modifying the formulation of probabilistic constraints, Tu proposed an inverse measure approach, called Performance Measure Approach (PMA) (Tu 1999; Tu and Choi 1997; Tu et al. 1999; Tu 2001) which is proved to be consistent with the RIA but is inherently robust and more efficient if the probabilistic constraint is inactive. Both RIA and PMA employ double loop strategy with analysis loop (inner loop for reliability analysis) nested within the synthesis loop (outer loop for design optimization).

Due to the nature of double loop optimization, the computational cost is usually high. A couple of new strategies were proposed to improve the efficiency (Yang and Gu 2004). Sequential Optimization and Reliability Assessment (SORA) method (Du and Chen 2002b) decouples optimization loop from the reliability analysis loop and each deterministic optimization loop followed by a series of MPP searches. This method shifts the boundaries of violated constraints to the feasible direction based on the reliability results obtained in the previous cycle. Thus it improves design quickly from cycle to cycle and ameliorates the computational efficiency. Other single loop methods(Chen et al. 1997; Kwak and Lee 1987; Liang et al. 2004; Wang and Kodiyalam 2002) are also developed to provide efficient RBDO. In this method, the relationship between random variables and its mean is found through the Karush-Kuhn-Tucher (KKT) optimality condition. The double loop RBDO formulation is transformed to a single loop deterministic optimization problem and expensive MPP search is avoided. However, there is no guarantee that an active reliability constraint converges to its own MPP, and the required reliability may not be satisfied.

Sensitivity in Reliability Analysis

When RBDO problems are solved using gradient-based optimization algorithms, sensitivities of reliability or probability of failure with respect to the design parameters are required. Probability sensitivity can be used to identify those insignificant random variables during the design stage. In the moment-based approaches such as FORM, the sensitivity can be obtained accompanied by the reliability analysis without extra function evaluation once MPP is located (Karamchandani and Cornell 1992; Yu et al. 1997). Wu(Wu 1994) proposed an adaptive importance sampling(AIS) method to calculate reliability and AIS-based reliability sensitivity coefficients. Liu et al(Liu et al. 2004)

compare four widely-used probability sensitivity analysis(PSA) methods, which include Sobol' indices, Wu's sensitivity coefficients, the MPP based sensitivity coefficients and the Kullback-Leibler entropy based method. The merits behind each method are reviewed in details.

Dimension Reduction Strategy

In reliability analysis, the computational cost of multidimensional integration is high. Xu and Rahman(Rahman and Xu 2004; Xu and Rahman 2004) use series expansions to decompose the multidimensional problem to lower dimensional integration, such as univariate and bivariate integrations. Compared to multidimensional integration, the total computation of univarate integrations is much lower. Recent development in statistics introduces global sensitivity analysis (GSA)(Saltelli et al. 2000; Saltelli et al. 1999; Sobol 1993; Sobol 2001), which studies how the variance in the output of a computational model can be apportioned, qualitatively and quantitatively, to different sources of variation. Considering the contribution of the variance of design variables to performance variances are not of same importance, Kim et al proposed an adaptive reduction method using total sensitivity indices to reduce the problem dimensions (Kim et al. 2004a).

Robust Design

Robust design, known as Taguchi parameter design (Taguchi 1986; Taguchi 1987), is to design a product in such a way that the performance variance is insensitive to variation of design variables which is beyond the control of designer. Wang & Kodiyalam(Wang and Kodiyalam 2002) formulated robust design as an optimization problem by minimizing the variation of system response. Since the material cost has to be considered as well as manufacturing cost, Chen and Du's formulation compromises cost

reduction with performance variance control(Du and Chen 2002a). A robust design can also be achieved by using traditional optimization techniques to minimize the performance sensitivities. Chen & Choi formulated the robust design by minimizing a total cost function and sum of squares of magnitudes of first-order design sensitivities(Chen and Choi 1996), which requires the evaluation of second-order sensitivity analysis. This is a different philosophy compared to the variance based approach. It is more focus on the local behavior of the system performance and can achieve local robustness. The final design by minimizing local sensitivity cannot guarantee the robustness of system globally if the input variances are considerable.

By summarizing approaches popularly applied in robust design, Park et al. (Park et al. 2006) define robust design methodologies into two different category: Taguchi method and robust optimization. Under the context of multi-scale and multi-disciplinary applications, Allen et al.(Allen et al. 2006) reviewed robust design methods and categorizes robust design into four different types based on the sources of variability.

Fatigue Life Prediction

In 1829, Albert found that a metal subjected to a repeated load will fail at a stress level lower than that required to cause failure on a single application of the load. Then the question comes out: how parts fail under time-varying or non-static conditions? Such phenomenon is called fatigue. The first approach developed to carry out fatigue analysis is the nominal stress method, which is still widely used in applications where the applied stress varies with constant amplitude within the elastic range of the material and the number of cycles to failure is large. The nominal stress method works well in high cycle fatigue analysis but does not fit for the low cycle fatigue analysis where the material has a significant part in the plastic region.

August Wöhler(Wohler 1860) carried out experiments to obtain a plot of cyclic stress level versus the logarithm of life in mid-19th century, which is well known as *S-N* curve. Basquin proposed a stress-life(*S-N*) relationship(Basquin 1910) which can be plotted as a straight line using log scales. *S-N* approach is applicable to situations where cyclic loading is essentially elastic, so the *S-N* curve should be confined on the life axis to numbers greater than about 10^5 cycles in order to ensure no significant plasticity occurs. Most basic fatigue data are collected in the laboratory by testing procedures which employ fully reversed loading. However, most realistic service loads involve non-zero mean stresses. Therefore, the influence of mean stress on fatigue life should be considered so that the fully reversed laboratory data can be used in the evaluation of real service life. Since the tests required to determine the influence of mean stress are quite expensive, several empirical relationships(Gerber 1874; Goodman 1899; Soderberg 1939) which related alternating stress amplitude to mean stress have been developed. Among the proposed relationships, two are widely used, which are based on Goodman(Goodman 1899) and Gerber(Gerber 1874).

S-N approach works well when the cyclic loading is essentially elastic, which means in high cycle fatigue life evaluation. While using this method, it assumes that most of the life is consumed by nucleating cracks (around 0.01 mm) and nominal stresses and material strength control fatigue life. Accurate determinations of miscellaneous effects factor K_f for each geometry and material are also required.

The advantage of *S-N* approach is apparent since changes in material and geometry can easily be evaluated and large empirical database for steel with standard notch shape is available. However, the limitation should also be accounted. This method does not

consider the effects of plasticity, and mean stress effect evaluation is often in error. As the matter of fact, the requirement of empirical K_f for good results is also a kind of disadvantage.

As mentioned above, when the cyclic loads are relatively large and have a significant amount of plastic deformation, the components will suffer relatively short lives. This type of fatigue behavior is called low-cycle fatigue or strain-controlled fatigue.

The analytical procedure in dealing with strain-controlled fatigue is called the strain-life, local stress-strain or critical location approach. In 1950's, Coffin and Manson(Coffin 1954; Manson 1954) suggested that the plastic strength component of a fatigue cycle may also be considered in fatigue life prediction by a simple power law. In order to account for the mean stress effects, two correction methods are proposed by Morrow and Smith, Topper & Watson (STW)(Smith et al. 1970), respectively.

Local Strain-Life (ε-N) method assumes that the local stresses and strains control the fatigue behavior. In this method, the plastic effects and mean stress effects are considered well. The limitation is that it also needs the empirical K_f. In the local strain-life approach, the most of the life is consumed by micro-crack growth (0.1-1mm).

To account for macro-crack growth(>1mm), the fracture mechanics-based crack propagation method is proposed(Hoeppner and Krupp 1974; Paris 1964; Paris and Erdogan 1963). In this method, major assumption is that nominal stress and crack size control the fatigue life and the initial crack size is determined accurately. It is the only method to directly deal with cracks. However, the complex sequence effects and accurate initial crack size are difficult to be determined.

Linear elastic fracture mechanics (LEFM) is a new branch of engineering. The earliest work was done by Inglis(Inglis 1913) but the major developments were carried out by Griffth(Griffith 1921) at Royal Aircraft Factory(RAF,UK) in 1921 and Irwin(Irwin 1956) in the USA in 1956.

In LEFM theory, the driving force for a crack to extend is not the stress or strain but the stress intensity factor, known as K. The stress intensity factor uniquely describes the crack tip stress field independent of global geometry by embodying both the stress and the crack size. The relationship of the crack growth in the sense that the rate of crack growth, da/dN, with respect to the cyclic range of the stress intensity factor, ΔK, was derived by Paul C. Paris(Paris et al. 1961) in 1961, known as Paris Law.

In reality, mechanical component are seldom subjected to purely constant amplitude loading history. The irregular stress history must be counted as a series of constant amplitude stresses. In addition, it is difficult to define a cycle in an irregular stress history. Since the reverse of stress curve can be easily found according to the sign change of the stress history curve, cycle counting techniques such as rain-flow counting method(Matsuishi and Endo 1968) are developed to combine reversals to form cycles. After that, cumulative damages can be calculated by Miner's law(Miner 1945).

For most realistic structures or components, stress or strain fields are multi-axial. Fatigue life prediction methods for multi-axial loading also have been developed(Bannatine et al. 1990; Fuchs and Stephens 1980; Miller et al. 1966). In addition to some traditional method such as maximum principle stress/strain method, maximum shear stress/strain method and Von Mises' effective stress/strain method; Miller and Brown formulized the critical plane approach(Brown and Miller 1973) from

the observation that the stress and strain normal to the plane with maximum shear has been recognized to strongly influence the development of fatigue crack. No consensus has been reached on the methods of multi-axial fatigue life prediction. All these methods have their own advantages in the specific application.

So far, fatigue life analysis has been separated into two categories, (a) crack initiation, including *S*-*N* and ε-*N* method, and (b) crack propagation. The criteria for the fatigue life of a component in engineering design depend on material properties or work conditions. In general, the automotive industry usually applies crack initiation criteria because of the nature of the product and use. On the other hand, the aircraft industry mainly uses crack propagation criteria by periodic inspection and fatigue crack monitoring to achieve and maintain structural safety.

CHAPTER 3
UNCERTAINTY ANALYSIS USING STOCHASTIC RESPONSE SURFACE

Introduction

Uncertainty modeling and reliability analysis are the key issues in the reliability based design process. Uncertainty modeling can be decomposed into three fundamental steps: i) uncertainty characterization of model inputs, ii) propagation of uncertainty, and iii) uncertainty management/decision making. The uncertainty in model inputs can be represented in terms of standardized normal random variables (*srv*) with mean zero and variance equal to one. The selection is supported by the fact that they are widely used and well-behaved. For other types of random variables, an appropriate transformation must be employed. It is assumed that the model inputs are independent so each one is expressed directly as a function of a *srv* through a proper transformation. Devroye(Devroye 1986) presents the required transformation techniques and approximations for a variety of probability distributions. More arbitrary probability distributions can be approximated using algebraic manipulations or by series expansions.

For uncertainty propagation, Monte Carlo Simulation (MCS) may be the most common choice because of the accuracy and robustness, but the dilemma of MCS is that the required large number of samples that makes it impractical for computationally demanding models. There are several remedies to reduce the number of samples in MCS, such as importance sampling(Melchers 2001) and separable MCS(Smarslok and Haftka 2006). However, they require special knowledge of the problem or special form of the response. Several computationally efficient methods were proposed in last two decades

with reasonable accuracy in many structural problems, such as first- and second-reliability method (FORM/SORM), and response surface method (RSM). The stochastic response surface (SRS) can be viewed as an extension of classical deterministic response surfaces for model outputs constructed using uncertain inputs and performance data collected at heuristically selected collocation points. The polynomial expansion uses Hermite polynomial bases for the space of square-integrable probability density function (PDF) and provides a closed form solution of model outputs from a significant lower number of model simulations than those required by conventional methods such as modified Monte Carlo methods and Latin hypercube sampling.

In this chapter, a surrogate-based uncertainty model using stochastic response surface (SRS) is introduced. Reliability analysis using Monte Carlo simulation on this surrogate model shows promising results in terms of accuracy and efficiency. The proposed method is compared with the first-order reliability method (FORM) and MCS.

Description of Uncertainty Model

When the inputs of a system are uncertain or described as random variables/parameters, the output or response from this system will have a stochastic behavior as well. Let us assume that these random inputs are given in an n-dimensional vector $\mathbf{X}$ with continuous joint distribution function $f_{\mathbf{X}}(\mathbf{x})$. As shown in Figure 3-1, the system state can have a Boolean description such that the system fails when the limit state $G(\mathbf{X}) < 0$. The probability of failure P_f can then be defined as a cumulative distribution function (CDF) over the failure region, as

$$P_f = \int_{G(\mathbf{X})\le 0} f_{\mathbf{X}}(\mathbf{x}) d\mathbf{x}. \tag{3.1}$$

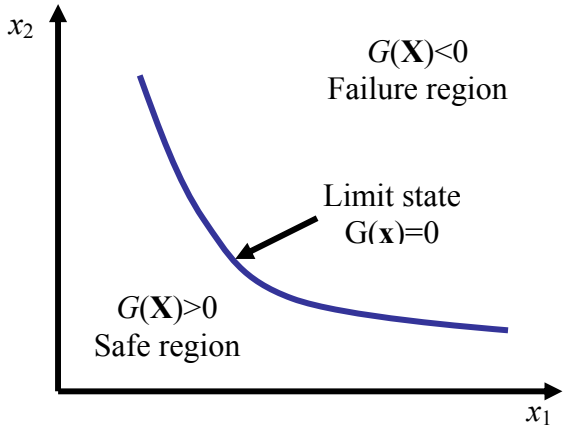

Figure 3-1. Limit state function divides the safe region from the failure region

Equation (3.1) is called the reliability integral. Since the integral domain defined by limit state function $G(\mathbf{X})$ is complex in the multi-dimensional random space, the reliability integral is difficult to calculate.

As introduced in the previous section, by transforming random variables from the original random space to the standard normal space, the limit state function can be expressed as a function of a set of *srvs* $\{u_i\}$. Then, P_f can be expressed in standard Gaussian space as

$$P_f = \int_{G(\mathbf{U})\le 0} \varphi_{\mathbf{U}}(\mathbf{u}) d\mathbf{u} \tag{3.2}$$

where $\varphi(\bullet)$ is the standard normal PDF and **U** is the vector of standard random variables. The transformation between **X** and **U** is denoted as **U**=T(**X**).

In FORM, the probability level of a system is usually represented by the reliability index or safety index β. For instance, if $\Phi(\bullet)$ is the CDF of the standard random variable, the failure probability can often be represented by the reliability index $\beta = -\Phi^{-1}(P_f)$.

Stochastic Response Surface Method (SRSM)

Polynomial Chaos Expansion (PCE) in Gaussian Space

Orthogonal polynomials have many useful properties in the solution of mathematical and physical problems. Just as Fourier series provide a convenient method of expanding a periodic function in a series of linearly independent terms, orthogonal polynomials provide a natural way to solve, expand, and interpret solutions to many types of important differential equations.

Orthogonal polynomials associated with the generalized polynomial chaos (Askey-Chaos) are different according to different weight functions. The type of polynomials is decided by the match between the specific weight function and the standard probability density function (PDF). The corresponding type of polynomials and their associated random variables are listed in Table 3-1.

Table 3-1. The type of polynomials and corresponding random variables for different Askey-Chaos (N≥0 denotes a finite integer)

	Random variable	Orthogonal polynomials	Support range
Continuous	Gaussian	Hermite	(-∞,∞)
	Gamma	Laguerre	[0, ∞)
	Beta	Jacobi	[a,b]
	Uniform	Legendre	[a,b]
Discrete	Poisson	Charlier	{0,1,2,…}
	Binomial	Krawtchouk	{0,1,2,…,N}
	Negative Binomial	Meixner	{0,1,2,…}
	Hypergeometric	Hahn	{0,1,2,…,N}

For example, in Table 3-1, Hermite polynomial chaos expansion requires the weight functions to be Gaussian probability density function, and it satisfies the following orthogonal relation:

$$\int_{x_k} f_k(x_k)\Gamma_k^i(x_k)\Gamma_k^j(x_k)dx_k = C\delta_{ij}, \qquad \forall i, j \tag{3.3}$$

where $f_k(x_k)$ is Gaussian PDF for variable x_k, $\Gamma_k^i(x_k)$ is the Hermite polynomial basis, and upper indices *i,j* denote for two different polynomials.

In this research, the uncertainty propagation is based on stochastic response surfaces (polynomial chaos expansion). The SRS(Isukapalli et al. 1998; Webster et al. 1996) can be view as an extension of classical deterministic response surfaces(Khuri and Cornell 1996; Myers and Montgomery 1995) for model outputs constructed using uncertain inputs and performance data collected at heuristically selected collocation points. The polynomial expansion uses Hermite polynomial bases for the space of square-integrable probability density function (PDF) and provides a closed form solution of model outputs from a significant lower number of model simulations than those required by conventional methods such as modified Monte Carlo methods and Latin hypercube sampling.

Let *n* be the number of random variables and *p* the order of polynomial. The model output can then be expressed in terms of the *srv* $\{u_i\}$ as:

$$G^p = a_0^p + \sum_{i=1}^{n} a_i^p \Gamma_1(u_i) + \sum_{i=1}^{n}\sum_{j=1}^{i} a_{ij}^p \Gamma_2(u_i,u_j) + \sum_{i=1}^{n}\sum_{j=1}^{i}\sum_{k=1}^{j} a_{ijk}^p \Gamma_3(u_i,u_j,u_k) + \cdots \qquad (3.4)$$

where G^p is the model output, the $a_i^p, a_{ij}^p, \ldots$ are deterministic coefficients to be estimated, and the $\Gamma_p(u_1,\ldots,u_p)$ are multidimensional Hermite polynomials of degree *p*:

$$\Gamma_p(u_i,\ldots,u_p) = (-1)^p e^{1/2\mathbf{u}^T\mathbf{u}} \frac{\partial^p}{\partial u_i \ldots \partial u_p} e^{-1/2\mathbf{u}^T\mathbf{u}} \qquad (3.5)$$

where **u** is a vector of *p* independent and identically distributed normal random variables selected among the *n* random variables that represent the model input uncertainties. Equation (3.4) is also called polynomial chaos expansion. The Hermite polynomials $\Gamma_p(u_i,\ldots,u_p)$ are set of orthogonal polynomials with weighting function $e^{-u^2/2}$, which

has the same form with the PDF of standard random variables. In this research, a modified version of Hermite polynomial(Isukapalli et al. 1998) is used. The first four terms are u, $u^2 - 1$, $u^3 - 3u$, and $u^4 - 6u^2 + 3$, when a single random variable is involved. The use of the Hermite polynomials has two purposes: (1) they are used to determine the sampling points, and (2) they are used as bases for polynomial approximation. In general, the approximation accuracy increases with the order of the polynomial, which should be selected reflecting accuracy needs and computational constraints.

The expressions for the 2nd- and 3rd-order polynomials in *n* dimensions (later used in the numerical examples) are:

2nd-order:

$$G^{(2)}(\mathbf{u}) = a_0^{(2)} + \sum_{i=1}^{n} a_i^{(2)} u_i + \sum_{i=1}^{n} a_{ii}^{(2)} (u_i^2 - 1) + \sum_{i=1}^{n-1} \sum_{j>i}^{n} a_{ij}^{(2)} u_i u_j \tag{3.6}$$

3rd-order:

$$\begin{aligned} G^{(3)}(\mathbf{u}) = a_0^{(3)} &+ \sum_{i=1}^{n} a_i^{(3)} u_i + \sum_{i=1}^{n} a_{ii}^{(3)} ({u_i}^2 - 1) \\ &+ \sum_{i=1}^{n} a_{iii}^{(3)} ({u_i}^3 - 3u_i) + \sum_{i=1}^{n-1} \sum_{j>i}^{n} a_{ij}^{(3)} u_i u_j \\ &+ \sum_{i=1}^{n} \sum_{j=1, j\neq i}^{n} a_{ijj}^{(3)} (u_i {u_j}^2 - u_i) + \sum_{i=1}^{n-2} \sum_{j>i}^{n-1} \sum_{k>j}^{n} a_{ijk}^{(3)} u_i u_j u_k \end{aligned} \tag{3.7}$$

The number of unknown coefficients is determined by dimension of the design space *n*. For 2nd and 3rd order expansion, if the number of unknowns is denoted by $N^{(2)}$, $N^{(3)}$, respectively:

$$N^{(2)} = 1 + 2n + \frac{n(n-1)}{2} \tag{3.8}$$

$$N^{(3)} = 1 + 3n + \frac{3n(n-1)}{2} + \frac{n(n-1)(n-2)}{6} \tag{3.9}$$

For $n = 2$, 4, and 8, for example, $N^{(2)} = 6$, 15, and 45; and $N^{(3)} = 10$, 35, and 165, respectively.

The coefficients in the polynomial chaos expansion are calculated using the least square method, considering samples of input/output pairs. Since all inputs are represented using *srv*, more accurate estimates for the coefficients can be expected, in the sense of statistics, if the probability distribution of the u_i's is considered. The idea of Gaussian Quadrature of numerical integral can be borrowed to generate collocation points(Webster et al. 1996). In Gaussian Quadrature, the function arguments are given by the roots of the next higher polynomial. Similarly, the roots of the next higher order polynomial are used as the points at which the approximation being solved, which is proposed as the orthogonal collocation method by Villadsen and Michelsen (Villadsen and Michelsen 1978).

For example, to solve for a three dimensional second order polynomial chaos expansion, the roots of the third order Hermite polynomial, $-\sqrt{3}$, 0 and $\sqrt{3}$ are used, thus the possible collocation points are (0,0,0),($-\sqrt{3}$, $-\sqrt{3}$, $-\sqrt{3}$),($-\sqrt{3}$,0, $\sqrt{3}$),etc.. There are 27 possible collocation points in this case. However, in equation(3.9), there are only 10 unknown coefficients. Similarly, for higher dimensional systems and higher order approximations, the number of available collocation points is always greater than the number of unknowns, which introduces a problem of selecting the appropriate collocation points. For a good approximation in polynomial chaos expansion, the choice of collocation points is critical. Hence, a set of points near the high probability region is heuristically selected among the roots of the one-order higher polynomial under restrictions of symmetry and closeness to the mean.

Since the origin always corresponds to the highest probability in standard Gaussian space, the exclusion of the origin as a collocation point could potentially lead to a poor

estimation. Thus, when the roots of high-order polynomial do not include zero, it is added in addition to the standard orthogonal collocation method.

The Hermite polynomials (orthogonal with respect to the Gaussian PDF) provide several attractive features, namely, more robust estimates of the coefficients with respect to those obtained using non-orthogonal polynomials(Gautschi 1996); it converges to any process with finite second order moments(Cameron and Martin 1947); and the convergence is optimal (exponential) for Gaussian processes(Xiu et al. 2002). In addition, the selected SRS approach includes a sampling scheme (collocation method) designed to provide a good approximation of the model output (inspired by the Gaussian Quadrature approach) in the higher probability region with limited observations. Once the coefficients are calculated, statistical properties of the prediction, such as mean and variance can be analytically obtained, and sensitivity analyses can be readily conducted.

Numerical Example of Stochastic Response Surface

As an illustration of the efficiency and convergence properties of the SRS approach, consider the construction of the PDF associated with a simple analytical function represented by:

$$y(x) = e^{x} \tag{3.10}$$

with x being a normally distributed random variable, as $N(0,0.4^2)$. Note that in this case the analytical expression of the PDF is known. The SRS for 2nd- and 3rd-order polynomials are shown in Eqs.(3.11) and (3.12), respectively.

$$y^{(2)} = 1.0833 + 0.4328u + 0.0833(u^2 - 1) \tag{3.11}$$

$$y^{(3)} = 1.0843 + 0.4333u + 0.0863(u^2 - 1) + 0.0112(u^3 - 3u) \tag{3.12}$$

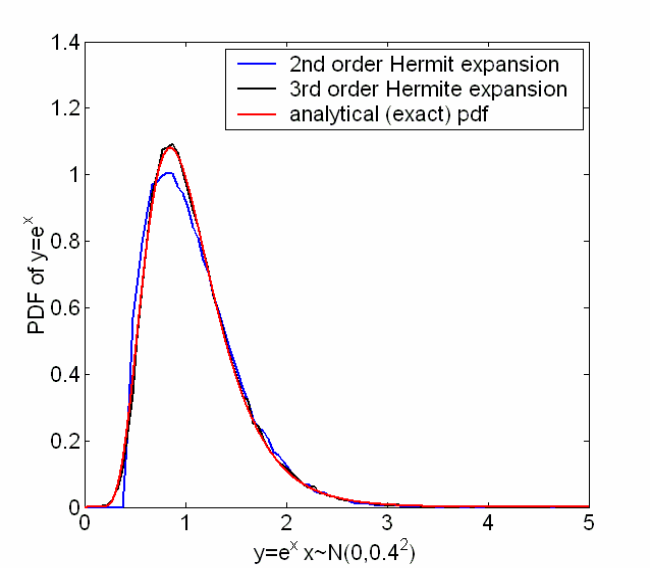

Figure 3-2. PDF of performance function $y(x) = e^x$

In this particular example, the accuracy of the proposed SRS is compared with the analytical solution. Figure 3-2 shows the PDF obtained from MCS applied to the SRS and from the exact solution.

A good agreement is observed in the PDF approximation, and the root mean square errors decreases with higher order polynomials, showing the convergence of the proposed SRS (Table 3-2).

Table 3-2. Root mean square error of PDF compared with the exact PDF of performance function $y=e^x$

Polynomial order	Errors
2	0.03835
3	0.00969

To illustrate the effectiveness of the SRS in the application to the structural problem, consider a torque-arm model in Figure 3-3 that is often used in shape optimization(Kim et al. 2003). The locations of boundary curves have uncertainties due

to manufacturing tolerances, modeled as probabilistic distributions. Thus, the relative locations of corner points of the boundary curves are defined as random variables with $x_i \sim N(d_i, 0.1^2)$. The mean values d_i of these random variables are chosen as design parameters, while the standard deviation remains constant during the design process.

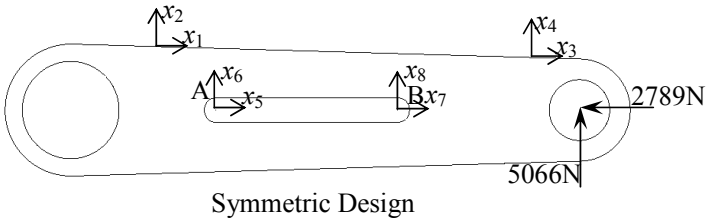

Figure 2-3: Shape design parameters for the torque

Figure 3-3. Shape design parameters for the torque arm

The torque arm model consists of eight random variables. In order to show how the SRS is constructed and the PDF of the model output is calculated, we choose the three random parameters (x_2, x_6, and x_8) that contribute most significantly to the stress performance at points A and B in Figure 3-3. In the deterministic analysis with mean value, the maximum stress of $\sigma_A = 319$MPa occurs at location A. The stress limit is established to be $\sigma_{max} = 800$MPa. In the reliability analysis the performance function is defined such that $G \leq 0$ is considered a failure. Thus, the performance function can be defined as $G(\mathbf{x}) = \sigma_{max} - \sigma_A(\mathbf{x})$. The number of unknown coefficients is a function of the dimension n of the random variables. For 2nd- and 3rd-order expansion, the numbers of coefficients, denoted by N_2 and N_3, are 10 and 20, respectively. There are 27 possible collocation points and 10 unknown coefficients in the case of 2nd-order expansion. For robust estimation, the number of collocation points in general should be at least twice the number of coefficients. In this particular example, all possible collocation points are

used. After coefficients are obtained, MCS with 100,000 samples is used to obtain the PDF.

Figure 3-4 shows the PDF associated with G(**x**) when different orders of polynomial approximations are used. The PDF obtained from the direct MCS with 100,000 sample points is also plotted. It is clear that the PDF from the 3rd-order is much closer than that of the 2nd-order to the PDF from the MCS.

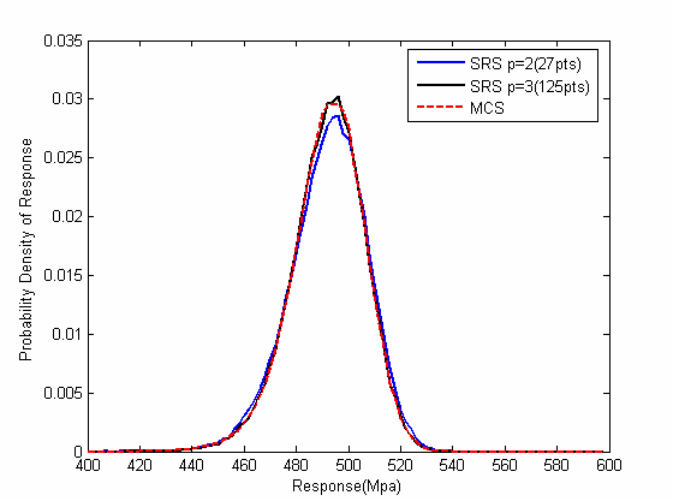

Figure 3-4. PDF of performance function G(**x**) – torque arm model

In order to compare the accuracy of the probability estimation through proposed SRS, let us check the probability of response being larger than 520MPa. In Table 3-3, the probability obtained from MCS is regarded as the reference. The relative error (ε) of failure probability from MCS estimation with sample size of N can be calculated using the following equation:

$$\varepsilon = k\sqrt{\frac{1-P_f}{N \cdot P_f}} \tag{3.13}$$

where k denotes the confidence level, for confidence level of 95%, k=1.96, which can be verified from standard normal table. Thus, in Table 3-3, number of MCS sample is 100,000, the error in P_f will be less than 5% with 95% confidence.

As shown in Table 3-3, it is clear that the SRS provides a convergent probability result as the order increases. With third order SRS, the accuracy of reliability analysis is significantly improved, compared to FORM.

Table 3-3. Comparison of probability of G>520MPa obtained from different uncertainty analysis methods (Full sampling without using local sensitivity)

Method	FORM	2nd order SRS	3rd order SRS	MCS
Prob. of G>520MPa	1.875%	2.061%	1.682%	1.566%
Relative error*	19.732%	31.609%	7.407%	–

*Relative error: $\left|\frac{prob(approx.) - prob(MCS)}{prob(MCS)}\right| \times 100\%$

Improving Efficiency of SRS Using Local Sensitivity Information

In the proposed SRS, the number of sampling points depends on the number of unknown coefficients. Although the proposed method is accurate and robust, we have to address the curse of dimensionality: as the number of random variables increases, the number of coefficients rapidly increases, as can be seen in Eqs. (3.8) and (3.9).

In addition to the efficient collocation method, the number of simulations can be reduced even further when local sensitivity is available. Recently, Isukapalli et al.(Isukapalli et al. 2000) used an automatic differentiation program to calculate the local sensitivity of the model output with respect to random variables and used them to construct the SRS. Their results showed that local sensitivity can significantly reduce the number of sampling points as more information is available. The computational cost of the automatic differentiation, however, is often higher than that of direct analysis(Van Keulen et al. 2004). However, in the application to the structural analysis, local sensitivity can be obtained at a reasonable computational cost. At each sampling point, the local sensitivity is a partial derivative of the limit state with respect to random

variables. Hence, if local sensitivity information is available, then n+1 data at each sampling point can be used for constructing the proposed SRS, which significantly reduces the required number of sampling points.

Continuum-Based Design Sensitivity Analysis

In this research, the continuum-based design sensitivity analysis(Choi and Kim 2004a) is utilized to calculate the gradient of the performance function with respect to random variables. Even if the idea can be used in a broader context, only structural problems are considered in this research. Let $\mathbf{z}$ be the displacement and $\bar{\mathbf{z}}$ be the displacement variation that belongs to the space $\mathbb{Z}$ of kinematically admissible displacements. For given body force **f** and surface traction force **t**, the variational equation in the continuum domain Ω is formulated as

$$a(\mathbf{z},\bar{\mathbf{z}}) = l(\bar{\mathbf{z}}), \tag{3.14}$$

for all $\bar{\mathbf{z}} \in \mathbb{Z}$. In Eq. (3.14), the structural bilinear and load linear forms are defined, respectively, as

$$a(\mathbf{z},\bar{\mathbf{z}}) = \iint_{\Omega} \sigma_{ij}(\mathbf{z})\varepsilon_{ij}(\bar{\mathbf{z}})d\Omega \tag{3.15}$$

$$l(\bar{\mathbf{z}}) = \iint_{\Omega} f_i \bar{z}_i d\Omega + \int_{\Gamma_T} t_i \bar{z}_i d\Gamma \tag{3.16}$$

where ε_{ij} are components of the engineering strain tensor, and σ_{ij} are components of the stress tensor. In linear elastic materials, the constitutive relation can be given as

$$\sigma_{ij}(\mathbf{z}) = c_{ijkl}\varepsilon_{kl}(\mathbf{z}) \tag{3.17}$$

where the constitutive tensor c_{ijkl} is constant. The summation rule is used for the repeated indices.

In order to solve Eq.(3.14) numerically, the finite-element-based method or the meshfree method can be employed, which ends up solving the following form of matrix equation:

$$[\mathbf{K}]\{\mathbf{D}\} = \{\mathbf{F}\} \tag{3.18}$$

where [**K**] is the stiffness matrix, {**F**} the discrete force vector, and {**D**} the vector of nodal displacements. The major computational cost in solving Eq.(3.18) is related to L-U factorization of the coefficient matrix. As will be shown later, the efficiency of sensitivity calculation comes from the fact that sensitivity analysis uses the same coefficient matrix that is already factorized when Eq.(3.18) is solved.

In design sensitivity analysis, the variational Eq.(3.14) is differentiated with respect to design variables. In shape design, the design variable does not appear explicitly in the governing equation. Rather, the shape of the domain that a structural component occupies is treated as a design variable. Thus, a formal procedure is required to obtain the design sensitivity expression.

As shown in Figure 3-5, suppose that the initial structural domain Ω is changed into the perturbed domain Ω_τ in which the parameter τ controls the shape perturbation amount. By defining the design changing direction to be $\mathbf{V}(x)$, the material point at the perturbed design can be denoted as $\mathbf{x}_\tau = \mathbf{x} + \tau\mathbf{V}(\mathbf{x})$. The solution $\mathbf{z}_\tau(\mathbf{x}_\tau)$ of the structural problem is assumed a differentiable function with respect to shape design. The sensitivity of $\mathbf{z}_\tau(\mathbf{x}_\tau)$ at $\mathbf{x}_\tau$ is defined as

$$\dot{\mathbf{z}} = \lim_{\tau \to 0} \frac{\mathbf{z}_\tau(\mathbf{x} + \tau\mathbf{V}(\mathbf{x})) - \mathbf{z}(\mathbf{x})}{\tau} \tag{3.19}$$

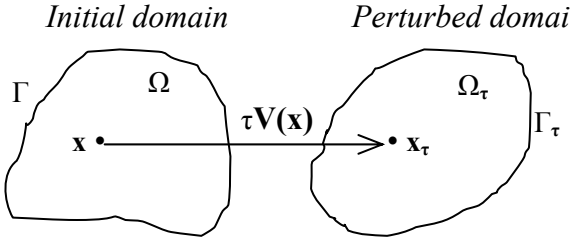

Figure 3-5. Variation of a structural domain according to the design velocity field **V(x)**

The design sensitivity equation is obtained by taking the material derivative of the variational equation(3.14) . The derivative of the structural energy form then becomes

$$\frac{d}{d\tau} a_{\Omega_\tau}(\mathbf{z}_\tau, \overline{\mathbf{z}}_\tau)\big|_{\tau=0} = a_\Omega(\dot{\mathbf{z}}, \overline{\mathbf{z}}) + a'_{\mathbf{V}}(\mathbf{z}, \overline{\mathbf{z}}) \tag{3.20}$$

The first term on the right-hand side represents an implicit dependence on the design through the state variable, while the second term, the structural fictitious load, denotes an explicit dependence on the design velocity **V(x)**, defined as

$$a'_V(\mathbf{z}, \mathbf{z}) = \iint_\Omega [\varepsilon^V_{ij}(\overline{\mathbf{z}})\sigma_{ij}(\mathbf{z}) + \varepsilon_{ij}(\overline{\mathbf{z}})c_{ijkl}\varepsilon^V_{kl}(\mathbf{z}) + \varepsilon_{ij}(\overline{\mathbf{z}})\sigma_{ij}(\mathbf{z})div\mathbf{V}]d\Omega \tag{3.21}$$

where

$$\varepsilon^V_{ij}(\mathbf{z}) = -\frac{1}{2}\left(\frac{\partial z_i}{\partial x_k}\frac{\partial V_k}{\partial x_j} + \frac{\partial z_j}{\partial x_k}\frac{\partial V_k}{\partial x_i}\right) \tag{3.22}$$

If the applied load is independent of displacement, i.e., conservative, then

$$\begin{aligned} l'_V(\overline{\mathbf{z}}) &= \iint_\Omega [\overline{z}_i \frac{\partial f_i}{\partial x_j} V_j + \overline{z}_i f_i \frac{\partial V_j}{\partial x_j}]d\Omega \\ &+ \int_\Gamma [\overline{z}_i \frac{\partial t_i}{\partial x_j} V_j + \kappa \overline{z}_i t_i V_n]d\Gamma \end{aligned} \tag{3.23}$$

is the external fictitious load form, where V_n is the normal component of the design velocity on the boundary, and κ is the curvature of the boundary. The design sensitivity equation is obtained from Eq. (3.20) to (3.23) as

$$a(\dot{\mathbf{z}}, \overline{\mathbf{z}}) = l'_V(\overline{\mathbf{z}}) - a'_V(\mathbf{z}, \overline{\mathbf{z}}) \tag{3.24}$$

for all $\overline{\mathbf{z}} \in \mathbb{Z}$.

Note that by substituting $\dot{\mathbf{z}}$ into $\mathbf{z}$, the left-hand side of the design sensitivity equation (3.24) takes the same form as that of the response analysis in Eq.(3.14). Thus, the same stiffness matrix [**K**] can be used for sensitivity analysis and response analysis, with a different right-hand side.

Once the sensitivity $\dot{\mathbf{z}}$ of the field vector is calculated, the sensitivity of the performance function with respect to design variable u_i can be calculated using the chain rule of differentiation, as

$$\frac{dy(\mathbf{z};\mathbf{x})}{du_i} = \frac{\partial y(\mathbf{z};\mathbf{x})}{\partial u_i} + \frac{\partial y(\mathbf{z};\mathbf{x})}{\partial \mathbf{z}}\dot{\mathbf{z}} \tag{3.25}$$

When finite element analysis is used, the sensitivity equation can be solved inexpensively because the coefficient matrix is already factorized when solving Eq.(3.14) and the sensitivity equation uses the same coefficient matrix. The computational cost of sensitivity analysis is usually less than 20% of the original analysis cost. The computational efficiency of the uncertainty propagation approach is critical to RBDO since as previously stated at each design cycle the updated version of the PDF for the constraint function (related to model outputs) is required.

Constructing SRS Using Local Sensitivity

In SRS, the system response can be approximated as polynomial expansion when k sampling data are available, the linear regression equation can be written as

$$\{\mathbf{y}\} = \begin{Bmatrix} y_1 \\ y_2 \\ \vdots \\ y_k \end{Bmatrix} = \begin{bmatrix} 1 & u_1 & u_1^2 - 1 & \cdots \\ 1 & u_2 & u_2^2 - 1 & \cdots \\ \vdots & \vdots & \vdots & \vdots \\ 1 & u_3 & u_3^2 - 1 & \cdots \end{bmatrix} \begin{Bmatrix} a_0 \\ a_1 \\ \vdots \\ a_N \end{Bmatrix} = [\mathbf{A}]\{\mathbf{a}\} \tag{3.26}$$

The above equation is the standard form for linear regression to solve for unknown coefficients $\{\mathbf{a}\}$. When the sensitivity information is available, additional information at each sampling point can be used in calculating the coefficients. By differentiating Eq.(3.4) with respect to random variable u_i and by applying the same regression process in Eq.(3.26), we have

$$\left\{\frac{d\mathbf{y}}{du_i}\right\} = \left[\frac{\partial \mathbf{A}}{\partial u_i}\right]\{\mathbf{a}\} \tag{3.27}$$

Equations (3.26) and (3.27) can be combined to obtain the following regression equations:

$$\begin{Bmatrix} \mathbf{y} \\ \dfrac{d\mathbf{y}}{du_1} \\ \vdots \\ \dfrac{d\mathbf{y}}{du_n} \end{Bmatrix} = \begin{bmatrix} \mathbf{A} \\ \dfrac{\partial \mathbf{A}}{\partial u_1} \\ \vdots \\ \dfrac{\partial \mathbf{A}}{\partial u_n} \end{bmatrix} \{\mathbf{a}\} \tag{3.28}$$

Let $\{\mathbf{Y}\} = \begin{Bmatrix} \mathbf{y} & \dfrac{d\mathbf{y}}{du_1} & \cdots & \dfrac{d\mathbf{y}}{du_n} \end{Bmatrix}^T$, $\{\mathbf{B}\} = \begin{bmatrix} \mathbf{A} & \dfrac{\partial \mathbf{A}}{\partial u_i} & \cdots & \dfrac{\partial \mathbf{A}}{\partial u_n} \end{bmatrix}^T$, Eq. (3.28) can be written as

$$\{\mathbf{Y}\} = [\mathbf{B}]\{\mathbf{a}\} \tag{3.29}$$

Thus, the coefficients of SRS can be obtained using least square regression, such that

$$\{\mathbf{a}\} = \left([\mathbf{B}]^T [\mathbf{B}] \right)^{-1} [\mathbf{B}]^T \{\mathbf{Y}\} \tag{3.30}$$

Note that the sensitivity $\dfrac{\partial \mathbf{y}}{\partial u_i}$ can be calculated using the transformation of random variables, as

$$\frac{\partial \mathbf{y}}{\partial u_i} = \frac{\partial y}{\partial x_i} \frac{\partial x_i}{\partial u_i} \tag{3.31}$$

As introduced in the previous section, the local sensitivity $\partial \mathbf{y} / \partial x_i$ can be obtained implicitly through Eq. (3.25), where design variable is represented by u_i instead of x_i since notation x has been used as space coordinate. Since the transformation between *srv* and variables with other types of distribution are also mathematically well developed, $\partial x_i / \partial u_i$ can be obtained explicitly. Therefore, Eq.(3.30) provides an explicit solution for obtaining coefficients of SRS.

Numerical Example – Torque Arm Model

In order to show the effectiveness of the proposed SRS with local sensitivity, the same torque arm problem with previous example is used. All conditions are the same as before. By taking advantage of using sensitivity information to build stochastic response surface, the number of collocation points is reduced significantly. Here for the second-order polynomial chaos expansion, 7 points have been used, while 31 points for the third-order case. At each sampling point, the function value and sensitivity information are used to construct the SRS.

The PDF obtained from the SRS with sensitivity is plotted in Figure 3-6 along with that from MCS with 100,000 samples. In the case of 2nd-order, the SRS with sensitivity is more accurate than the SRS without sensitivity (Figures 3-4 & 3-6). In order to calculate the accuracy, the probability of $G \geq 520MPa$ is calculated using FORM, second- and third-order SRS (Table 3-4). Since no analytical solution is available, MCS with 100,000 samples is used as a reference. Both SRS are more accurate than FORM.

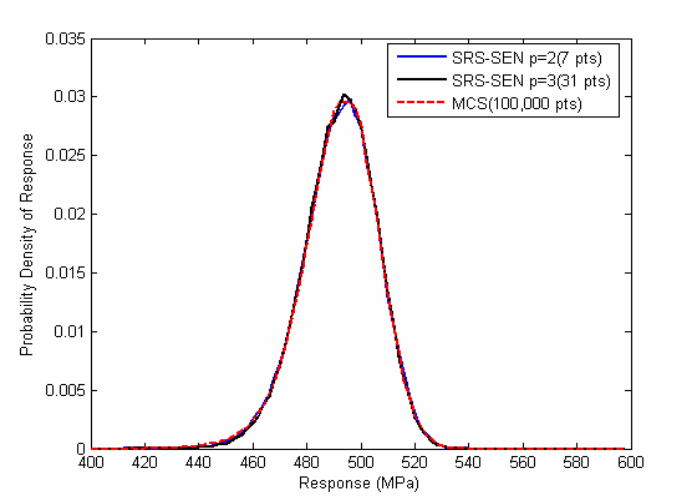

Figure 3-6. PDF of performance fuction G(**x**) – Torque model at initial design (SRS with sensitivity)

Table 3-4. Comparison of probability of G>520MPa obtained from different uncertainty analysis methods (reduced sampling using local sensitivity) ;

Method	FORM	2nd order SRS	3rd order SRS	MCS
Prob. of G>520MPa	1.875%	1.520%	1.545%	1.566%
Relative error*	19.732%	2.937%	1.341%	–

*Relative error: $\left|\frac{prob(approx.)-prob(MCS)}{prob(MCS)}\right|\times 100\%$

Table 3-5 compares the probability of G>520 MPa of second order SRS with/without using local sensitivity with that of MCS, which is regarded as the reference of exact value. With local sensitivity and seven sampling points, SRS provides more accurate probabilistic result than that without utilizing local sensitivity and twenty-seven sampling points. The accuracy is improved by using local sensitivity while computational cost is reduced.

Table 3-5. Comparison of probability of G>520MPa obtained with/without local sensitivity (7/27 sampling points) using 2nd order SRS

Method	2nd order SRS using 27 sampling points without sensitivity	2rd order SRS using 7 sampling points with sensitivity	MCS (100,000 samples)
Prob. of G>520MPa	0.2061%	1.520%	1.566%
Relative error*	31.6091%	2.937%	–

*Relative error: $\left|\frac{prob(approx.)-prob(MCS)}{prob(MCS)}\right|\times 100\%$

Summary

In this chapter, a stochastic response surface method (SRSM) using polynomial chaos expansion is used in calculating structural reliability. Compared with FORM, which is based on the linear approximation at the most probability point, it provides more accurate result for nonlinear responses. In addition, orthogonal polynomial basis provide

a convergent behavior as the order of polynomial is increased. A nonlinear function has been used as numerical example to show its accuracy and convergence.

Since continuum based sensitivity results were obtained during structure analysis, the computational cost is further reduced by providing gradient information while fitting response surface. SRSM has been applied on a structural problem to show its effectiveness. When sensitivity information is provided, numerical results show that even lower number of sampling point can provide more accurate result.

CHAPTER 4
RELIABILITY-BASED DESIGN OPTIMIZATION

Although statistical methods of uncertainties quantification have been studied intensively for decades, traditional deterministic design optimization still takes no advantage in these scientific advances and compensates uncertainties based on experience; for example, the safety factor. Such an optimization scheme usually yields either unsafe or too conservative design due to the lack of uncertainty quantification. In order to impose existing knowledge of uncertainty to engineering design process, reliability-based design optimization (RBDO) methodologies have been proposed and developed(Chandu and Grandi 1995; Chen et al. 1997; Du and Chen 2002b; Enevoldsen and Sorensen 1994; Grandhi and L.P. 1998; Kim et al. 2004b; Kwak and Lee 1987; Liang et al. 2004; Tu 1999; Tu and Choi 1997; Youn et al. 2003), where the system reliability or probability of failure is used to evaluate the system performance. Compared to the deterministic optimization, RBDO provides margins on reliability by quantifying the uncertainty in the response of structural system due to input uncertainty.

General RBDO Model

Design optimization has been introduced to structural engineering for decades(Arora 2004; Haftka and Gurdal 1991; Vanderplaats 2001). Its methodologies have been well developed mathematically, and applications in product development are flourishing. The underlying design philosophy is to reduce the cost by pushing the design to its performance margin. In traditional deterministic design, an optimization problem is formulated as

$$\begin{aligned} &\text{minimize} && \text{Cost}(\mathbf{d}) \\ &\text{subject to} && G_j(\mathbf{d}) \le G_{j-allowable}, \quad j = 1,2,\ldots,np \\ & && \mathbf{d}_L \le \mathbf{d} \le \mathbf{d}_U \end{aligned} \tag{4.1}$$

where $G_j(\mathbf{d})$ is the constraint function, for example, stress; $G_{j-allowable}$ is the corresponding maximum constraint allowable; and $\mathbf{d}$ denotes the vector of the deterministic design variables. The objective is to minimize the cost while meeting the system constraints.

A system design depends on the system design variables. In deterministic optimization, both objective and constraints only depend on the design vector **d** which contains all deterministic design variables d_i. In reliability-based design, design is based on a randomly distributed system vector, e.g., denoted by **X**, which contains random variable X_i. In RBDO, the mean value μ_i or the standard deviation σ_i of the system variable X_i can be used as the design variable. In some cases, uncontrollable random variables may contribute to the uncertainty of the performance.

Instead of directly setting constraints on deterministic performance, the RBDO problem(Chandu and Grandi 1995; Enevoldsen and Sorensen 1994; Grandhi and L.P. 1998; Wu and Wang 1996) can generally be defined by setting constraints to be uncertainty measures, such as probability of failure. It is then formulated as

$$\begin{aligned} &\text{minimize} && \text{Cost}(\mathbf{d}) \\ &\text{subject to} && P(G_j(\mathbf{x}) < 0) \le \bar{P}_{f,j}, \quad j = 1,2,\ldots,np \\ & && \mathbf{d}_L \le \mathbf{d} \le \mathbf{d}_U \end{aligned} \tag{4.2}$$

where the cost can be any function of the design variable $\mathbf{d} = [d_i]^T$, (i =1, 2, …, n) and $\bar{P}_{f,j}$ is the prescribed failure probability limit for the *jth* constraint.

Reliability Index Approach (RIA) and Performance Measure Approach (PMA)

In the RBDO formulation described in the previous section, each prescribed failure probability limit $\overline{P}_f$ is often represented by the reliability target index as $\beta_t = -\Phi^{-1}(\overline{P}_f)$. Hence, any probabilistic constraint in Eq. (4.2) can be rewritten using equation as

$$F_G(0) \le \Phi(-\beta_t) \tag{4.3}$$

where $F_G(0)=P(G<0)$ is the cumulative distribution function(CDF) of G at the failed region. Equation(4.3) can also be expressed in another way through inverse transformations

$$\beta_s = -\Phi^{-1}(F_G(0)) \ge \beta_t \tag{4.4}$$

where β_s is traditionally called the reliability index. The expression of probability constraint in Eq. (4.4) leads to the so called reliability index approach (RIA)(Tu and Choi 1997; Tu 2001; Youn 2001).

The two forms of constraint described in equations (4.2)and (4.4) are basically the same.

In FORM/SORM based RBDO, an inner loop optimization is used to find the most probability point (MPP) in the standard Gaussian space. RIA may cause singularity because β_s approaches infinity or negative infinity when the failure probability is zero or one. In that case, inner loop optimizer may fail to find the MPP.

There is an alternative way to avoid singularity(Tu and Choi 1997) based on a different concept of reliability measure. For any given target probability, a certain level of performance can be reached to meet the reliability requirement. Tu(Tu and Choi 1997) proposed an inverse measure approach called performance measure approach (PMA) based on FORM by transforming Eq.(4.4) to

$$g^* = F_G^{-1}(\Phi(-\beta_t)) \ge 0 \tag{4.5}$$

where g^* is named the target probabilistic performance measure. In PMA, Eq.(4.5) is used as probabilistic constraint of RBDO. PMA has been proved to be consistent with RIA in prescribing the probabilistic constraint, but their differences in probabilistic constraint evaluation can be significant (Tu 1999). PMA is more robust in FORM/SORM than RIA based on the fact that RIA may yield singularity; that is, β_s approaches infinity or negative infinity. In addition, for an inactive probabilistic constraint, PMA is more efficient than RIA.

Known as an inverse measure approach, PMA can also be implemented on the sampling based uncertainty estimation method. For example, in MCS, a performance measure that meets reliability requirement can be obtained from the order statistics of sampled performance values.

Figure 4-1 shows the general numerical procedure of RBDO. The effect and efficiency of inverse measure approach has been investigated for FORM/SORM(Tu 1999; Tu and Choi 1997). In this research, RIA and PMA as two different philosophies for probability constraint evaluation are also addressed for SRS-based RBDO.

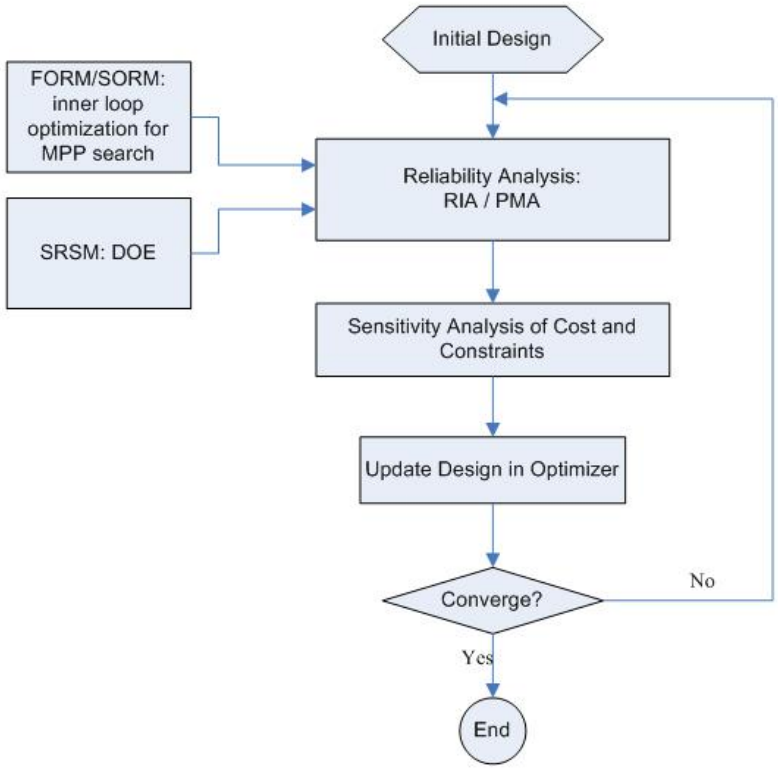

Figure 4-1. Flow chart for reliability-based design optimization

Probability Sensitivity Analysis (PSA)

Similar to the traditional design sensitivity, where sensitivity quantifies the effect of deterministic design variable to the structure response, probability sensitivity provides the quantitative estimation of the changing of failure probability or reliability with respect to the changes of random parameters, such as means or standard deviations of random design variables.

In RBDO, the gradient based optimizer needs sensitivity information to carry out optimization. Automatic differentiation using finite differentiation leads to a significantly extra computational cost, especially when there are many design variables.

In RBDO, if constraints are set with the probability of failure being less than a certain threshold, the gradient of probability with respect to the random input is required.

In this research, probability sensitivity analysis is utilized to calculate the gradient information.

First, the probability sensitivity calculation in FORM is introduced by taking advantage of structural sensitivity analysis. It can be shown that one can obtain accurate probability sensitivity without extra simulation cost. Since SRSM shows an advantage for nonlinear response, sampling based probability sensitivity is also introduced. For inverse measure approach, sensitivity for both FORM and sampling based RBDO can be obtained.

Probability Sensitivity Analysis in FORM

In first order reliability method (FORM), reliability index (β) can be obtained by following equation

$$\beta = (\mathbf{U}^{*\mathrm{T}}\mathbf{U}^{*})^{1/2} \tag{4.6}$$

where $\mathbf{U}^{*}$ is the vector of MPP. The derivative of failure probability with respect to the design variables in FORM can then be written as

$$\frac{\partial P_f}{\partial \eta} = \frac{\partial \Phi(-\beta)}{\partial \eta} = \frac{\partial \Phi(-\beta)}{\partial \beta}\frac{\partial \beta}{\partial \eta} = -\varphi(-\beta)\frac{\partial \beta}{\partial \eta} \tag{4.7}$$

where φ(•) is the PDF of the standard random variable. Thus, the sensitivity of the failure probability is directly related to that of the reliability index, which can be obtained by

$$\frac{\partial \beta}{\partial \eta} = \frac{\partial (\mathbf{U}^{*\mathrm{T}}\mathbf{U}^{*})^{1/2}}{\partial \eta} = \frac{1}{\beta}\mathbf{U}^{*\mathrm{T}}\frac{\partial \mathbf{U}^{*}}{\partial \eta} \tag{4.8}$$

For a random variable $\eta = \theta_i$

$$\begin{aligned}\frac{\partial \beta}{\partial \theta_i} &= \frac{1}{\beta}\mathbf{U}^{*\mathrm{T}}\left[\frac{\partial \mathbf{T}(\mathbf{X}^*,\boldsymbol{\theta})}{\partial \theta_i}+\frac{\partial \mathbf{T}(\mathbf{X}^*,\boldsymbol{\theta})}{\partial \mathbf{X}}\frac{\partial \mathbf{X}^*}{\partial \theta_i}\right] \\ &= \frac{1}{\beta}\mathbf{U}^{*\mathrm{T}}\frac{\partial \mathbf{T}(\mathbf{X}^*,\boldsymbol{\theta})}{\partial \theta_i}+\frac{1}{\beta}\mathbf{U}^{*\mathrm{T}}\frac{\partial T(\mathbf{X}^*,\boldsymbol{\theta})}{\partial \mathbf{X}}\frac{\partial \mathbf{X}^*}{\partial \theta_i} \\ &= \frac{1}{\beta}\mathbf{U}^{*\mathrm{T}}\frac{\partial \mathbf{T}(\mathbf{X}^*,\boldsymbol{\theta})}{\partial \theta_i}\end{aligned} \tag{4.9}$$

Since the reliability index and the most probable point are available from the reliability analysis, the sensitivity can be easily obtained. If the computationally expensive structure analysis code does not come with sensitivity analysis, a finite difference method is widely used to provide gradient information for searching the most probability point (MPP). The computational cost of finite difference method is proportional to the number of design variables. Using design sensitivity analysis, we can avoid the finite difference calculation and provide more accurate gradient information to the line search for MPP.

In the finite difference method, the gradient of the limit state in the standard normal space is defined as

$$\nabla g(\mathbf{U}) = \lim_{\Delta \mathbf{U}\to 0}\frac{g(\mathbf{U}+\Delta \mathbf{U})-g(\mathbf{U})}{\Delta \mathbf{U}} \tag{4.10}$$

Every iteration in line search needs to perturb each design variable to evaluate the gradient. If the sensitivity information can be obtained from a structural analysis code, there is a more efficient way to obtain the gradient information for MPP search. The gradient $\nabla g(\mathbf{U})$ can be computed as

$$\nabla g(\mathbf{U}) = \nabla g(\mathbf{X})\frac{\partial \mathbf{T}^{-1}(\mathbf{U})}{\partial \mathbf{U}} \tag{4.11}$$

where $\mathbf{T}:\ \mathbf{X}\to\mathbf{U}$.

The transformation $\mathbf{T}$ from original random design space to the standard Gaussian space can usually be obtained explicitly, and the gradient $\nabla g(\mathbf{X}^*)$ is provided by design sensitivity analysis.

In this section, the torque arm model described in Chapter 3 is used to evaluate the accuracy of the probability sensitivity analysis using FORM. At the initial design, the probabilistic parameters of eight random variables are considered as design variables. Each random variable is assumed to be normally distributed with a mean of zero and a standard deviation 0.1. The sensitivity of reliability index is calculated based on Eq.(4.9). Since the transformation $\mathbf{T}$ is an explicit function of probabilistic parameters, the sensitivity can easily be calculated with reliability analysis.

Table 4-1 shows the sensitivity results with respect to mean ($\partial\beta/\partial\mu_i$) and standard deviation ($\partial\beta/\partial\sigma_i$). The accuracy of the sensitivity is compared with that of the finite difference method with 1% perturbation size.

Table 4-1. Probability sensitivity with respect to random parameters (unit: centimeter)

design	$\frac{\partial\beta}{\partial\mu_i}$	$\frac{\Delta\beta}{\Delta\mu_i}$	$\frac{\Delta\beta/\Delta\mu_i}{\partial\beta/\partial\mu_i}\times 100\%$	$\frac{\partial\beta}{\partial\sigma_i}$	$\frac{\Delta\beta}{\Delta\sigma_i}$	$\frac{\Delta\beta/\Delta\sigma_i}{\partial\beta/\partial\sigma_i}\times 100\%$
x_1	0.376	0.377	100.26	-0.030	-0.030	100.00
x_2	5.243	5.243	100.00	-5.773	-5.775	100.03
x_3	0.034	0.034	100.00	-0.000	-0.000	100.00
x_4	0.106	0.106	100.00	-0.002	-0.002	100.00
x_5	0.055	0.055	100.00	-0.001	-0.001	100.00
x_6	-7.244	-7.244	100.00	-11.022	-11.011	99.90
x_7	-0.140	-0.140	100.00	-0.004	-0.004	100.00
x_8	-4.457	-4.457	100.00	-4.171	-4.173	100.05

In Table 4-1, the first column represents eight random variables that have normal distributions. All random variables are assumed to be independent. Since the mean value and the standard deviation are considered as probabilistic parameters, there are 16 cases

in the sensitivity calculations. The second and fifth columns represent the sensitivity results obtained from the analytical derivative, while the third and sixth columns are sensitivity results from the finite difference method. A very good agreement between the two methods is observed.

Table 4-2 shows the computational efficiency of the proposed analytical sensitivity calculation. The gradient information is provided from design sensitivity analysis in MPP search in the standard HL-RF method(Hasofer and Lind 1974; Liu and Kiereghian 1991). The computational savings are about 90% compared to the case when only the function values are provided. Once the reliability analysis is finished, the sensitivity of reliability index requires additional 17 function evaluations for the finite difference method, while only a single analysis is enough for the proposed method because the analytical expression in Eq.(4.9) and (4.11) is used.

Table 4-2. Computational efficiency of analytical method for probability sensitivity

	Finite differential method	Analytical method
number of analyses in MPP search	90	10
number of analyses in sensitivity calculation	17	1
Total number of analysis	107	11

Probability Sensitivity Analysis Using SRSM

In RBDO, the probability of failure can be formulated as

$$P_f = \int_{G(\mathbf{X})\le 0} f(\mathbf{x})d\mathbf{x} \tag{4.12}$$

where $G(\mathbf{X}) \le 0$ is the failure region and $f(\bullet)$ is the joint probability density function(PDF).

By introducing an indication function $I(G(\mathbf{X}) \le 0)$ such that I=1 if $G(\mathbf{X}) \le 0$ and I=0 otherwise, Eq.(4.12) can be rewritten as

$$P_f = \int_{\Omega_x} I(G(\mathbf{x}) \le 0) f(\mathbf{x}) d\mathbf{x} \tag{4.13}$$

where $\Omega_{\mathbf{X}}$ denotes the entire random design space.

Since Eq.(4.12) is used as a constraint in RBDO, the sensitivity of P_f is required. The derivative of failure probability can be written as

$$\begin{aligned} \frac{\partial P_f}{\partial \theta} &= \int_{\Omega_x} I(G(\mathbf{x}) \le 0) \frac{\partial f(\mathbf{x})}{\partial \theta} d\mathbf{x} = \int_{\Omega_x} I(G(\mathbf{x}) \le 0) \cdot \left[\frac{\partial f(\mathbf{x})}{f(\mathbf{x}) \partial \theta} \right] f(\mathbf{x}) d\mathbf{x} \\ &= \int_{\Omega_u} I(G(\mathbf{u}) \le 0) \cdot \left[\frac{\partial f(\mathbf{x})}{f(\mathbf{x}) \partial \theta} \right]_{\mathbf{x}=\mathbf{T}^{-1}(\mathbf{u})} \varphi(\mathbf{u}) d\mathbf{u} \end{aligned} \tag{4.14}$$

where $\Omega_{\mathbf{u}}$ denotes the entire standard normal space. Explicit expression of Eq.(4.14) for different distribution types and numerical examples are derived in Appendix A. The accuracy of the sensitivity results are also presented in Appendix A for the case of various distribution types.

Reliability-Based Design Optimization Using SRSM

Although RIA and PMA are theoretically consistent in prescribing the probability constraint, there are still significant differences in probabilistic constraint evaluation. The RBDO based on RIA and PMA may lead to either different convergence or efficiency.

In this section, an RBDO problem is formulated for the same torque-arm model in Chapter 3 using the concepts of RIA and PMA. A 3rd-order SRS is constructed for uncertainty analysis for both RIA and PMA.

When the reliability index is used as a constraint in RBDO, it sometimes experiences numerical difficulty because it can have a value of infinity for very safe design. When SRSM is used in evaluating the probabilistic constraint in RBDO, the problem of singularity can be avoided naturally since the value of failure probability can always be obtained from MCS. The accuracy and convergence of SRSM have been

illustrated in the previous chapter. Although SRSM usually requires more performance evaluation compared to FORM, it is still an affordable and applicable approach to obtain more accurate results for the highly nonlinear system.

RBDO with RIA

In this section, the RBDO problem of the torque arm model is solved using RIA. Stochastic response surface is used in uncertainty analysis to evaluate probability constraints. RBDO formulation of Eq. (4.2) can be used straightforwardly to solve the problem. For the torque-arm problem, the objective is to minimize the weight while meeting the requirement of reliability constraint. If we define that the structure fails when stresses in this structure reach yield stress, such that

$$G_i(\mathbf{x}) = \sigma_i(\mathbf{x}) - \sigma_y \le 0 \tag{4.15}$$

where **x** is the random input variables, $\sigma_i(\mathbf{x})$ is stress response for *i*th constraint, σ_y denotes yield stress.

The RBDO problem is then defined as

$$\begin{aligned} &\text{Minimize} && Mass(\mathbf{d}) \\ &\text{subject to} && P(G_i(\mathbf{x}) \le 0) \le \Phi(-\beta_{t_i}), \quad i = 1,\ldots,NC \\ &&& \mathbf{d}^L \le \mathbf{d} \le \mathbf{d}^U \end{aligned} \tag{4.16}$$

where β_t is the target reliability index and $\Phi(\ )$ is the cumulative density function of srv.

During the optimization, a $\beta_t = 3$ is used, which corresponds to 99.87% reliability. Since the maximum stress location can shift, the probabilities of failure at eight different locations are chosen as constraints in Eq. (4.16). The constraints can be evaluated using the SRS. The SRS needs to be reconstructed at each design cycle.

Table 4-3 shows the properties of the random variables and the lower and upper bounds of their mean values (design variables). Note that the design variables are the

relative change of the corner points and the initial values of all design variables are zero. The lower and upper bounds are chosen such that the topology of the boundary is maintained throughout the whole design process.

Table 4-3. Definition of random design variables and their bounds. The values of design variables at optimum design are shown in the 5th column (unit: centimeter).

Random Variables	$\mathbf{d}^L$	$\mathbf{d}$ (Initial)	$\mathbf{d}^U$	$\mathbf{d}^{opt}$ (optimum)	Standard Deviation	Distribution type
d_1	–3.0	0.0	1.0	-2.5226	0.1	Normal
d_2	–0.5	0.0	1.0	-0.4583	0.1	Normal
d_3	–1.0	0.0	1.0	-0.9978	0.1	Normal
d_4	–2.7	0.0	1.0	-2.4663	0.1	Normal
d_5	–5.5	0.0	1.0	-2.1598	0.1	Normal
d_6	–0.5	0.0	2.0	1.9274	0.1	Normal
d_7	–1.0	0.0	7.0	2.3701	0.1	Normal
d_8	–0.5	0.0	1.0	-0.0619	0.1	Normal

The design optimization problem is solved using the sequential linear programming technique. The optimization process converges after 14 design cycles and 27 performance evaluations where the relative convergence criterion has been met in two consecutive designs. The optimum values of the design variables are shown in the 5th column in Table 4-3. Figure 4-2 shows the optimum design and analysis results at the mean values. The major changes occur at design parameters d_4, d_5, d_6 and d_7. Even if the maximum stress constraint is set to 800MPa, the active constraint at optimum design converges to a lower value so that the variance of the input parameters can be accounted for. In Figure 4-2 the maximum value shows 739MPa, which is the extrapolated nodal stress. The actual element stress at the active constraint is about 618MPa, which is much lower than the extrapolate stress show on the figure. Figure 4-3 provides the optimization history of the cost function. As a result of the optimization process, the mass of the structure is reduced from 0.878kg to 0.497kg (a reduction of about 43.4 %).

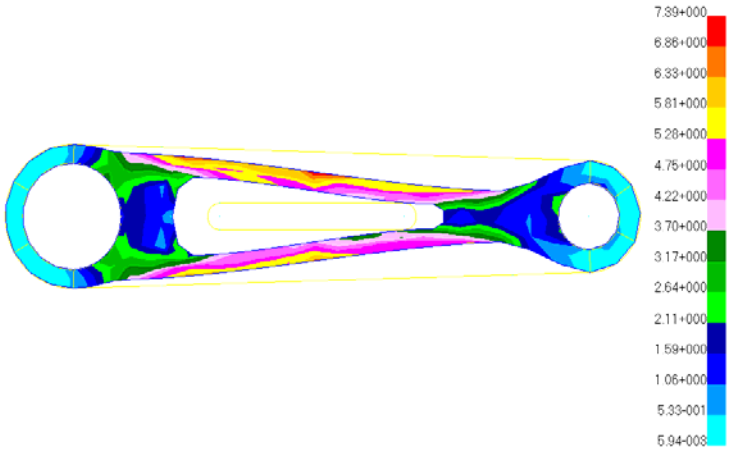

Figure 4-2. Optimum design and stress distribution of the torque arm model with 8 random variables.

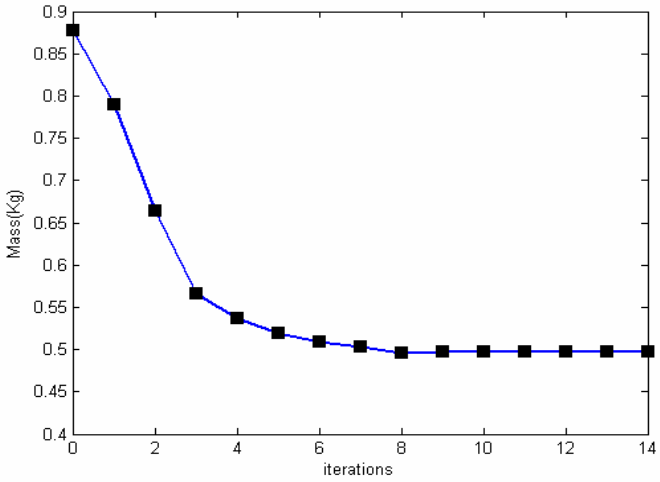

Figure 4-3. Optimization history of cost function (mass) for the torque arm model with 8 random variables.

In order to observe the impact of the accuracy of the uncertainty propagation procedure at the optimum design, a 3rd-order SRS is considered at the optimum design (Figure 4-4). Table 4-4 shows the values of the reliability indices for the active constraint at the optimum design obtained from MCS with100,000 samples, the proposed SRS approach, and the FORM. The MCS result is used as a reference mark to compare the other two methods, which has about 1.5% error in estimating reliability index with confidence level of 95%. The proposed SRS approach exhibits a lower error than the

corresponding to the FORM and compares very well with the exact result (namely, 3) and that obtained using MCS (0.6% error)

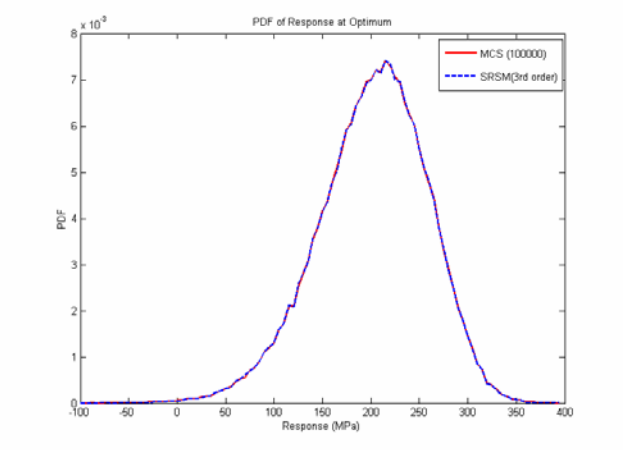

Figure 4-4. PDF of the performance function at the optimum for the torque-arm problem

Table 4-4. Reliability Index of active constraint at optimal design

	Reliability Index	Error (%)
MCS	3.0307	–
SRS	3.0115	0.633
FORM	2.9532	2.556

RBDO with Inverse Measure

As we discussed in section 3.2, enlightened by PMA, an inverse measure approach can also be applied in SRS based RBDO. In this section, the inverse measure approach is applied on reliability based design optimization for the torque arm model. As discussed in section 3.2, the design problem can be formulated as

$$\begin{aligned} &\text{Minimize} && Mass(\mathbf{d}) \\ &\text{subject to} && G_i(u^*) \geq 0, \quad i = 1,\ldots,NC \\ & && \mathbf{d}^L \leq \mathbf{d} \leq \mathbf{d}^U \end{aligned} \tag{4.17}$$

where G_i is the i-th constraint. If the total sample size of Monte-Carlo simulation for SRS is N and allowed maximum probability of failure is P_f, then G_i can be found by ordering samples and selecting pth smallest sample.

$$p = N \times P_f \tag{4.18}$$

Thus, the evaluation of reliability constraints is transformed to find the *p*th order statistic of sampling. One of the advantages of this approach is that the sensitivity of performance based constraint measure can be obtained directly through structure sensitivity analysis:

$$\frac{\partial G(u^*)}{\partial \theta} = \frac{\partial G(x^*)}{\partial \theta} = \frac{\partial G(x^*)}{\partial x_i} \frac{\partial T^{-1}(u^*; d)}{\partial \theta} \tag{4.19}$$

For example, if $\theta = \mu_i$, and $X \sim Normal(u_i, \sigma_i^2)$

$$\begin{aligned} \frac{\partial G(u^*)}{\partial \mu_i} &= \frac{\partial G(x^*)}{\partial \mu_i} = \frac{\partial G(x^*)}{\partial x_i} \frac{\partial T^{-1}(u^*; d)}{\partial \mu_i} \\ &= \frac{\partial G(x^*)}{\partial x_i} \end{aligned} \tag{4.20}$$

Summary

In this chapter, reliability based design optimization using stochastic response surface is discussed. Procedures for both RIA and PMA are investigated and formulated. A torque arm problem shown in Chapter 3 has been used to demonstrate the feasibility of RBDO using SRS.

Since accurate, sensitivity calculation is important to the convergence of gradient based optimizer, probability sensitivity using FORM and SRS is presented. It is shown that probability sensitivity in SRS based sampling approach can be also obtained with minimal increase of computational cost. If the SRS is accurate enough, the accuracy of sensitivities obtained also have convergent with respect to the increasing of the sampling size.

CHAPTER 5
GLOBAL SENSITIVITY ANALYSIS FOR EFFICIENT RBDO

Introduction

In industrial applications, a system usually involves considerable number of random variables. As stated in the previous two chapters, the increasing number of random variables boosts the computational cost of reliability analysis significantly. Structural reliability analysis which involves a computationally demanding model is limited by the relatively high number of required function analyses for uncertainty. Even if the local sensitivity information described in chapter 3 can reduce the number of required simulations, the dimension of the SRS will still increase according to the number of random variables. Design engineers want to reduce the number of variables based on their contribution to the output performance. However, it is challenging to identify the importance of a random variable in the process of uncertainty propagation. Those random variables with extremely low contribution to the performance variance can be filtered out to reduce the computational cost of uncertainty propagation.

Recent development in statistics introduces global sensitivity analysis (GSA)(Saltelli et al. 2000; Saltelli et al. 1999; Sobol 1993; Sobol 2001), which studies how the variance in the output of a computational model can be apportioned, qualitatively and quantitatively, to different sources of variations. In this chapter, global variance-based sensitivity analysis has been applied on structural model to illustrate different roles of random variables in uncertainty propagation. Effort has been made to reduce the dimension of random space in the RBDO process.

To reduce the number of simulations required to construct the SRS even further, unessential random variables are fixed during the construction of the SRS. A random variable is considered unessential (and hence it is fixed) if its contribution to the variance of the model output is below a given threshold. Global sensitivity indices considering only main factors are calculated to quantify the model input contributions to the output variability hence establishing which factors influence the model prediction the most so that: i) resources can be focused to reduce or account for uncertainty where it is most appropriate, or ii) unessential variables can be fixed without significantly affecting the output variability. The latter application is the one of interest in the context of this chapter.

The RBDO problem in the previous chapter was solved with all random variables. However, some random variables did not significantly contribute to the variance of the stress function. Thus, a large amount of computational cost can be saved if the random variables whose contribution to the variance of the output is small are considered as deterministic variables at their mean values. This section describes how the global sensitivity indices considering only main factors can be used for deciding unessential random variables during the construction of stochastic response surfaces.

Sensitivity Analysis

As defined by Saltelli(Saltelli et al. 2000), sensitivity analysis studies the relationships between information flowing in and out of the model. In engineering design application, sensitivity usually refers to the derivative of performance measure with respect the input design variable. This derivative is used directly in deterministic design as sensitivity information is required by the gradient-based optimizer. In this research, this derivative is called local sensitivity, which has been applied in constructing SRS in

the previous chapters. Local sensitivity analysis concentrates on the local impact of the design variables. It is carried out by computing partial derivatives of the output performance with respect to the input variable at the current design point. In structural optimization, substantial research has been done on the local sensitivity(Choi and Kim 2004a; Choi and Kim 2004b).

Another choice of sensitivity measure explores what happens to the performance variance if all design variables are allowed a finite variation. Global sensitivity techniques apportion the output uncertainty to the uncertainty in the input factors. A couple of techniques have been developed in recent two decades. In this research, Sobol's sensitivity indices(Sobol 1993; Sobol 2001), which is based on the decomposition of function into summands of increasing dimension, will be discussed and applied to the constraint evaluation of RBDO.

Variance-Based Global Sensitivity Analysis (GSA)

Variance-based methods are the most rigorous and theoretically sound approaches (Chen et al. 2005; Saltelli et al. 2000; Saltelli et al. 1999; Sobol 1993; Sobol 2001)for global sensitivity calculations. This section describes the fundamentals of the variance-based approach and illustrates how the polynomial chaos expansions are particularly suited for this task.

The variance based methods: (i) decompose the model output variance as the sum of partial variances, and then, (ii) establish the relative contribution of each random variable (global sensitivity indexes) to the model output variance. In order to accomplish step (i), the model output is decompose as a linear combination of functions of increasing dimensionality as described by the following expression:

$$f(\mathbf{x}) = a_0 + \sum_{i=1}^{n} a_i f_i(x_i) + \sum_{i=1}^{n}\sum_{j>i}^{n} a_{ij} f_{ij}(x_i, x_j) + \ldots + a_{12\ldots n} f_{12\ldots n}(x_1, x_2, \ldots, x_n) \quad (5.1)$$

subject to the restriction that the integral of the weighted product of any two different functions is zero. Formally,

$$\int \cdots \int p(\mathbf{x}) f_{i_1,\ldots,i_s}(x_{i_1},\ldots,x_{i_s}) f_{j_1,\ldots,j_s}(x_{j_1},\ldots,x_{j_s}) d\mathbf{x} = 0, \quad \text{for} \quad i_1,\ldots,i_s \neq j_1,\ldots,j_s \quad (5.2)$$

where p(x) is the joint PDF of input random variable x. If, for example, the weighting function is the uniform distribution for the random variables or the Gaussian probability distribution, the functions of interest can be shown to be Legendre and Hermite orthogonal polynomials, respectively.

The model output variance can now be calculated using a well-known result in statistics. The result establishes that the variance of the linear combination of random variables (U_i) can be expressed as:

$$V\left(b_0 + \sum_{i=1}^{n} b_i U_i\right) = \sum_{i=1}^{n} b_i^2 V(U_i) + 2\sum_{i=1}^{n}\sum_{j>i}^{n} COV(U_i, U_j) \quad (5.3)$$

Hence, the model output variance can be shown to be:

$$V(f) = \sum_{i=1}^{n} a_i^2 V(f_i) + \sum_{i=1}^{n}\sum_{j>i}^{n} a_{ij}^2 V(f_{ij}) + \ldots + a_{12\ldots n}^2 V(f_{12\ldots n}) \quad (5.4)$$

where the terms represent partial variances and each V(·) may be found by definition as:

$$V(f) = \int [\, f(x) - E(\, f(x))]^2 \, p(x)\, dx \quad (5.5)$$

In the above formula, $f(x)$ represents the function under consideration and the symbol E(·) denotes expected value. There are no covariance terms in Eq.(5.4) because of the orthogonality property shown in Eq.(5.2).

The global sensitivity index S_i that considers only main factor is called main sensitivity index, which associated with each of the random variables which is represented by Eq. (5.4):

$$S_i = \frac{{a_i}^2 V(f_i(x_i))}{V(f)} \tag{5.6}$$

A sensitivity index that considers the interaction of two or more factors is called interaction sensitivity index. Thus, as denoted by Chan and Saltelli(Saltelli et al. 2000), the summation of all sensitivity indices, involving both main and interaction effect of i-th random variable, is called total sensitivity index. Sobol(Sobol 2001) suggested to use total sensitivity indices to fix unessential variables. If total sensitivity index for certainty variable extremely small compare to 1, that means the contribution of the variable is neglectable and the variable can be considered as a deterministic one.

Global Sensitivity Analysis Using Polynomial Chaos Expansion

The polynomial chaos expansion is particularly suited for computing global sensitivity indices because: (1) The model output is already decomposed as a sum of functions of increasing dimensionality; (2) the functions are orthogonal with respect to the Gaussian measure (Hermite polynomials); and (3) the variance of the bases are analytically available. For example, the variances of the functions associated with a two dimensional chaos expansion of order 2 are shown in Table 5-1.

Table 5-1. Variances of the Hermite bases up to the second order

Function f	V(f)
X_1	1
X_2	1
${X_1}^2 - 1$	2
X_1X_2	1
${X_2}^2 - 1$	2

In addition, given the polynomial chaos expansion (i.e., the coefficients of the linear combination of Hermite polynomials), the model output variance and global sensitivity indices can be easily computed using Eqs. (5.4) and (5.6), respectively. In both

equations, the variances V(·), are readily available for polynomial chaos expansions of arbitrary order and number of variables.

In order to show the effect of the global sensitivity, let us consider the torque arm model presented in chapter 3. The eight random design variables are normally distributed with standard deviation of 0.1. A cubic stochastic response surface with eight variables in standard normal space has been constructed to approximate the stress response. Global sensitivity indices for main factor have been calculated to quantify the contribution of each random variable to performance variability. Figure 5-1 shows that three design variables(x_2,x_6,x_8) makes most contribution to the total variance, influences from other variables are extremely small. That means, at the initial design, that the randomness of those variables with low global sensitivity indices can be ignorable. If only three variables are considered in constructing SRS instead of eight, the computational cost will be saved significantly, while maintaining the same level of variability.

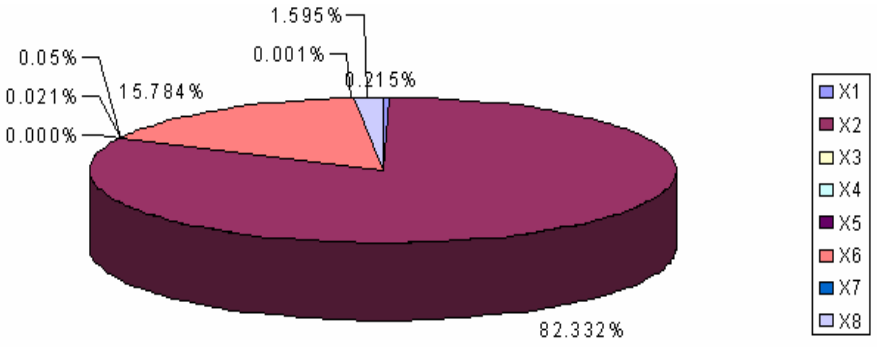

Figure 5-1. Global sensitivity indices for torque arm model at initial design

Adaptive Reduction of Random Design Space Using GSA in RBDO

The idea of adaptive reduction of random variables is based on the main factor of each random variable. If it is smaller than a threshold, it is fixed in constructing SRS. For

that purpose, a linear polynomial chaos expansion is enough to obtain the main factors of GSI. The current algorithm with linear polynomial chaos expansion for the reduction of random variables can be modified to use a sensitivity index that accounts for interactions. These interactions will only appear in higher order polynomial chaos expansions. The choice of a non-linear polynomial chaos expansion would reduce the computational efficiency of the proposed approach with unclear significant advantages.

As stated at the beginning of this section, once the global sensitivity indices are calculated, variables that have the least influence on the model prediction (unessential variables) can be identified and eventually held fixed without significantly affecting the output variability. The procedure is adaptive because the global sensitivity indices are calculated at each design iteration and as a result different sets of random variables may be fixed throughout the RBDO process. A flow chart of RBDO using this strategy is shown in Figure 5-2.

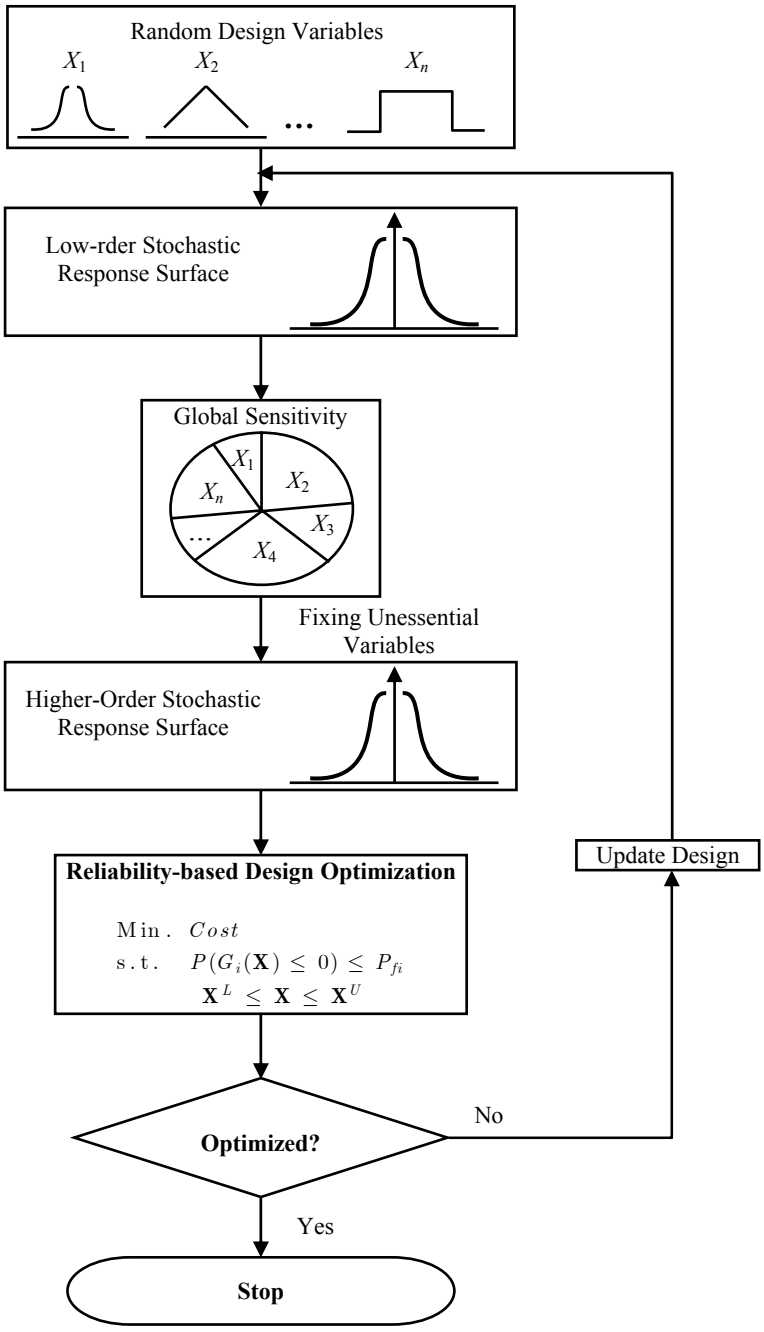

Figure 5-2. Adaptive reduction of unessential random design variables using global sensitivity indices in RBDO. Low-order SRS is used for global sensitivity analysis, while a high-order SRS is used to evaluate the reliability of the system.

At the initial design stage, a lower-order stochastic response surface is constructed using all random variables. In this particular example the first-order SRS is constructed using 17 sampling points. At the initial design, the first-order SRS with eight random variables can be expressed as,

$$\begin{aligned} G^1 &= a_0 + a_1u_1 + a_2u_2 + a_3u_3 + a_4u_4 + a_5u_5 + a_6u_6 + a_7u_7 + a_8u_8 \\ &= 4.95 + 0.0063u_1 + 0.117u_2 + 0.00008u_3 - 0.0019u_4 \\ &\quad +0.0026u_5 - 0.052u_6 - 0.0002u_7 - 0.016u_8 \end{aligned} \tag{5.7}$$

One useful aspect of the polynomial chaos expansion is that the coefficients in Eq. (5.7) are a measure of the contribution of the corresponding random variable to the variation of the output, and these coefficients will not change significantly in higher-order SRS. On the other hand, typically the global sensitivity index associated with a particular variable is responsible for most of its contribution to the output variance. Thus, evaluating the global sensitivity indices using the first-order SRS can be justified. Since all random variables are transformed into standard normal random variables, the variance of G^1 can be evaluated analytically. Using Eq. (5.6) and (5.7) and assuming the design variables are independent, the global sensitivity index can be calculated as:

$$S_i = \frac{a_i^2}{\sum_{j=1}^{n} a_j^2} \tag{5.8}$$

Note that the denominator in Eq. (5.8) is the total variance of G^1 using the first-order approximation. Thus, the global sensitivity index, S_i, is the ratio of the contribution of i-th random variable to the total variance. If the global sensitivity index of a specific variable is less than a threshold value, the variable is considered as deterministic and fixed at its mean value.

In order to show the advantage of fixing unessential random variables, the global sensitivity indices of the torque-arm model are calculated. Table 5-2 shows the global sensitivity indices of the torque-arm model using the first-order SRS at the initial design. The total variance of stress function is 1.670×10^{-2}. Based on the global sensitivity indices, there are only three random variables whose contribution is greater than 1.0%; i.e., u_2, u_6, and u_8. Thus in the reliability analysis, only these three random variables are used in constructing the third-order SRS, which now requires only 19 sampling points for 10 unknown coefficients. All other random variables are considered as deterministic variables at their mean values. If the total number of sampling points for both lower- (17) and higher-order (19) polynomial expansions are compared with the higher-order SRS using all random variables (89), a significant reduction of the number of sampling points was achieved.

Table 5-2. Global sensitivity indices considering only main factors for the torque arm model at the initial design. Only three random variables (u_2, u_6, and u_8) are preserved when a threshold value of 1.0% is in place.

SRV	Variance	GSI (%)
u_1	3.916×10^{-5}	0.235
u_2	1.369×10^{-2}	**82.0**
u_3	6.403×10^{-9}	0.00003834
u_4	3.667×10^{-6}	0.02197
u_5	6.864×10^{-6}	0.04109
u_6	2.702×10^{-3}	**16.179**
u_7	4.818×10^{-8}	0.0002885
u_8	2.538×10^{-4}	**1.519**

The RBDO problem, defined in Eq.(5.2) in chapter 4 is now solved using the proposed adaptive reduction of random variables. The optimization algorithm converges after the 17-th iteration. As shown in Figure 5-3, the optimum design using the adaptively reduced SRS is slightly different from that with all random variables in chapter 4. The

former has a longer interior cutout than the latter. This can be explained from the fact that the model with reduced random variables has less variability than the full model. Furthermore, the optimum value achieved using the adaptively reduced SRS converges to a lower value than the one without adaptive reduction). The total mass of the torque arm is reduced by 54.8%. The difference between the two approaches is approximately 1.8%.

The number of active random variables associated with the modeling of the first constraint during the design iterations are listed in Table 5-3. On average, four random variables were preserved, which implies that only 29 sampling points were required for constructing the SRS. This is three times less than the SRS approach without adaptive reduction (89 sampling points).

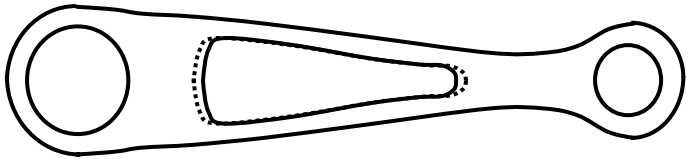

Figure 5-3. Optimum designs for the full SRS (solid line) and adaptively reduced SRS (dotted line). Because some variables are fixed, the interior cutout of the design from the adaptively reduced SRS is larger than that from the full SRS.

Table 5-3. Comparison of the number of random variables in each design cycle. The threshold of 1.0% is used. The first constraint is listed.

Iter	Full SRS	Reduced SRS
1	8	3
2	8	3
3	8	3
4	8	3
5	8	4
6	8	4
7	8	5
8	8	4
⋮	⋮	⋮
17	8	4
⋮	⋮	⋮

Summary

In this chapter, a dimension reduction technique using global sensitivity indices is introduced. Since the variances of the Hermite polynomial bases are analytically available, the SRS is suitable to compute global sensitivity indices. Its application to RBDO is also presented. In the RBDO procedure, the global sensitivity indices that are calculated using the lower-order SRS are used to fix unessential random variables, a higher-order SRS with reduced dimension is then used in evaluating the probability constraint. Fixing the unessential random variables accelerates the design optimization process. The RBDO result obtained in this way is compared to that from previous chapter, which shows little difference because of the loss of variability in fixing random variables.

CHAPTER 6
FATIGUE RELIABILITY-BASED LOAD TOLERANCE DESIGN

Introduction

Traditional reliability-based structural design usually makes assumptions on randomness of factors involved in modeling a structural system such as design variables, material properties, etc. These parameters are relatively well controlled so that the variability is usually small. However, it is also important to consider the capacity of the system subject to working conditions, e.g., uncertain loadings, because the uncertainty in load or force is much larger than that of others. The variability of the load is often ignored in the design stage and is difficulty to quantify it. Without knowing the accurate uncertainty characteristics of input load, it is hard to rely on the reliability of the output. In this chapter, a different approach from the traditional RBDO is taken by asking how much load a system can support. The amount of load, which a structural system can support, becomes an important information for evaluating a design.

As an illustration, the fatigue reliability-based load tolerance of the front loader frame of CAT 994D wheel loader is studied. Besides the uncertainty in the material properties, which can be incorporated in S-N curve(Ayyub et al. 2002; Chopra and Shack), uncertainties are also investigated on both mean and amplitude of a given dynamic load. Either the variation of load amplitude or mean may affect the fatigue life of the structural system. This research presents a reliability based load design method, which provides the load envelope for a structure subject to fatigue failure mode. Both one dimensional and multidimensional problems are addressed.

Since service loads are subjective such that the load characteristic of one operator may completely different from that of others. In order to perform reliability analysis, it is necessary to know uncertainty characteristics of inputs. However, distribution type and parameters of loads are often unknown. In this chapter, instead of modeling variability in parameters by assuming specific type of random distribution, the effect of different distribution types on the system response is investigated by introducing the concept of conservative distribution type, which provides a safer way to model uncertainties.

Fatigue Life Prediction

Recent developments in the computer-aided analysis provide a reasonable simulation for fatigue life prediction at early design stage for components under complex dynamic loads. For most automotive components, fatigue analysis means to find crack initiation fatigue life. Figure 6-1 illustrates the procedure to the crack initiation fatigue life prediction.

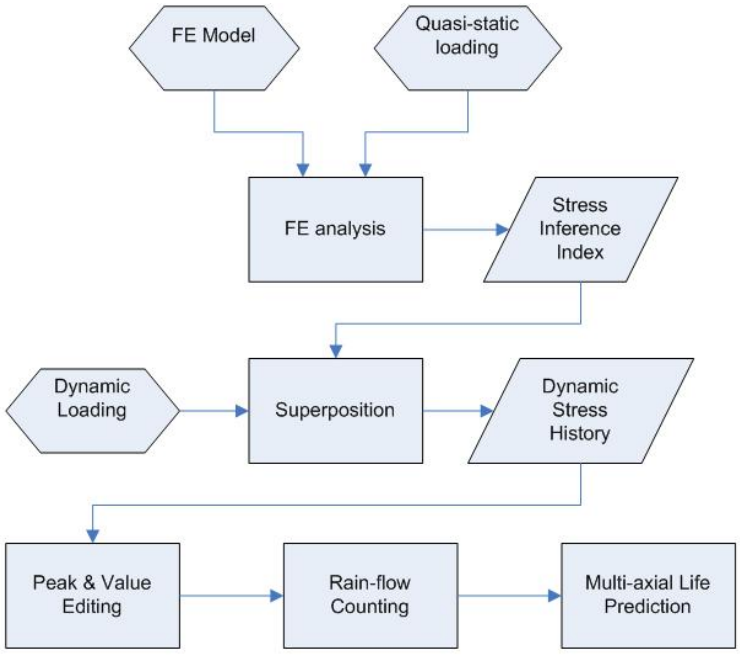

Figure 6-1. Flow chart for fatigue life prediction

Crack Initiation Fatigue Life Prediction

Two major crack initiation fatigue life prediction methods are stress-based and strain-based methods. The stress-life ($S-N$) approach employs relationship between the stress amplitude and the fatigue life. This method is based primarily on linear elastic stress analysis. The advantage of stress-life approach is apparent since changes in material and geometry can easily be evaluated and large empirical database for steel with standard notch shape is available. However, the effects of plasticity are not considered in this method. The local strain-life($\varepsilon-N$) method assumes that the local strains control the fatigue behavior. The plastic effects are considered well in this method. It is similar to the stress-life approach in that it uses $\varepsilon-N$ curve instead of $S-N$ curve, but differs in that the strain is the variable related to the life, and also in that plastic deformation effects are specifically considered.

Machine parts are usually required to be durable and able to undertake high numbers of life cycles. The front loader frame of CAT 994D wheel loader is one of such case. The critical position of fatigue failure is usually at welding joints. Because the stress-life method is works well for the brittle material and provides a reasonable approximation for a high cycle fatigue crack initiation life, by taking advantage of the availability of a large amount of available uniaxial fatigue data, stress-life method is employed in this chapter.

Since the crack is usually initiated along the component surface, for saving unnecessary computation, FE based fatigue analysis chooses element along surface to calculate the fatigue life. For multi-axial application, the principal stress method has been applied using the planes perpendicular to the surface. Fatigue lives are calculated on eighteen planes spaced at 10 degree increment. On each plane the principal stresses are

used to calculate the time history of the stress normal to the plane. It has been shown that this method should only be used for fatigue analysis of 'brittle' metals like cast iron and very high strength steels, as it provides nonconservative results for most ductile metals. Based on the factor that material in our application is cast iron and the interested region is welding joints, the principal stress algorithm can offer the fatigue life calculation with reasonable accuracy. Using superposition of dynamic loadings and the quasi-static FE analysis, the dynamic stresses in the component are used to analyze multi-axial fatigue, based on principal stress using conventional *S-N* curve(Fe-safe 2004).

Most basic fatigue data are collected in the laboratory by testing procedures which employ fully reversed loading. However, realistic service loading usually involves nonzero mean stresses. Therefore, the influence of mean stress on fatigue life should be considered so that the fully reversed laboratory data can be used in the evaluation of real service life.

Since the tests required to determine the influence of mean stress are quite expensive, several empirical relationships which related alternating stress amplitude to mean stress have been developed. Among the proposed relationships, two are widely used, which are Goodman and Gerber models.

Goodman: $(S_a / S_e) + (S_m / S_u) = 1$

Gerber: $(S_a / S_e) + (S_m / S_u)^2 = 1$

where S_a : Alternating stress amplitude; S_e : Endurance stress limit

S_m : Mean stress; S_u : Ultimate strength

Experience shows that test data tend to fall between the Goodman and Gerber curves. In the application of fatigue life prediction of front loader frame of CAT 994D, Goodman relation is applied to address the mean stress effect.

Variable Amplitude Loading and Cumulative Damage

In real application, components are usually subject to complex dynamic loading which has variable amplitude. It requires identifying cycles and assessing fatigue life for each cycle. The rain-flow counting method(Matsuishi and Endo 1968) is the most commonly used cycle counting technique. This method defined cycles as closed stress-strain hysteretic loops as shown in the figure below:

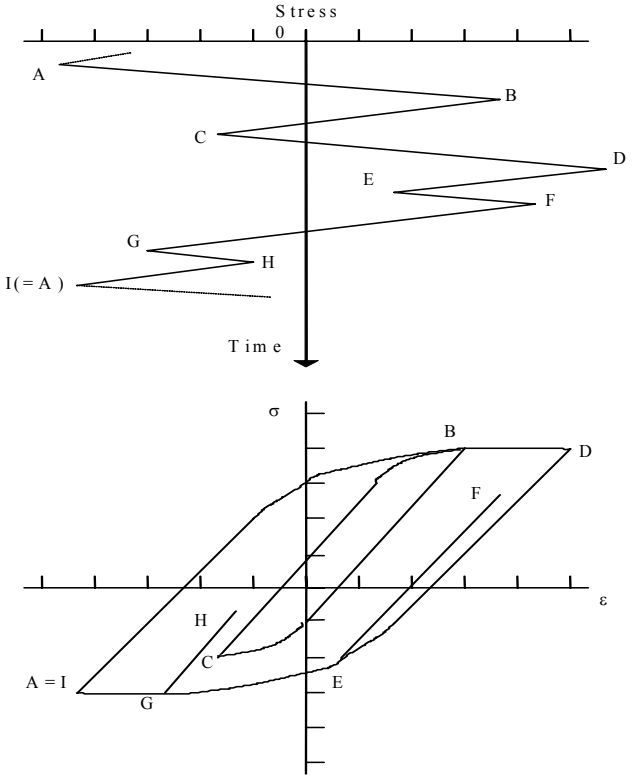

Figure 6-2. Rain-flow and hysteresis

An algorithm of rain-flow counting can be developed based on ASTM standard description. Although the rain-flow counting method is not based on an exact physical concept to account for fatigue damage accumulation, it is expected to provide a more realistic representation of the loading history.

Cumulative damage of each cycle can be obtained by the Palmgren-Miner hypothesis, which is referred to as the linear damage rule:

$$D_i = \sum_{j=1}^{n} \frac{n_j}{N_j} \tag{6.1}$$

in *i*-th cycle. In Eq. (6.1), D_i is the fraction of the damage; n_j is the counted number of cycles for *j*-th stress range; N_j is the cycles to fail; and *n* is the total number of stress ranges counted from rain flow. Failure is predicted to occur if

$$\sum_{i=1}^{N} D_i \geq 1 \tag{6.2}$$

where *N* is the number of cycles.

Thus, the fatigue life can be calculated as the number of applied load cycle until the cumulative damage reaches 1:

$$Life\ cycles = \frac{1}{\sum_{i=1}^{N} D_i} \tag{6.3}$$

Model Preparation for Fatigue Reliability Analysis

Finite Element Model

Figure 6-3 shows the component of a front loader frame of CAT 994D wheel loader, which is subjected to 26 channels of dynamic loading. As show in Figure 6-4, the finite element model consists of 49,313 grid points and 172,533 elements (24 beam, 280 gap, 952 hexagon, 1016 pentagon, 226 quadrilateral, 160,688 tetrahedron, 9,144 triangular, 203 rigid body elements). In order to apply for the displacement boundary

conditions and loads, pins are modeled using beam and gap elements. The existence of gap elements makes the problem nonlinear. However, if the gap status does not change during analysis, we can still consider the problem to be linear.

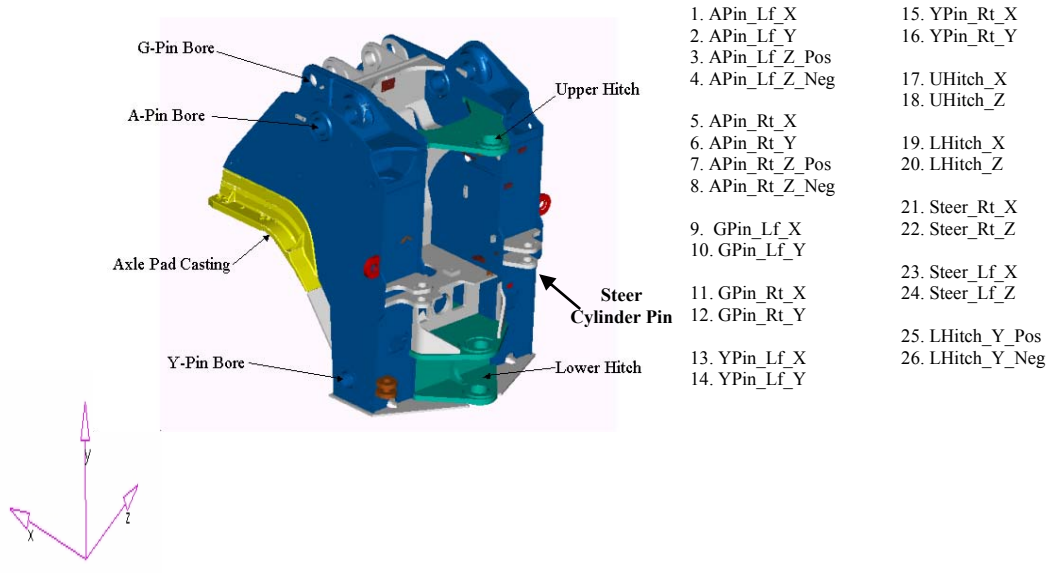

Figure 6-3. Front loader frame of CAT 994D wheel loader (subject to 26 channels of dynamic loading)

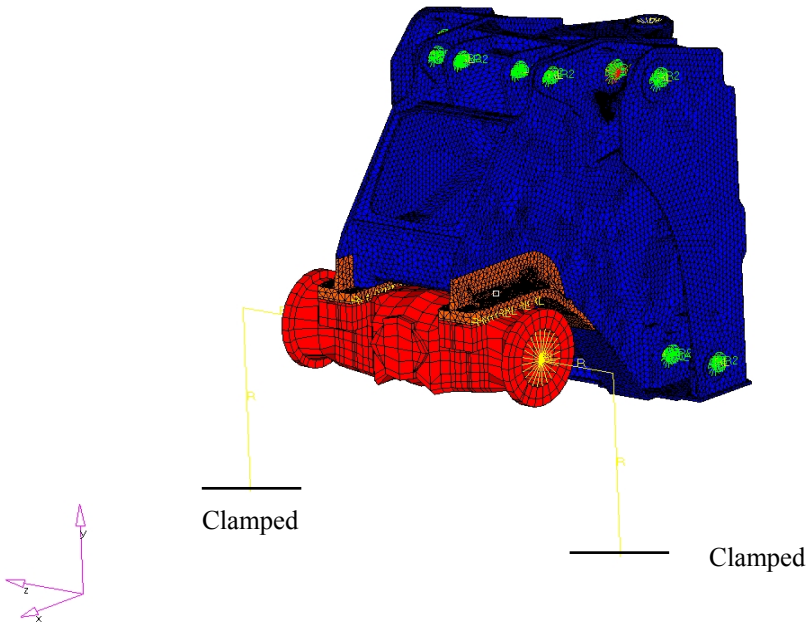

Figure 6-4. Finite element model for front frame

Dynamic Load History

In Figure 6-3, a total of 26 degrees-of-freedom are chosen for the application of dynamic loads. All loads are located in the center of the pins and the hitches. Even if the dynamic load $f(t)$ is applied to the system, it is assumed that the inertia is relatively small and the method of superposition can be applied. Thus, only a linear static analysis is enough with the unit load applied to each degree-of-freedom. The stress value from the unit load is called the stress influence coefficient. The dynamic stress can be obtained by multiplying these stress influence coefficients with the dynamic load history. Measured data of 26 channels are used for the dynamic loads with the duration of 46 minutes. This duration is defined as a working cycle. The dynamic load is sampled such that 9,383 data points are available for each channel.

Uncertainty in Material Properties and *S-N* Curve Interpolation

Based on available material properties and the component's working conditions, principle stress analysis using the Goodman model is used as the algorithm for fatigue life prediction. From superposition of quasi-static linear finite element analysis and dynamic loading, the stress data are obtained for each element. These stresses can be regard as 'true stress', which means *S-N* curve can be applied directly on principle stress life method without considering the stress concentrate factor. The *S-N* curve can be interpolated from nominal stress-life data. Considering the uncertainties of material properties, this interpolation will be implemented in a random manner. A lognormal distribution in S-N curve can be assumed to simplify the randomness. Although there is no rigorous statistical evaluation was performed, but this assumption seems reasonable empirically(Ayyub et al. 2002; Chopra and Shack).

Figure 6-5 shows the *S-N* curve obtained from stress- life data for cast iron used in the front frame. Solid line is the nominal S-N curve and two dashed lines represent the variation in S-N curve.

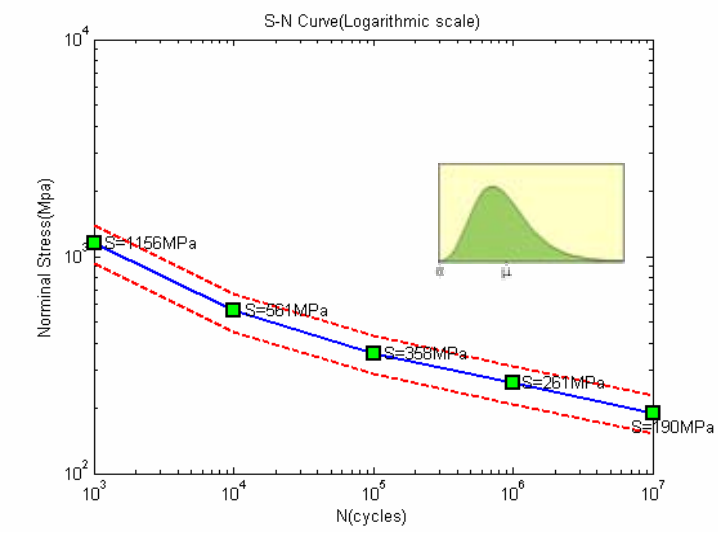

Figure 6-5. Material *S-N* curve with uncertainty

Uncertainty Modeling of Dynamic Loadings

Dynamic loadings are usually very complicated and may involve a lot of uncertainties. Figure 6-6 shows one channel of the dynamic load. The mean and amplitude of dynamic loading usually plays the most important role in fatigue life estimation. Therefore, for the purpose of illustration and simplification, uncertainties can be model based on these two quantities.

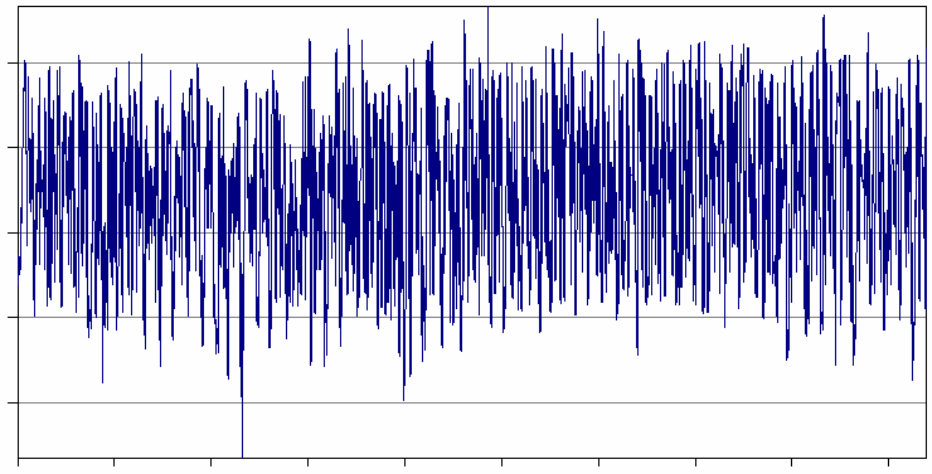

Figure 6-6. Illustration of one channel of dynamic loads

By combining the effects of the randomness of mean and amplitude of the loads, two load capacity coefficients α and γ are defined for the mean and amplitude, respectively. The dynamic load can be parameterized as

$$f(t) = \alpha f_{mean} + \gamma (f_0(t) - f_{mean}) \tag{6.4}$$

where α , γ are random parameters to describe the uncertainties of the loads called load capacity coefficient (LCC). In Eq. (6.4), $f_0(t)$ is the original dynamic loads and f_{mean} is the mean value of the initial loads. Due to the random parameters, the dynamic load $f(t)$ shows probabilistic behavior. Equation (6.4) provides a simple two dimensional model of

uncertainty in dynamic load history. Note that when both α and γ equal to one and fixed, the original deterministic loading history $f_0(t)$ is recovered. In the following section, one-dimensional problem will first be investigated by fixing one of them. For example, if we fix α at 1 and treat γ as a random variable, then uncertainty is modeled for the amplitude of the load.

Linear Estimation of Load Tolerance

The major challenge of the research is to estimate the load tolerance with respect to the reliability of fatigue life performance, which depends on the load history and uncertainty characterization. Identifying the load distribution is one of the most difficult tasks in the uncertainty analysis because different operating conditions will yield completely different distribution types. At this point, it is assumed that the load has a specific uncertainty characteristic (distribution type and corresponding parameters). When the variance of the load is fixed, for example, it is possible to construct the safety envelope by gradually changing the mean value of the applied load, which requires a large number of reliability analyses. When nonlinearity of the system is small, it is possible to estimate the safety envelope using the sensitivity information at the current load without requiring further reliability analyses. This estimation is based on the first-order Taylor series expansion method. For illustration, one-dimensional models (only considering single random variable) for the effect of amplitude and mean are separately investigated to meet the reliability requirement of fatigue life under uncertainty. In these one dimensional cases, the variation in S-N curve is ignored.

Variability of Dynamic Load Amplitude

In order to consider the variability of the dynamic load, the mean value of the load is first assumed to remain constant, while the amplitude of the load is varied randomly. From Eq. (6.4), the uncertainty caused by the amplitude can be represented using the following decomposition of the dynamic load:

$$f(t) = f_{mean} + \gamma(f_0(t) - f_{\text{mean}}) \tag{6.5}$$

When $\gamma = 1$, the original load history is recovered. When $\gamma = 0$, the dynamic load becomes a static load with the mean value. In this definition, γ cannot take a negative value.

Since γ is a random variable, it is necessary to assume the distribution type and distribution parameters for γ. First we assume that γ is normally distributed with the mean of one and the standard deviation of 0.25 (COV=0.25). The standard deviation is estimated from the initial dynamic load history. Since the first-order reliability analysis is performed using the standard random variable, we convert γ into the standard random variable u by

$$\begin{aligned} \gamma &= \mu + \sigma u \\ &= 1 + 0.25u \end{aligned} \tag{6.6}$$

where $u \sim N(0,1^2)$, $\gamma \sim N(1,0.25^2)$, μ = mean, σ = standard deviation.

For any given sample point u corresponding γ can be obtained from Eq. (6.6), and using γ a new dynamic load history can be obtained from Eq. (6.5). By applying this dynamic load history, we can calculate the fatigue life of the system. Since this procedure includes multiple steps, we can construct a (stochastic) response surface for the fatigue life and then perform the reliability analysis using the response surface.

Since the fatigue life changes in several orders of magnitudes, it would be better to construct the response surface for the logarithmic fatigue life. In one dimensional case, five collocation points are available from the DOE introduced in chapter 3. Using these five sampling points, a cubic stochastic response surface is constructed as a surrogate model for the logarithmic fatigue life as

$$L(\gamma) \equiv Log_{10}(Life) = 5.7075 - 0.7223u - 0.0581(u^2 - 1) + 0.0756(u^3 - 3u) \quad (6.7)$$

Note that in one dimensional case, the five collocation points available from previous DOE scheme are sometimes not enough to construct a high fidelity SRS, a couple of complementary sampling points can be chosen to construct a new SRS, which spread evenly between the original collocation points, i.e., four more point in the middle of intervals of the original five points have been chosen. The corresponding SRS logarithmic fatigue life becomes

$$L(\gamma) \equiv Log_{10}(Life) = 5.6976 - 0.6826u - 0.0541(u^2 - 1) + 0.0617(u^3 - 3u) \quad (6.8)$$

Various quantities for estimating the quality of SRS are shown in Table 6-1 for both five and nine sampling points scheme. The table shows nine points DOE schemes fit the data better based on significant improvement of PRESS (prediction error sum of squares). Table 6-2 lists the t-statistics for the evaluation of each coefficient in the above response surface. Although using more sampling points can increase the fidelity of estimation, it also increases the computational cost. In our specific problem, considering the saving of computation, the five sampling DOE scheme is sufficient.

Table 6-1. Quality of response surface

Error statistics	RMSE	SSe	R^2	R^2_{adj}	PRESS
5 sampling DOE	0.0406	0.0082	0.9980	0.9921	8.5671
9 sampling DOE	0.0511	0.0235	0.9965	0.9943	0.1503

Table 6-2. T-statistic of the coefficients

coefficient	1	2	3	4
t-statistics of 5 sampling DOE	122.7590	15.9279	3.5759	4.0828
t-statistics of 9 sampling DOE	229.1431	33.9519	4.9313	6.4894

The response surface in Eq. (6.7) shows that the mean of logarithmic fatigue life is 5.6976 and the standard deviation is about 0.6826. It also shows that the contribution of the higher-order terms is relatively small, compared with the constant and linear terms. Thus, we can conclude that the performance is mildly nonlinear with respect to the random variable.

Since the required life of the working component is 60,000 hours and each cycle corresponding to 46 minutes, the target of the fatigue life can be written in the logarithmic scale by

$$\begin{aligned} L_{\text{target}} &= Log_{10}(60,000 \text{ hours}) \\ &= Log_{10}(78,261 \text{ cycles}) . \\ &\approx 4.9 \end{aligned} \tag{6.9}$$

The system is considered to be failure when the predicted life from Eq. (6.7) is less than the target life in Eq. (6.9). Accordingly, we can define the probability of failure as

$$P_f[L(\alpha) - L_{\text{target}} \le 0] \le P_{\text{target}} , \tag{6.10}$$

where P_{target} is the target probability of failure. For example, when $P_{\text{target}} = 0.1$, the probability of failure should be less than 10%. Even though the interpretation of Eq. (6.10) is clear, it is often inconvenient because the probability changes in several orders of magnitudes. In reliability analysis, it is common to use the reliability index, which uses the notion of the standard random variable. Equation (6.10) can be rewritten in terms of the reliability index as

$$P_f \equiv \Phi(-\beta) \quad \leq \quad P_{\text{target}} \equiv \Phi(-\beta_{\text{target}}), \tag{6.11}$$

where β is called the reliability index and Φ is the cumulative distribution function of the standard random variable. When $P_{\text{target}} = 0.1$, $\beta_{\text{target}} \approx 1.3$. The advantage of using the reliability index will be clear in the following numerical results.

With the response surface in Eq. (6.7), reliability analysis is carried out using the first-order reliability method (FORM) at $\mu_\gamma = 1$. The results of reliability analysis are as follows:

$$\begin{aligned} P_f &= 17.81\% \\ \beta &= 0.922456 \\ \frac{\partial \beta}{\partial \mu_\gamma} &= -3.972 \end{aligned} \tag{6.12}$$

where $\partial\beta/\partial\mu_\gamma$ is the sensitivity of the reliability index with respect to the mean value of γ. Since $P_{\text{target}} = 0.1$ and $\beta_{\text{target}} = 1.3$, the current system does not satisfy the reliability requirement.

From the mild nonlinear property of the response, we can estimate the mean value of γ that can satisfy the required reliability. The linear approximation of the mean value can be obtained from

$$\mu_{\gamma estimate} = 1 - (\beta_{\mu_\gamma = 1} - \beta_{target}) / \frac{\partial \beta_{\mu_\gamma = 1}}{\partial \mu_\gamma} = 0.9049, \tag{6.13}$$

which means that the mean value of γ needs to be decreased about 10% from the original load amplitude in order to satisfy the required reliability.

In order to verify the accuracy of the estimated result, several sampling points are taken and reliability analyses are performed. Figure 6-7 shows the reliability index with respect to μ_γ, while Figure 6-8 shows the probability of failure P_f with respect to μ_γ. The solid line is linearly approximated reliability using sensitivity information. The reliability

index is almost linear and the estimation using sensitivity is close to the actual reliability index. When the target probability of failure is 0.1 and γ has the distribution of $N(\mu_\gamma, 0.25^2)$, the safety envelope can be defined as

$$0 \le \mu_\gamma \le 0.9049 . \tag{6.14}$$

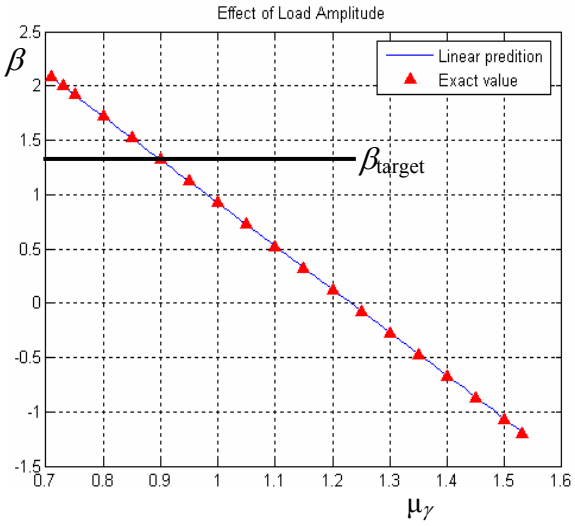

Figure 6-7. Reliability index β with respect to random parameter μ_γ

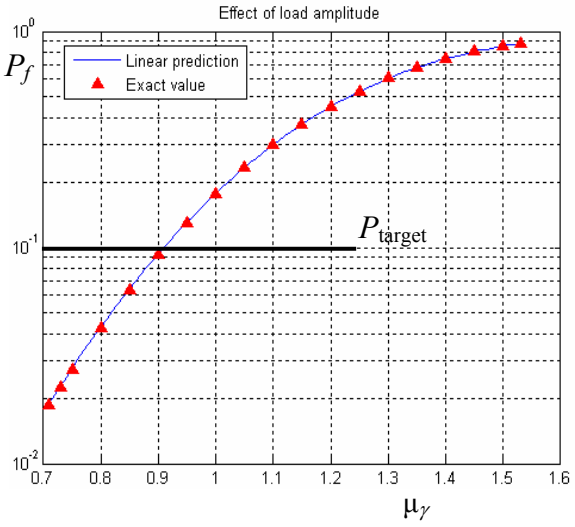

Figure 6-8. Probability of failure P_f with respect to random parameter μ_γ

The result means that current design, considering 25% standard deviation in the load amplitude, is not enough to achieve 90% reliability. The structure should work under

milder working condition, which means either lower the mean of the load amplitude by about 10% or provide more accurate estimation of the initial load to reduce the variance.

Variability of Mean of Dynamic Load

Since both mean and amplitude are used to describe the dynamic load history, both of their effects under uncertainty are studied separately. When the mean value of the load is assumed to be varied randomly and the load amplitude remains as the initial load, the uncertainty in load can be modeled as:

$$f(t) = \alpha f_{mean} + (f_0(t) - f_{mean}) \tag{6.15}$$

Same as the case of load amplitude, when $\alpha = 1$, the applied load is identical to the original load history. When $\alpha = 0$, the applied load has the same amplitude with the original load history but the mean value is zero. In this definition, α can be a negative value.

Since α is a random variable, it is necessary to assume the distribution type and distribution parameters for α. First we assume that α is normally distributed with the mean of one and the standard deviation of 0.25 (COV=0.25). Since the first-order reliability analysis is performed using the standard random variable, we convert α into the standard random variable u by

$$\begin{aligned} \alpha &= \mu + \sigma u \\ &= 1 + 0.25u \end{aligned}, \tag{6.16}$$

where $u \sim N(0,1^2)$, $\alpha \sim N(1,0.25^2)$, μ = mean, σ = standard deviation.

By following the same procedure with previous section, using nine sampling points, we can construct a cubic stochastic response surface as a surrogate model for the logarithmic fatigue life as

$$L(\alpha) \equiv Log_{10}(Life) = 5.6906 - 0.0905u - 0.0013(u^2 - 1) - 0.0003(u^3 - 3u). \tag{6.17}$$

If we compare the response surface in Eq. (6.17) with the case of amplitude change in Eq.(6.7), the mean values of the both cases are close but the standard deviations are quite different. From this result, we can conclude that the variance of the mean value does not contribute significantly to the variance of the fatigue life.

Using the response surface in Eq. (6.17), reliability analysis is carried out using the first-order reliability method (FORM) at $\mu_\alpha = 1$. The results of reliability analysis are as follows:

$$\begin{aligned} P_f &\approx 10^{-8} \\ \beta &= 6.3435 \\ \frac{\partial \beta}{\partial \mu_\alpha} &= -4.012 \end{aligned} \tag{6.18}$$

Since $P_{\text{target}} = 0.1$ and $\beta_{\text{target}} = 1.3$, the current system satisfies the reliability requirement. The linear approximation of the mean value can be obtained from

$$\mu_{\alpha estimate} = 1 - (\beta_{\mu_\alpha = 1} - \beta_{\text{target}}) / \frac{\partial \beta_{\mu_\alpha = 1}}{\partial \mu_\alpha} = 2.257, \tag{6.19}$$

which means that the system satisfies the reliability requirement even if the mean value of α is increased up to 225% from the original load. This observation is consistent with the conventional notion of fatigue analysis in which the effect of the amplitude is significant while that of the mean is not.

In order to verify the accuracy of the estimated result, several sampling points are taken and reliability analyses are performed. Figure 6-9 shows the reliability index with respect to μ_α, while Figure 6-10 shows the probability of failure P_f with respect to μ_α. The solid line is linearly approximated reliability using sensitivity information. The reliability index is almost linear and the estimation using sensitivity is close to the actual

reliability index. When the target probability of failure is 0.1 and α has the distribution of N(μ_α,0.25^2), the safety envelope can be defined as

$$0 \le \mu_\alpha \le 2.257 . \tag{6.20}$$

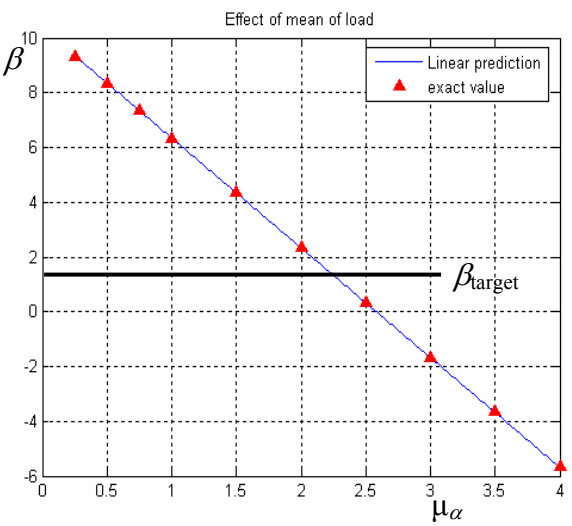

Figure 6-9. Reliability index β with respect to random parameter μ_α

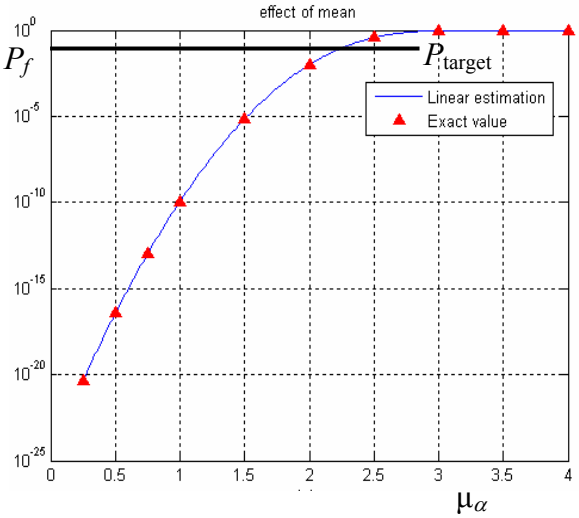

Figure 6-10. Probability of failure P_f with respect to random parameter μ_α

Safety Envelope Concept for Load Tolerance Design

The safety envelope is defined as the magnitudes of the input design variables when the system fails. When design variables are loads, it is called the load envelope. In one dimensional case, this is simply the range of the allowed loads, e.g., the range of

mean value of α or γ in the previous section. In multi-dimensional case, the combination of various loads constitutes an envelope, which is convex in linear systems. Such information is very useful as a capacity of the current design, a future reference for design upgrade, maintenance and control. Figure 6-11 shows a schematic illustration of the safety envelope when two variables are involved. In such a complex situation, a systematic way of searching the boundary of the safety envelope needs to be developed.

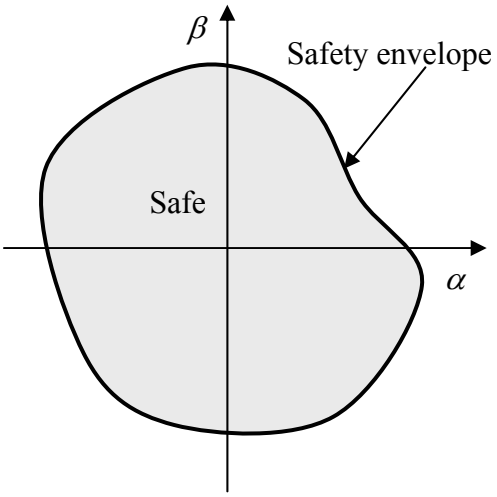

Figure 6-11. Safety envelope for two variables

When the relationship between the safety of the system and the applied loads is linear or mildly nonlinear, linear approximation can produce a very effective way of estimating the safety envelope.

In context of reliability based safety measure, the target of safety envelope is that failure probability cannot reach over the prescribed value.

Numerical Path Following Algorithm

According to the reliability based safety envelope concept introduced above, when target reliability has been specified, a safety envelope can be constructed using numerical path following algorithm to search the boundary of the safety envelope(Allgower and

Georg 1990). In this research, a systematic way of searching the boundary of the safety envelope is proposed using a predictor–corrector method, which is similar to the Euler–Newton continuation method(Allgower and Georg 1990; Kwak and Kim 2002). When the relationship between the safety of the structure and the applied loads is linear or mildly nonlinear, this approach can produce an efficient way of estimating the safety envelope. In the context of reliability–based safety measure, the boundary of the safety envelope is the location where the probability of failure is equal to the target probability.

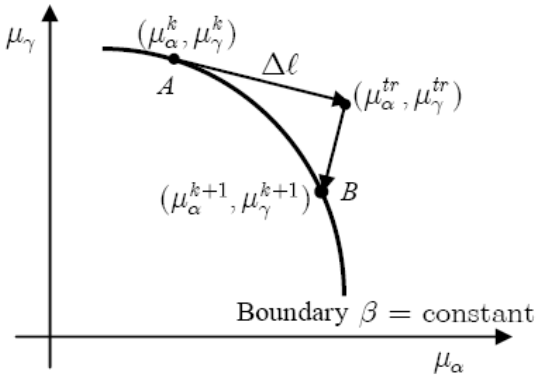

Figure 6-12. Predictor-corrector algorithm

The predictor–corrector algorithm(Figure 6-12) is explained below with two random variables, α and γ. First, the distribution type of random variables is assumed. The effect of different distribution types on the safety envelope can be investigated by following the same procedure as in the previous section. It is clear that the two parameters must have non-negative values, which means that the safety envelope only exists in the first quadrant. The capacity of the structure with respect to (μ_α, μ_γ) is interesting. If the required probability of failure is P_{target} (i.e., $\beta_{\text{target}} = -\Phi^{-1}(P_{\text{target}})$), the following steps can been taken to construct the safety envelope:

Step 1: Set k=1. Set the move limit Δl and a small parameter ε. Initialize $(\mu_\alpha, \mu_\gamma)=(\mu_\alpha^0, \mu_\gamma^0)$.

Step 2: Find an initial state $(\mu_\alpha^1, \mu_\gamma^1)$ such that $\beta(\mu_\alpha^1, \mu_\gamma^1)= \beta_{target}$.

Step 3: Determine the trial state (predictor).

The trial state can be obtained by moving in the tangent direction of the boundary of the envelope. From the first-order Taylor series expansion of $\beta(\mu_\alpha^k, \mu_\gamma^k)$=constant and from the move limit of Δl, the following two conditions can be used to determine the trial increments:

$$(\Delta\mu_\alpha^{tr})^2 + (\Delta\mu_\gamma^{tr})^2 = \Delta l \tag{6.21}$$

$$\left.\frac{\partial\beta}{\partial\mu_\alpha}\right|_{\mu_\alpha=\mu_\alpha^k} \cdot \Delta\mu_\alpha^{tr} + \left.\frac{\partial\beta}{\partial\mu_\gamma}\right|_{\mu_\gamma=\mu_\gamma^k} \cdot \Delta\mu_\gamma^{tr} = 0 \tag{6.22}$$

Of the two possible directions, the one that provides a clockwise (or counter clockwise) direction is selected. Then, the trial state can be obtained by

$$\begin{aligned} \mu_\alpha^{tr} &= \mu_\alpha^k + \Delta\mu_\alpha^{tr} \\ \mu_\gamma^{tr} &= \mu_\gamma^k + \Delta\mu_\gamma^{tr} \end{aligned} \tag{6.23}$$

According to the convex property of the envelope, the trial state in Eq.(6.23) can be either inside or outside the envelope. The reliability index at the trial state is $\beta^{tr}=\beta(\mu_\alpha^{tr}, \mu_\gamma^{tr})$.

Step 4: Return to the boundary of the envelope (corrector).

Since the trial state is not on the boundary, it needs to be returned to the boundary of the envelope. The correcting direction is perpendicular to the trial direction.

$$\beta_{\text{target}} = \beta^{tr} + \left.\frac{\partial\beta}{\partial\mu_\alpha}\right|_{\mu_\alpha=\mu_\alpha^{tr}} \cdot \Delta\mu_\alpha^{cr} + \left.\frac{\partial\beta}{\partial\mu_\gamma}\right|_{\mu_\gamma=\mu_\gamma^k} \cdot \Delta\mu_\gamma^{cr} \tag{6.24}$$

$$\Delta\mu_\alpha^{cr} \cdot \Delta\mu_\alpha^{tr} + \Delta\mu_\gamma^{cr} \cdot \Delta\mu_\gamma^{tr} = 0 \tag{6.25}$$

Then, the new state on the boundary of the envelope can be obtained by

$$\begin{aligned} \mu_\alpha^{k+1} &= \mu_\alpha^{pr} + \Delta\mu_\alpha^{cr} \\ \mu_\gamma^{k+1} &= \mu_\gamma^{pr} + \Delta\mu_\gamma^{cr} \end{aligned} \tag{6.26}$$

Step 5: Stop if $\left\| \left(\mu_\alpha^{k+1}, \mu_\gamma^{k+1}\right) - \left(\mu_\alpha^{0}, \mu_\gamma^{0}\right) \right\| \le \varepsilon$.

Step 6: Otherwise, set k=k+1 and go to step 3.

As schematically explained in Figure 6-12, the limit of the envelope is first found in one parameter μ_α, while μ_γ is fixed (Point *A*). The reliability result and sensitivity information are calculated at this point, from which the new search direction is found using sensitivity information and linear Taylor series expansion. The trial state can be obtained by moving the parameters by Δl in the search direction. From the trial state, the location of the boundary can be recovered by moving in the perpendicular direction to the search direction. Using linear search, a new position *B* on the envelope can be found. This sequence can be repeated to create a closed safety envelope. As expected, the accuracy of the safety envelope can be improved by using a smaller size of the move limit.

Example for Multi-Dimensional Load Envelope

In the uncertainty model of the dynamic loading formulated in Eq. (6.4) for the front loader frame of CAT 994D, suppose both mean(α) and amplitude(γ) of the dynamical are normally distributed with standard deviation of 0.25. As discussed in previous section, uncertainty in S-N curve will be modeled as lognormal distributed with a constant coefficient of variance of 0.1 in this problem. A reliability based load tolerance

design method can be applied to construct the safety envelope for the dynamic loads with respect to the mean values of both random parameters related to the load.

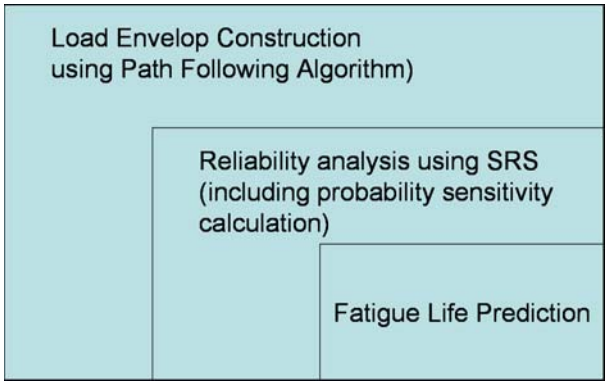

Figure 6-13. Construction of load envelope

Figure 6-13 provides the procedures for the construction of fatigue reliability based load envelope.

In the front loader frame problem, it is obvious that the mean of α and γ are positive value. Load tolerance can only be defined as nonnegative values. If the required probability of failure is 10% ($\beta_{target} = 1.3$), following steps can be taken to construct the load envelope:

Step 1: Find the initial point ($\mu_\alpha \geq 0$) on the envelope ($\beta(\mu_\alpha, \mu_\gamma) = 1.3$);

Step 2: Find the next solution on load envelope using Euler-Newton continuation to meet the constraint $\beta = 1.3$;

Step 3: Since only $\mu_\alpha, \mu_\gamma \geq 0$ is meaningful, continue step 2 until the curve end in this region;

Figure 6-14 shows the two-dimensional safety envelope for the loader frame while LCCs are both normally distributed. It is clear from the figure that the system has much

more safety margin in the average value than that of the amplitude which is consistent with the one-dimensional case.

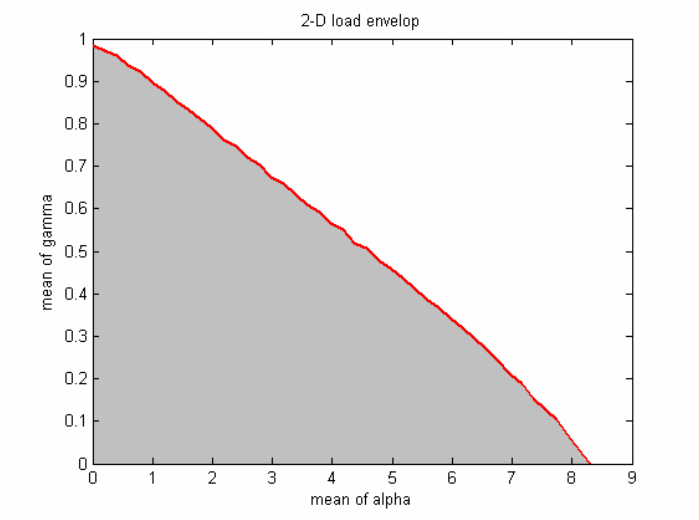

Figure 6-14. Safety envelop for fatigue reliability of CAT 994D front loader frame

Conservative Distribution Type

In the previous section, the load has been assumed a specific uncertainty characteristic (distribution type and corresponding parameters). Identifying the load distribution, however, is one of the most difficult tasks in the uncertainty analysis because different operating conditions will yield completely different distribution types. Thus, design engineers often look for a conservative distribution type. As can be seen in Figure 6-15 and Figure 6-16, for example, log-normal distribution is more important when the amplitude of the applied load is small, whereas normal distribution is more important when the amplitude is large. Using the sensitivity information and linear approximation, it would be possible to predict which distribution type has a significant effect on the load tolerance. Once dominant distribution type is selected, the detailed load tolerance can be constructed.

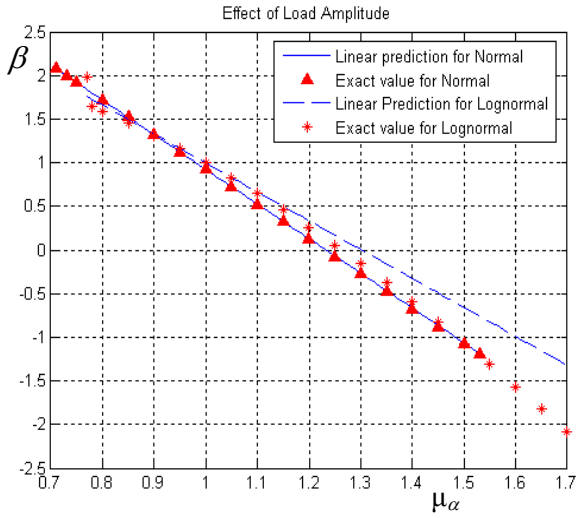

Figure 6-15. Reliability index β with respect to random parameter μ_α

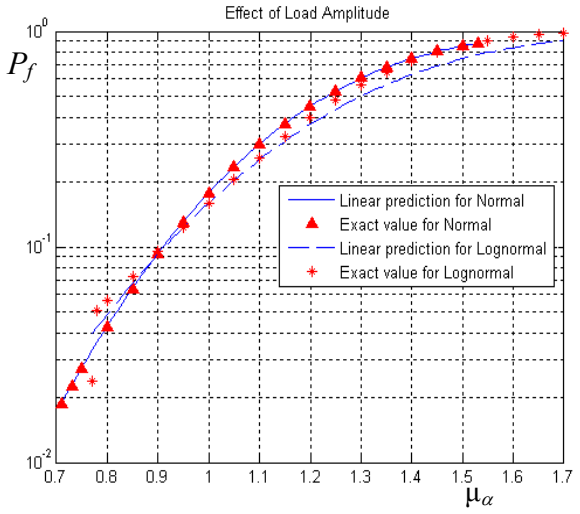

Figure 6-16. Probability of failure P_f with respect to random parameter μ_α

In two-dimensional case stated in the previous section, based on the same average value and standard deviation of LCCs but different distribution types, e.g., lognormal distribution, the effect of normal and lognormal distribution on safety envelope is compared in Figure 6-17.

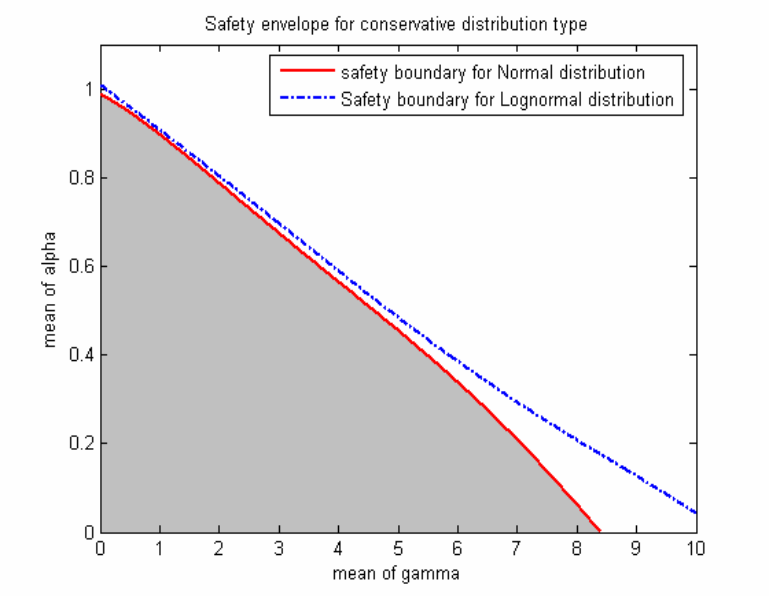

Figure 6-17. 2-D safety envelope for different distribution type with same random parameters

It is obvious that the structure working under dynamic load modeled with normal distribution is in more severe situation than that of lognormal distribution, which means uncertainties of dynamic load modeled by normal distribution is more conservative than the lognormal distribution while both of them have the same random parameters, i.e., mean and standard deviation. Following the same procedure, the safety boundary for different distribution type can be found. Thus, a conservative safety envelope is constructed by considering all the possible distribution type associated with different possibilities of working conditions. The completed safety envelope provides higher confidence of operation and offers a reference for future design upgrade.

Summary

In this chapter, fatigue reliability based load tolerance design for industrial equipment has been studied. A concept of safety envelope has been introduced for fatigue reliability based load tolerance design. The systematic road map of safety envelope has

been presented. FE-based fatigue evaluation, SRS-based reliability and sensitivity analysis, path following algorithm are integrated to construct a design reference for a structure. By considering the difficulties to obtain the uncertainty characteristics, conservative distribution type is considered to offer safer design of load without complete knowledge of uncertainty properties. The procedure of safety envelope construction has been presented for a two dimensional load model with considering the material uncertainty.

CHAPTER 7
ROBUST DESIGN USING STOCHASTIC RESPONSE SURFACE

Introduction

In the previous chapter, the objective of RBDO is to minimize the cost of product while meeting reliability level of performance. In quality engineering, it has been realized that the deviation from target value of performance due to the uncontrollable input variances/noises results in quality loss, which is a measure of dissatisfaction from the customers' point of view. Thus, robust design, which targets on making the performance of the product insensitive (robust) to the noise factors, has been gaining increasing attention in recent research activities.

Traditionally, the performance variance is evaluated either using the Monte-Carlo simulation (MCS) or linear approximation. The computational cost of MCS and the lack of accuracy of the linear approximation have been issues in robust design. In this chapter, an efficient and accurate method of evaluating the performance variance is proposed using the polynomial chaos expansion (Ghanem and Spanos 1991; Isukapalli et al. 1998). The proposed method has comparable accuracy with MCS, while requiring much less computational cost. By selecting appropriate bases of the surrogate model, the performance variance is calculated analytically. In addition, the derivatives of the performance variance with respect to design variables and input random parameters are calculated consistently with the variance calculation method, which is critical information for design optimization algorithm.

In general, the robust design problem should not be formulated to reduce the variance alone. Even if robustness is a requirement from quality point of view, a good design should also satisfy the requirement of the performance. In most of cases, quality and performance requirement are two competing design objectives. Thus, the robust design problem becomes a multi-objective optimization problem. In multi-objective optimization, there are multiple optimum designs in a sense that one objective function cannot be reduced further without increasing other objective functions. The optimal set is referred to as the Pareto optimal set and yields a set of possible answers from which the engineer may choose the desired values of the design variables.

In this chapter, a numerical example of a cantilever beam with both linear and nonlinear performance is used to show the advantage of SRS-based variance calculations. The variance calculated from the proposed method is compared with that from traditional approximation using first-order Tyler series expansion. Robust design for the natural frequency of a micro-scale cantilever composite beam is also presented. Since the objective is to design a structure whose lowest natural frequency reaches resonance frequency with lower variability, the robust design is modeled as a multi-objective optimization problem with two competitive targets, one for performance mean and another for the standard deviation of the performance. A Pareto optimal front is then obtained by setting one objective as a constraint and by gradually changing its constraint limit. It turns out that controlling design variables makes less change of variance of the performance than performance mean. It is more important to control the input variance itself rather than the design variable in this problem. Global sensitivity is then introduced

at the optimum design to address the importance of different input variance, which means that random variables should be paid more attention to reduce total performance variance.

Performance Variance Calculation Using SRS

One important issue for robust design is to evaluate the performance variance. Traditionally, a linear approximation using Taylor series expansion is often employed for that purpose (Koch et al. 2004). However, the error of approximation increases according to the nonlinearity of the performance. In addition, the coupled effect of input variances cannot be counted in the linear model.

As we introduced in chapter 5, performance variance can be obtained by SRS at each design stage. The advantage of the polynomial chaos expansion becomes clear in evaluating the variance. In general, the polynomial chaos expansion in a surrogate model provides an analytical solution for the variance, since Hermite basis functions are orthogonal with respect to the Gaussian measure and the variance of the bases are analytically available. It is convenient to obtain output variance though the sum of partial variances based on the coefficients of each term.

If the polynomial bases are generally defined as $\Psi_i(\boldsymbol{\xi})$ with $\boldsymbol{\xi}$ being the vector of standard random variable, the SRS in Eq. (2.4) can be re-written as

$$g(\boldsymbol{\xi}) = \sum_{i=1}^{N} a_i \cdot \Psi_i(\boldsymbol{\xi}) \tag{7.1}$$

where g is the approximated system performance and N is the number of coefficients in SRS. Since the above expression is linear with respect to the unknown coefficients, the performance variance can be written as

$$\mathrm{Var}(g) = \sum_{i=1}^{N} {a_i}^2 \cdot \mathrm{Var}[\Psi_i(\boldsymbol{\xi})] \tag{7.2}$$

Thus, the analytical expression of the performance variation can be obtained if the variations of the polynomial bases are available. When input variables are SRV, the analytical variations of Hermite bases can be found in Ghanem and Spanos (Ghanem and Spanos 1991).

Variance Sensitivity

The robust design problem in this paper is formulated as an optimization problem that minimizes the performance variation in Eq.(7.2). In gradient-based optimization algorithms, calculation of sensitivity information is a critical issue for saving the computational cost and making the algorithm converge. The finite difference method requires a complete recalculation of the performance variation (Haftka and Gurdal 1991). The goal is to calculate the gradient information without carrying out a complete recalculation of the performance variance. From the fact that the SRV in the polynomial chaos remains constant while the design changes, the regression coefficients only depend on design variables. Thus, in the proposed polynomial chaos expansion, the gradient of the performance variance with respect to j-th design parameter, d_j, can be written as

$$\frac{\partial \operatorname{Var}(g)}{\partial d_j} = \sum_{i=1}^{N} 2a_i \frac{\partial a_i}{\partial d_j} \operatorname{Var}[\Psi_i(\boldsymbol{\xi})] \tag{7.3}$$

It is clear that the derivatives of the regression coefficients are enough to calculate the derivative of performance variation.

In the linear regression method, the coefficients of SRS are obtained from

$$\mathbf{a} = (\mathbf{X}^T\mathbf{X})^{-1}\mathbf{X}^T\mathbf{g} \tag{7.4}$$

where $\mathbf{g} = [g_1, g_2, \ldots, g_M]^{\mathrm{T}}$ is the vector of performance functions at sampling points, and $\mathbf{X}$ is the matrix of bases at sampling points, defined as

$$\mathbf{X} = [\mathbf{Y_i(\xi)}] = \begin{bmatrix} \Psi_1(\xi_1) & \Psi_2(\xi_1) & \dots & \Psi_N(\xi_1) \\ \Psi_1(\xi_2) & \Psi_2(\xi_2) & \dots & \Psi_N(\xi_2) \\ \vdots & \vdots & \ddots & \vdots \\ \Psi_1(\xi_M) & \Psi_2(\xi_M) & \dots & \Psi_N(\xi_M) \end{bmatrix}_{M \times N} \tag{7.5}$$

In the above equation, *M* is number of sampling points, and *N* is the number of bases. Then, the derivatives of the coefficients can be obtained from

$$\frac{\partial \mathbf{a}}{\partial d_j} = ((\mathbf{X}^T\mathbf{X})^{-1}\mathbf{X}^T \frac{\partial \mathbf{g}}{\partial d_j} \tag{7.6}$$

The last term, $\partial \mathbf{g} / \partial d_j$, is the derivative of performance function at sampling points, which can be calculated using design sensitivity analysis (see Choi and Kim (Choi and Kim 2004a; Choi and Kim 2004b)). By substituting Eq. (7.6)into Eq.(7.3), the derivative of performance variation can be obtained. This procedure of calculating sensitivity of the performance variation is much more efficient than the traditional finite difference method because most information, such as **a** and **X**, is already available from the performance variation calculation. The only term required for sensitivity analysis is $\partial \mathbf{g} / \partial d_j$.

When finite element analysis is used as a computational tool for calculating the performance function, sensitivity analysis provides an efficient tool for calculating the performance derivative. In the context of structural analysis, for example, the discrete system is often represented using a matrix equation of the form **[K]**{**D**} = {**F**}. The performance function **g** in Eq. (7.4) can be expressed as a function of the nodal solution {**D**}. Thus, the sensitivity of the performance can be easily calculated if that of the nodal solution is available. When the design variables are defined, the matrix equation can be differentiated with respect to them to obtain

$$[\mathbf{K}]\left\{\frac{\partial \mathbf{D}}{\partial d_j}\right\} = \left\{\frac{\partial \mathbf{F}}{\partial d_j}\right\} - \left[\frac{\partial \mathbf{K}}{\partial d_j}\right]\{\mathbf{D}\} \tag{7.7}$$

Equation (7.7) can be solved inexpensively because the matrix [**K**] is already factorized. The computational cost of sensitivity analysis is usually less than 20% of the original analysis cost, so, local sensitivity can in fact be obtained efficiently.

As an illustrative example, a cantilevered beam (Figure 7-1) is taken from literature (Qu and Haftka 2004; Wu et al. 2001). Two failure modes are considered in this example: (1) the maximum stress of the beam should be less than the strength of the material [Eq.(7.8)], and the tip deflection should be less than the allowable displacement [Eq.(7.9)]. These two constraints can be expressed by

$$g_1 = R - (\frac{600}{wt^2}Y + \frac{600}{w^2t}X) \geq 0 \tag{7.8}$$

$$g_2 = D_0 - \frac{4L^3}{Ewt}\sqrt{\left(\frac{Y}{t^2}\right)^2 + \left(\frac{X}{w^2}\right)^2} \geq 0 \tag{7.9}$$

where R is the yield strength, E is the elastic modulus, X and Y are the independent horizontal and vertical loads shown in Figure 7-1. D_0 is the allowable tip displacement which is given as 2.25 in.

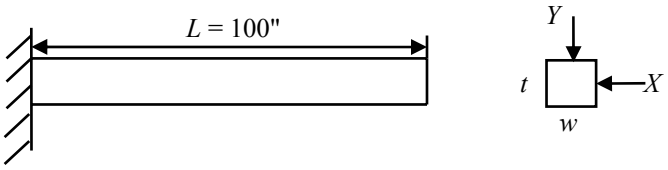

Figure 7-1. Cantilever beam subject to two direction loads

Two cross-sectional dimensions, w and t, are considered as controllable design variables. Five uncontrollable random variables are defined in Table 7-1.

Table 7-1. Random variables for cantilevered beam structure

Random variable	X	Y	R	E
Distribution type	Normal $(500,100^2)$ lb	Normal $(1000,100^2)$ lb	Normal $(40000,2000^2)$psi	Normal $(29E6,(1.45e6)^2)$psi

It is obvious that the strength constraint defined in Eq.(7.8) is a linear function of the random inputs. For linear performance, the variance can be analytically obtained as

$$\mathrm{Var}(g_1) = \mathrm{Var}(R) + (\frac{600}{wt^2})^2 \mathrm{Var}(Y) + (\frac{600}{w^2 t})^2 \mathrm{Var}(X) \tag{7.10}$$

Using this property, the accuracy of the proposed variance estimation in Eq.(7.10) can be verified. Table 7-2 shows the comparison between the variance from the SRS-based method and that from analytical approach. The variance is calculated at the deterministic optimal design (w = 1.9574", t = 3.9149").

Table 7-2. Variance estimation of linear performance (strength)

Analytical variance	Variance from SRS (3rd-order)
2.4e7	2.4e7

In the case of strength constraint, it is possible to find the analytical expression of the variance. However, in the case of nonlinear performance, such as deflection constraint in Eq.(7.9), there is no easy way of calculating this analytical expression except for the first-order approximation. The linear approximation of the deflection constraint becomes

$$\mathrm{Var}(g_2)_{\mathrm{linear}} = \left(\frac{\partial g_2}{\partial X}\right)^2 \mathrm{Var}(X) + \left(\frac{\partial g_2}{\partial Y}\right)^2 \mathrm{Var}(Y) + \left(\frac{\partial g_2}{\partial E}\right)^2 \mathrm{Var}(E) \tag{7.11}$$

Due to the error involved in the linear approximation, MCS is the only method that can verify the accuracy of variance calculation. Since MCS is a sampling-based method, the estimated variance always has variability. Let σ^2 be the variance of a random variable and let s^2 be the unbiased estimator of σ^2. When n number of samples are used, the variance of the MCS-estimated performance variance can be predicted by (Ang and Tang 1975)

$$\mathrm{Var}(s^2) = \frac{\sigma^4}{n}\left(\frac{\mu_4}{\sigma^4} - \frac{n-3}{n-1}\right) \tag{7.12}$$

where $\mu_4 = E(X-\mu)^4$ is the fourth central moment of random variable X. μ_4 / σ^4 is called kurtosis.

For the nonlinear performance in Eq.(7.9), the third-order SRS is used to approximate the deflection and the expression in Eq. (7.2) is used to evaluate the performance variance. Table 7-3 compares the variance obtained from these three methods. As expected, the linear approximation has about 1% error compared with MCS, while SRS-based variance is within the confidence range of MCS. The error in the linear approximation will increase proportionally to the nonlinearity of the function.

Table 7-3. Variance estimation of nonlinear performance (deflection)

$\mathrm{Var}(g_2)_{\mathrm{MCS}}$ (500,000 samples)	$\mathrm{Var}(g_2)_{\mathrm{linear}}$	$\mathrm{Var}(g_2)_{\mathrm{SRS}}$
0.1947 (standard deviation = 3.9248E−4)	0.1966	0.1948

Based on the accuracy of the proposed method in calculating performance variance, the variance sensitivity in Eq. (7.3) is also tested using the cantilevered beam model. Table 7-4 and Table 7-5 show the variance sensitivities obtained from the proposed method compared with those from the central finite difference method (FDM). In FDM, the design variables are perturbed by 2% and the variance is recalculated using the SRS. When the performance is linear with respect to random variables, the analytical sensitivity can be obtained, for example, by differentiating Eq. (7.10) with respect to the design variables. In Table 7-4, the sensitivity obtained from SRS agrees well with that of the analytical sensitivity. The finite difference sensitivity shows a small error because the variance is still a nonlinear function with respect to the design variable.

Table 7-4. Sensitivity of variance for linear performance (strength)

∂Var/∂w (SRS)	∂Var/∂w (FDM)	∂Var/∂w (Analytical)	∂Var/∂t (SRS)	∂Var/∂t (FDM)	∂Var/∂t (Analytical)
−3.6784E7	−3.6801E7	−3.6785E7	−1.2261E7	−1.2265E7	−1.2261E7

Table 7-5. Sensitivity of variance for nonlinear performance (deflection)

∂Var/∂w (SRS)	∂Var/∂w (FDM)	∂Var/∂t (SRS)	∂Var/∂t (FDM)
−0.6538	−0.6544	−0.0712	−0.0712

Robust Design – Two-Layer Beam

Dynamic Response of Two-layer Beam

The robust design problem formulation is demonstrated using a cantilevered, composite beam, shown in Figure 7-2. When an electric field is applied to the piezoelectric (PZT) part, it will generate a bending moment and deform the beam. On the other hand, when the base is oscillating with a specific frequency, the deformation of the beam will induce an electric field through PZT, which can be used as an energy reclamation device. System dynamic response of the composite beam is highly coupled and the closed-form solution is difficult to obtain (De Rosa 1994; Jang and Bert 1989a; Jang and Bert 1989b). In this chapter, a lumped element modeling technique (LEM, (Li et al. 2006)) is used to obtain the approximate solution for the system. Under the quasi-static assumption, the LEM can estimate the first fundamental natural frequency with accuracy. First, the effective mechanical compliance (C_e) and the effective mass (M_e) can be calculated by lumping the total strain energy and kinetic energy, respectively. The detailed procedure is summarized in the Appendix B. The first natural frequency is then calculated using the following expression (Li et al. 2006).

$$f_n = \frac{1}{2\pi}\sqrt{\frac{1}{C_e M_e}} \tag{7.13}$$

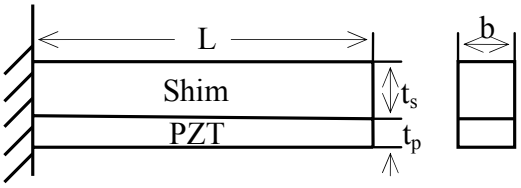

Figure 7-2. Piezoelectric cantilevered composite beam

When the composite beam is used as an energy reclamation device, the maximum efficiency can be obtained when the excitation frequency and the natural frequency are resonant. Thus, the design goal is to find design variables such that the natural frequency is as close as possible to the excitation frequency. However, due to the uncertainty of the material properties, the performance function (natural frequency) in Eq. (7.13)is not a deterministic quantity. Thus, the additional design goal is to minimize the variance of the natural frequency due to the input random variable inputs.

Robust Design for Two-Layer Beam

When a robust design problem is formulated in such a way that only the variance of the output is minimized, the optimization problem may find an inappropriate design without considering the mean value of the performance. Thus, it would be appropriate to consider both the variance and the mean value simultaneously. In this section, the robust design problem is formulated as a two-objective optimization: one for the variance and the other for the mean value. When two objectives are competing with each other, there will be no single optimum design. Instead, a Pareto optimal front can be constructed, which represents the best combinations between the competing objective functions. Due to the uncertainty in inputs, all constraints are modeled as reliability constraints.

In the two-layer composite beam problem, the goal is to design a structure with natural frequency close to the prescribed value. Considering the uncertainties involved in input variables however, the natural frequency at any design will have certain variations, which should also be minimized. In addition, the reliabilities for the stress and deflection constraints should be considered. In reliability-based robust design, the reliability constraints are imposed by pushing the mean value to certain levels of standard deviation in the conservation direction. Thus, the robust design problem is formulated as

$$\begin{aligned} &\text{Minimize } g_1 = \left|\mu_f - f_0\right| \text{ and } g_2 = \sqrt{\text{Var}(f)} \\ &\text{s.t.} \qquad (\mu_\sigma - R) + k\sqrt{\text{Var}(\sigma - R)} \le 0 \\ &\qquad\quad (\mu_w - D_0) + k\sqrt{\text{Var}(w - D_0)} \le 0 \end{aligned} \tag{7.14}$$

where μ_f is the mean of the first natural frequency; f_0 is the excitation frequency; σ is the maximum stress; R is the material strength, which is assumed as 11,743Pa; w is the tip deflection and D_0 is the allowable maximum tip deflection, which is 7.138 nanometer; and k is the user-defined constant for specific target reliability level. It is assumed that uncertainties only exist in the material properties such as elastic modulus and material density. Table 7-6 lists the random parameters of these quantities. All random variables are assumed to be normally distributed and the standard deviation for the elastic modulus is 10% of the mean value and that of the density is 5%.

Table 7-6. Random parameters for the composite beam structure

Random variable	Mean	Standard deviation
Young's modus of shim (E_s)	169 GPa	16.9 GPa
Density of shim (ρ_s)	2330 kg/m3	116 kg/m3
Young's modus of PZT (E_p)	60 GPa	6 GPa
Density of PZT (ρ_p)	7500 kg/m3	375 kg/m3

In the composite beam problem, three design variables are defined: beam length L, shim thickness t_s, and PZT layer thickness t_p. The robust design problem involves three deterministic design variables and four random parameters. For given design variables, the SRS for the performance functions, such as natural frequency, stress, and tip deflection, are constructed according to Eq.(2.4). Then, the performance variances are calculated from Eq. (7.2) and variance sensitivity from Eq.(7.3). The values and sensitivities of the two objective functions g_1 and g_2 with respect to the three design variables are summarized in Table 7-7 at the initial design (t_s = 6μm, t_p = 0.2μm, L = 1000μm). Table 7-7 shows that for given design, the mean of the frequency will change at least 15 times more than the frequency variance. Thus, it is easier to change the mean values than to change the frequency variance. This observation leads to the idea of controlling the input variances directly rather than controlling the design variables in the following section.

Table 7-7. Sensitivities of objective functions at the initial design (t_s = 6μm, t_p = 0.2μm, L = 1000μm)

g1(Hz)	g2(Hz)	∂g1/∂ts (Hz/m)	∂g1/∂tp (Hz/m)	∂g1/∂L (Hz/m)	∂g2/∂ts (Hz/m)	∂g2/∂tp (Hz/m)	∂g2/∂L (Hz/m)
834.88	144.54	−491.02	562.05	5.335	27.15	−36.55	−0.29

Since two objective functions are competing with each other, there will be no single optimum design. In such a case, the value of one objective function is fixed and then the minimum value of the other objective function can be found. By repeating this procedure for different values, a Pareto optimal front can be constructed. Figure 7-3 shows the Pareto optimal front of the two-objective optimization problem in Eq.(7.14).

All points in the Pareto front are optimum design in a sense that one objective function cannot be reduced further without increasing the other objective function.

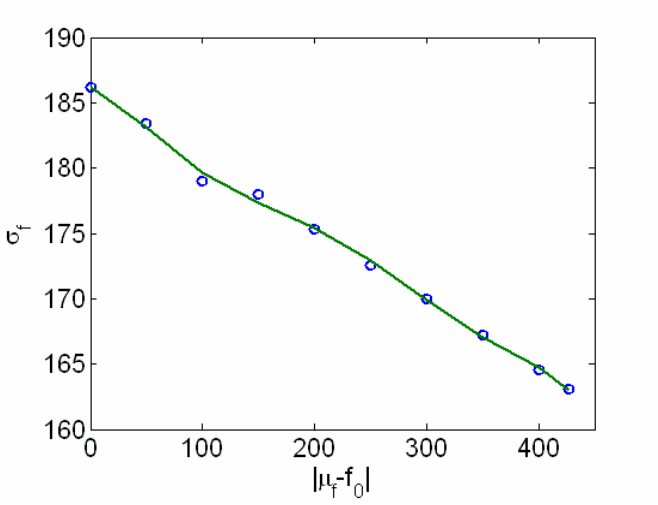

Figure 7-3. Pareto optimal front for the robust design of the composite beam

Global Sensitivity Analysis

In Figure 7-3, the change in the mean value (abscissa) is more significant than that in the standard deviation (ordinate), which is consistent with the observation in Table 7-7. This result indicates that when the design variables are deterministic, it is relatively easier to change the mean value rather than the performance variance. The performance variance can be changed more effectively by controlling input variance. However, controlling input variance accompanies manufacturing cost or large numbers of coupon tests. Thus, in practice, it is important to find the contribution of random variables to the performance variance and then spend more resources in controlling the most significant random variable.

In Table 7-8, the contribution of random input variables to the performance variance is summarized in terms of total sensitivity indices in Eq.(4.6). It can be found

that the contributions of ρ_s and E_s are more than 99% of the performance variance. Thus, it will be meaningful to reduce the variance of the shim rather than that of the PZT.

Table 7-8. Total sensitivity indices for the composite beam structure (t_s = 6μm, t_p = 0.2μm, L = 1000μm)

$S_{E_p}^{\text{total}}$	$S_{\rho_p}^{\text{total}}$	$S_{E_S}^{\text{total}}$	$S_{\rho_S}^{\text{total}}$
0.00%	0.96%	85.87%	13.17%

Robust Design by Tolerance Control

In the previous section, the input variances were considered as uncontrollable variables and only deterministic design variables were considered. However, in tolerance design, the design variables are fixed, while the variances of random variables are changed to further reduce the output variances. However, in such a problem, the optimum design will reduce all input variances to zero. Thus, the robust design will turn out to be zero variance.

In practice, reducing input variance requires cost. Different costs are anticipated in reducing the variance of different inputs. The cost of controlling individual input variance can be represented by a cost-tolerance model (Chase and Greenwood 1988). Thus, a more appropriate robust design problem will be: for a given investment, how much individual variance should be reduced in order to minimize the performance variance. Based on the total budget of controlling input variability, the robust design problem can be written as

$$\begin{aligned} &\text{Minimize}\,\text{Var}[\,g(\sigma_1,\sigma_2,...,\sigma_n)\,] \\ &\text{s.t.} \qquad \sum_{i=1}^{n} C_i(\sigma_i) \le C_{\text{total}} \end{aligned} \tag{7.15}$$

where σ_i is the standard deviation of i-th random variable, C_i is the cost function of controlling i-th standard deviation, and C_{total} is the total investment.

Similar to the robust design problem with deterministic design variables, the optimization problem in Eq. (7.15) requires the derivative of the performance variance. The only difference now is that the derivative is taken with respect to the input variance. By substituting *j*-th design variable d_j in Eq. (7.3) to *j*-th random parameter σ_j, the gradient of output variance in Eq. (7.15) with respect to *j*-th random parameter can be written as

$$\frac{\partial \operatorname{Var}(g)}{\partial \sigma_j} = \sum_{i=1}^{N} 2a_i \frac{\partial a_i}{\partial \sigma_j} \operatorname{Var}[\Psi_i(\boldsymbol{\xi})] \tag{7.16}$$

Similarly, the derivatives of the coefficients can be obtained from

$$\frac{\partial \mathbf{a}}{\partial \sigma_j} = (\mathbf{X}^T\mathbf{X})^{-1}\mathbf{X}^T \frac{\partial \mathbf{g}}{\partial \sigma_j} \tag{7.17}$$

Since all random variable are assumed to be independent, we have the following chain rule of differentiation:

$$\frac{\partial \mathbf{g}}{\partial \sigma_j} = \frac{\partial \mathbf{g}}{\partial T_j^{-1}(\xi_j)} \cdot \frac{\partial T_j^{-1}(\xi_j)}{\partial \sigma_j} \tag{7.18}$$

where T_j is the transformation of *j*-th random variable from original random space to standard normal space:

$$\xi_j = T_j(x_j) \tag{7.19}$$

Therefore, the sensitivity of performance variance with respect to random parameters can be obtained by combining Eqs.(7.16),(7.17) and (7.18) if the derivative $\partial \mathbf{g} / \partial T_j^{-1}(\xi_j) = \partial \mathbf{g} / \partial x_j$ is available.

As an illustration of the effectiveness and convergence properties of the proposed approach, the cantilevered beam model (Figure 7-1) is used. Based on the accurately estimated performance variance, the variance sensitivities with respect to input variances are calculated using the proposed method in Eq.(7.16). Table 7-9 and Table 7-10 show the sensitivities obtained from the proposed method along with those from the finite

difference method. Since the analytical sensitivity is available for the linear performance, Table 7-9 also lists the analytical sensitivity. It turns out that the proposed SRS-based sensitivity calculation method provides accurate sensitivity information. Since the proposed method only requires the calculation of performance sensitivity at sampling points [Eq.(7.18)], the computational cost will be much less than that of the finite difference method.

Table 7-9. Sensitivity of variance for linear performance (strength)

∂Var/ $\partial\sigma_X$ (SRS)	∂Var/ $\partial\sigma_X$ (FDM)	∂Var/ $\partial\sigma_X$ (Analytic)	∂Var/ $\partial\sigma_Y$ (SRS)	∂Var /$\partial\sigma_Y$ (FDM)	∂Var /$\partial\sigma_Y$ (Analytic)	∂Var /$\partial\sigma_R$ (SRS)	∂Var /$\partial\sigma_R$ (FDM)	∂Var /$\partial\sigma_R$ (Analytic)
3.2e5	3.2e5	3.2e5	8.0e4	8.0e4	8.0e4	4000	4000	4000

Table 7-10. Sensitivity of variance for nonlinear performance (deflection)

∂Var/$\partial\sigma_X$ (SRS)	∂Var/$\partial\sigma_X$ (FDM)	∂Var/$\partial\sigma_Y$ (SRS)	∂Var/$\partial\sigma_Y$ (FDM)	∂Var/$\partial\sigma_E$ (SRS)	∂Var/$\partial\sigma_E$ (FDM)
3.41e-3	3.41e-3	5.77e-5	5.77e-5	2.66e-8	2.66e-8

With performance variance and its sensitivity, the robust design problem with input variance control in Eq. (7.16) can be solved efficiently. Consider the robust design problem that minimizes the variance of natural frequency with strength and deflection constraints, as

$$\begin{aligned} &\text{Minimize} && \sqrt{\mathrm{Var}(\omega)} \\ &\text{s.t.} && E(g_1) - k\sigma(g_1) \geq 0 \\ & && E(g_2) - k\sigma(g_2) \geq 0 \\ & && \sum_{i=1}^{n} C_i(\sigma_i) \leq C_{tot} \end{aligned} \tag{7.20}$$

where g_1 and g_2 are strength and deflection constraints in Eq. (7.8) and (7.9), respectively. In this optimization problem, the deterministic design variables, w and t, are pre-determined (w = 2.73, t = 3.50) from the previous optimization. Now, the optimization is performed by changing the standard deviations of random input variables. In Eq.(7.20), ω is the first natural frequency of the beam defined as

$$\omega = (\beta L)^2 \sqrt{\frac{EI}{\rho A L^4}} = \frac{\beta^2 t}{2}\sqrt{\frac{E}{3\rho}} \tag{7.21}$$

and $E(\cdot)$ and $\sigma(\cdot)$ represent the expect value and standard deviation of random output, respectively, and $C_i(\sigma_i)$ is the cost-tolerance function for the i-th random variable. For a specific boundary condition, the term, β, is constant. Thus, the objective function to control the variance of natural frequency is modified to

$$\text{Minimize} \quad \sqrt{\text{Var}\left(\frac{\omega}{\beta^2}\right)} = \sqrt{\text{Var}\left(\frac{t}{2}\sqrt{\frac{E}{3\rho}}\right)} \tag{7.22}$$

Table 7-11 lists random variables and cost-tolerance functions (Chase and Greenwood 1988) for the random variables.

Table 7-11. Random variables and cost-tolerance functions

Variables	X	Y	R	E	ρ
Distribution	N(500,σ_1^2)lb	N(1000,σ_2^2)lb	N(40000,σ_3^2)psi	N(29E6,σ_4^2)psi	N(0.28, ,σ_5^2)
Cost-tolerance	1.5+200/σ_1	1.5+200/σ_2	1.5+1.6*10^7/ σ_3^2	200Exp(σ_4*10^{-6})	18Exp(-100σ_5)
σ_i	25≤σ_1≤200	50≤ σ_2≤400	1000≤ σ_3≤4000	106≤σ_4≤3*10^6	0.01≤ σ_5≤0.05

To demonstrate the robust design, total cost of controlling variance at the initial design has been chosen as cost constraint. Thus, the design goal is to minimize the performance variance, while maintaining the same cost with initial variance control. Table 7-12 shows that the standard deviation of natural frequency reduced from 452.5 Hz

to 325 Hz by redistributing the input variances. Since the natural frequency is independent of the applied loads and the two constraints are not active, the final design increased the variances of the first three random variables. The optimum design maintains the variance of the elastic modulus and halves the density, which is more cost effective than reducing the variance of the elastic modulus.

Table 7-12. Random variables and cost-tolerance functions

Design Variables	Initial design	Optimal design
σ_1	100	200
σ_2	100	400
σ_3	2000	4000
σ_4	1.45*106	1.45*106
σ_5	0.02	0.010762
Objective	452.5	325.0
C_{total}	17.8274	17.8274

Summary

In this chapter, SRS-based variance calculation is proposed to facilitate robust design application. Accurate variance sensitivity analysis is presented for the gradient-based optimizer. A simple cantilevered beam with two failure modes, one as linear and another as nonlinear, is used to illustrate the accuracy and robustness of variance calculation.

Robust design for the natural frequency of a cantilevered, composite beam showed that because controlling deterministic design variables makes less change of the performance variance than that of the performance mean, we found it is more important to control the input variance itself rather than the design variable in our specific problem. Global sensitivity is then introduced to address which random variables should be paid more attention to reduce total performance variance.

Finally, a cost model based robust design is proposed to control the input variance, an alternative way of tolerance design. Design sensitivity analysis of performance variance with respect to input variance has been proposed in mathematical programming. The cantilever beam model is used to illustrate the effectiveness of tolerance design.

CHAPTER 8
SUMMARY AND RECOMMENDATIONS

Although reliability-based design optimization has been studied intensively for decades, industrial applications in structural design are still limited by the significant amount of computational cost as well as accuracy in reliability analysis. RBDO techniques are under development and have large room for improvement.

To improve the efficiency of RBDO, there are two key factors: one is by introducing new RBDO strategies; and the other is by developing efficient and accurate uncertainty analysis methodologies. In the first category, two strategies are investigated in this research. The conventional RBDO strategy sets the required reliability as a constraint, while the inverse measure approach uses the performance measure at required reliability as a constraint. The mathematical equivalence of these two strategies has been discussed in section 3.2. However, since constraints are established using different measures, the convergence and optima may result in different ways.

In the second category, the improvement of efficiency of uncertainty analysis has always been a main concern. In this research, SRSM using local sensitivity information is implemented in uncertainty analysis. The convergence and accuracy of SRSM are investigated. During the implementation of SRSM to RBDO model, SRS-based probability sensitivity analysis is developed and tested in order to improve the convergence and efficiency of RBDO. The efficiency of SRSM is further improved significantly by utilizing variance-based global sensitivity analysis to reduce the dimension of random space.

In the manufacturing environment, the cost of controlling manufacture variations is often more than making the design insensitive to these variations. Thus, it is necessary to study robust design under the context of uncertainty. In this research, SRS-based variance calculation is proposed to facilitate the robust design application. It is shown that the proposed variance calculation is more accurate than the conventional first-order Taylor series expansion. The proposed method can include the higher-order terms as well as interactions. Accurate variance sensitivity analysis is further presented for the gradient-based optimizer. Numerical example shows that it is sometimes more important to control the input variance itself rather than the design variables. A cost model based robust design is then proposed to control the input variance with the same cost, an alternative way of tolerance design. Design sensitivity analysis of performance variance with respect to input variance has been proposed in mathematical programming. Numerical example is also used to illustrate the effectiveness of tolerance design.

As an integrated process, fatigue reliability-based load tolerance design involves finite element analysis, fatigue life prediction, reliability analysis and path following technique. The randomness of dynamic loads is subjective and difficult to control. In this research, different possible distribution types are considered to provide a conservative and safer load design. Implementing more distribution types of uncertainty in the load tolerance design and finding a more efficient way to construct the safety envelope are recommended for future research.

APPENDIX A
SAMPLING-BASED PROBABILITY SENSITIVITY ANALYSIS FOR DIFFERENT DISTRIBUTION TYPE

The derivative of failure probability can be written as

$$\frac{\partial P_f}{\partial \theta} = \int_{\Omega_{\mathbf{x}}} I(G(\mathbf{x}) \le 0) \frac{\partial f(\mathbf{x})}{\partial \theta} d\mathbf{x} = \int_{\Omega_{\mathbf{x}}} I(G(\mathbf{x}) \le 0) \cdot \left[\frac{\partial f(\mathbf{x})}{f(\mathbf{x}) \partial \theta} \right] f(\mathbf{x}) d\mathbf{x}$$
$$= \int_{\Omega_{\mathbf{u}}} I(G(\mathbf{u}) \le 0) \cdot \left[\frac{\partial f(\mathbf{x})}{f(\mathbf{x}) \partial \theta} \right]_{\mathbf{x}=\mathbf{T}^{-1}(\mathbf{u})} \varphi(\mathbf{u}) d\mathbf{u} \tag{A.1}$$

where θ is the random parameter, $\Omega_{\mathbf{x}}$, $\Omega_{\mathbf{u}}$ denote entire original design space and standard normal space, respectively; $G(\mathbf{X}) \le 0$ is failure region and $f(\bullet)$ is joint probability density function (PDF); $\varphi(\bullet)$ is standard normal PDF ; $I(G(\mathbf{X}) \le 0)$ is an indication function such that I=1 if $G(\mathbf{X}) \le 0$ and I=0 otherwise.

In this section, explicit mathematical expressions of sampling-based probability sensitivity analysis for different distribution types are derived. Numerical examples of analytical functions have been used to check the accuracy of the derivation.

Normal Distribution $X_i \sim N(\mu_i, \sigma_i^2)$

Case 1: $\theta = \mu_i$

$$\frac{\partial f(\mathbf{x})}{f(\mathbf{x}) \partial \mu_i}\Big|_{\mathbf{x}=\mathbf{T}^{-1}(\mathbf{u})} = \left[-\frac{x_i - \mu_i}{\sigma_i} \cdot (-\frac{1}{\sigma_i}) \right]_{\mathbf{x}=\mathbf{T}^{-1}(\mathbf{u})} = \frac{u_i}{\sigma_i} \tag{A.2}$$

$$\frac{\partial P_f}{\partial \mu_i} = \int_{\Omega_{\mathbf{u}}} I(G(\mathbf{u}) \le 0) \cdot \left[\frac{\partial f(\mathbf{x})}{f(\mathbf{x}) \partial u_i} \right]_{\mathbf{x}=\mathbf{T}^{-1}(\mathbf{u})} \varphi(\mathbf{u}) d\mathbf{u}$$
$$= \frac{1}{N} \sum_{j=1}^{N} I_j \frac{1}{\sigma_i} u_i^j \tag{A.3}$$

Case 2: $\theta = \sigma_i$

$$\frac{\partial f(\mathbf{x})}{f(\mathbf{x})\partial\sigma_i}\Big|_{\mathbf{x}=\mathbf{T}^{-1}(\mathbf{u})} = \left[(-\frac{x_i-\mu_i}{\sigma_i})\cdot(-\frac{x_i-\mu_i}{\sigma_i^2})-\frac{1}{\sigma_i}\right]_{\mathbf{x}=\mathbf{T}^{-1}(\mathbf{u})} = \frac{1}{\sigma_i}\cdot(u_i^2-1) \tag{A.4}$$

$$\begin{aligned}\frac{\partial P_f}{\partial\sigma_i} &= \int_{\Omega_\mathbf{u}} I(G(\mathbf{u})\le 0)\cdot\left[\frac{\partial f(\mathbf{x})}{f(\mathbf{x})\partial\sigma_i}\right]_{\mathbf{x}=\mathbf{T}^{-1}(\mathbf{u})}\varphi(\mathbf{u})d\mathbf{u} \\ &= \frac{1}{N}\sum_{j=1}^{N} I_j\frac{1}{\sigma_i}(u_i^j u_i^j-1)\end{aligned} \tag{A.5}$$

The accuracy of above sensitivity formulation is evaluated using a simple linear function. The random variable is normally distributed. In this particular example, FORM provides an exact solution. Consider a simple one-dimensional linear function represented by

$$\begin{cases} G(x) = 1.6 - 3x \\ x \sim Normal(0, 0.4^2) \end{cases} \tag{A.6}$$

A failure criterion for the performance function is set to be $G \le 0$.

In FORM, probability sensitivity can be obtained through the sensitivity of reliability index through

$$\frac{\partial P_f}{\partial\theta} = -\varphi(-\beta)\frac{\partial\beta}{\partial\theta} \tag{A.7}$$

Table A-1 compares the accuracy of P_f and its sensitivities with those from FORM. In the sampling-based probabilistic sensitivity calculation, 200,000 samples are used. A good agreement between two approaches is observed.

Table A-1: Accuracy of proposed probability sensitivity method for normal distribution using 200,000 sampling MCS

	FORM	Sampling based approach(200,000 samples)	Difference
P_f	0.0915	0.0914	0.11%
$dP_f/d\,\mu_x$	0.4100	0.4109	0.22%
$dPf/d\sigma_x$	0.5469	0.5484	0.27%

Uniform Distribution

The probability density function for uniform distribution can be written as:

$$f(x)=\frac{1}{b-a},\quad a\le x\le b \tag{A.8}$$

$$\mu=\frac{a+b}{2},\sigma=\frac{b-a}{\sqrt{12}} \tag{A.9}$$

Thus,

$$\begin{aligned} a&=\mu-\sqrt{3}\sigma\\ b&=\mu+\sqrt{3}\sigma \end{aligned} \tag{A.10}$$

This distribution can be modeled using a step function, as

$$H(x-a)=\begin{cases}1 & x\ge a\\ 0 & x<a\end{cases}, \tag{A.11}$$

However, it is not possible to calculate the sensitivity of the step function. Thus, an arctangent function is used to approximate the step function, as

$$\begin{aligned} f(x)&=\frac{1}{b-a}[H(x-a)-H(x-b)]\\ &\approx\frac{1}{(b-a)\pi}\left\{\arctan\left[c(x-a)\right]-\arctan\left[c(x-b)\right]\right\}\end{aligned} \tag{A.12}$$

when $c\to\infty$, $\frac{1}{(b-a)\pi}\left\{\arctan\left[c(x-a)\right]-\arctan\left[c(x-b)\right]\right\}\to f(x)$

The sensitivity of failure probability P_f to the mean of random variable x_i can be written as

$$\frac{\partial P_f}{\partial\mu_i}=\int_{\Omega_{\mathbf{X}}}\frac{\partial f(\mathbf{x})}{\partial\mu_i}d\mathbf{x} \tag{A.13}$$

For an N dimensional system, by assuming all system random variables are independent, the joint probability function is defined as

$$f(\mathbf{x})=\prod_{i=1}^{N}\frac{1}{(b_i-a_i)\pi}\left\{\arctan\left[c(x_i-a_i)\right]-\arctan\left[c(x_i-b_i)\right]\right\} \tag{A.14}$$

The derivative of this joint probability function can be written as

$$\begin{aligned}\frac{\partial f(\mathbf{x})}{\partial \mu_i} &= \frac{\partial f(\mathbf{x})}{\partial a_i}\frac{\partial a_i}{\partial \mu_i} + \frac{\partial f(\mathbf{x})}{\partial b_i}\frac{\partial b_i}{\partial \mu_i} \\ &= \frac{\partial f(\mathbf{x})}{\partial a_i} + \frac{\partial f(\mathbf{x})}{\partial b_i}\end{aligned} \tag{A.15}$$

From Eq.(A.13), sensitivity of failure probability with respect to mean value of design variable can be derived as

$$\begin{aligned}\frac{\partial P_f}{\partial \mu_i} &= \int_{\Omega_{\mathbf{X}}} I(G(\mathbf{x}) \le 0)\frac{\partial f(\mathbf{x})}{\partial \mu_i} d\mathbf{x} \\ &= \int_{\Omega_{\mathbf{X}}} I(G(\mathbf{x}) \le 0) \cdot \frac{c}{\pi(b_i - a_i)}\left[\frac{1}{1+c^2(x_i - b_i)^2} - \frac{1}{1+c^2(x_i - a_i)^2}\right] \\ &\cdot \prod_{\substack{j=1 \\ j\neq i}}^{N} \frac{1}{(b_j - a_j)\pi}\left\{\arctan\left[c(x_j - a_j)\right] - \arctan\left[c(x_j - b_j)\right]\right\} dx_1 \ldots dx_N \\ &= \int_{\Omega_{\mathbf{X}}} I(G(\mathbf{x}) \le 0) \cdot \left\{\frac{\frac{c}{\pi(b_i - a_i)}\left[\frac{1}{1+c^2(x_i - b_i)^2} - \frac{1}{1+c^2(x_i - a_i)^2}\right]}{\frac{1}{(b_i - a_i)\pi}\left\{\arctan\left[c(x_i - a_i)\right] - \arctan\left[c(x_i - b_i)\right]\right\}}\right\} f(\mathbf{x}) d\mathbf{x} \\ &= \int_{\Omega_{\mathbf{U}}} I(G(\mathbf{u}) \le 0) \cdot \left\{\frac{c\left[\frac{1}{1+c^2(x_i - b_i)^2} - \frac{1}{1+c^2(x_i - a_i)^2}\right]}{\arctan\left[c(x_i - a_i)\right] - \arctan\left[c(x_i - b_i)\right]}\right\}_{\mathbf{x}=\mathbf{T}^{-1}(\mathbf{u})} \varphi(\mathbf{u}) d\mathbf{u} \\ &= \frac{c}{N}\sum_{j=1}^{N}\left\{\frac{\frac{1}{1+c^2(x_i^j - b_i)^2} - \frac{1}{1+c^2(x_i^j - a_i)^2}}{\arctan\left[c(x_i^j - a_i)\right] - \arctan\left[c(x_i^j - b_i)\right]}\right\}_{\mathbf{x}=\mathbf{T}^{-1}(\mathbf{u})}\end{aligned} \tag{A.16}$$

The accuracy of the above sensitivity formula is used to calculate the sensitivity of the linear function in Eq. (A.6) with uniform distribution, as

$$\begin{cases} G(x) = 1.6 - 3x \\ x \sim Uniform(a,b) \\ where \;\; a = -2, b = 1 \end{cases} \tag{A.17}$$

When $G \le 0$, the performance function is considered to be fail.

For this linear function of uniform distributed variable x, the exact probability sensitivity is $\frac{1}{b-a}=\frac{1}{3}$. Table A-2 shows sensitivity results obtained from FORM and the sampling based approach. Although FORM cannot provide the exact solution for random variable with non-normal distribution, it is still a good approximation for reliability analysis. The sampling based approach is also a good estimation of both failure probability and probability sensitivity.

Table A-2: Accuracy of proposed probability sensitivity method for uniform distribution using 200,000 sampling MCS

	FORM	Sampling based approach (c=10000,200,000 samples)	Exact
P_f	0.1555	0.1556	0.1556 (7/45)
$dP_f/d\mu_x$	0.3334	0.3333	0.3333 (1/3)

Log-Normal Distribution

When a random variable x has lognormal distribution, the probability density function is defined as

$$f(x)=\frac{1}{\sqrt{2\pi}x\tilde{\sigma}}e^{-\frac{(\ln x-\tilde{\mu})^2}{2\tilde{\sigma}^2}} \tag{A.18}$$

where

$$\tilde{\sigma}^2=\ln(1+v^2)$$
$$\tilde{\mu}=\ln\mu-\frac{\tilde{\sigma}^2}{2}$$
$$v=\frac{\sigma}{\mu-a}$$

Transformation from standard normal space can be return as:

$$X=\mathbf{T}(U)=e^{\tilde{\mu}+\tilde{\sigma}U} \tag{A.19}$$

The sensitivity of failure probability P_f to the mean of random variable x_i can be written as

$$\frac{\partial P_f}{\partial \mu_i} = \int_{\Omega_{\mathbf{u}}} I(G(\mathbf{u}) \le 0) \cdot \left[\frac{\partial f(\mathbf{x})}{f(\mathbf{x}) \partial \mu_i} \right]_{\mathbf{x}=\mathbf{T}^{-1}(\mathbf{u})} \varphi(\mathbf{u}) d\mathbf{u} \tag{A.20}$$

For an *n* dimensional system, by assuming all system random variables are independent, the joint probability function is defined as

$$f(\mathbf{x}) = \prod_{i=1}^{n} \frac{1}{\sqrt{2\pi} x_i \tilde{\sigma}_i} e^{-\frac{[\ln(x_i) - \tilde{\mu}_i]^2}{2\tilde{\sigma}_i^2}} \tag{A.21}$$

Thus, we can have

$$\frac{\partial f(\mathbf{x})}{\partial \mu_i} = \frac{\partial f(\mathbf{x})}{\partial \tilde{\mu}_i} \frac{\partial \tilde{\mu}_i}{\partial \mu_i} + \frac{\partial f(\mathbf{x})}{\partial \tilde{\sigma}_i} \frac{\partial \tilde{\sigma}_i}{\partial \mu_i} \tag{A.22}$$

where

$$\frac{\partial f_i(x_i)}{\partial \tilde{\mu}_i} = f_i(x_i) \frac{\ln(x_i) - \tilde{\mu}_i}{\tilde{\sigma}_i^2} \Rightarrow \frac{\partial f(\mathbf{x})}{\partial \tilde{\mu}_i} = f(\mathbf{x}) \frac{\ln(x_i) - \tilde{\mu}_i}{\tilde{\sigma}_i^2} \tag{A.23}$$

$$\frac{\partial \tilde{\mu}_i}{\partial \mu_i} = \frac{1}{\mu_i} + \frac{v_i^2}{(\mu_i - a)(1 + v_i^2)} \tag{A.24}$$

$$\frac{\partial f_i(x_i)}{\partial \tilde{\sigma}_i} = -\frac{f_i(x_i)}{\tilde{\sigma}_i} + f_i(x_i) \frac{[\ln(x_i) - \tilde{\mu}_i]^2}{\tilde{\sigma}_i^3} \Rightarrow \frac{\partial f(\mathbf{x})}{\partial \tilde{\sigma}_i} = -\frac{f(\mathbf{x})}{\tilde{\sigma}_i} + f(\mathbf{x}) \frac{[\ln(x_i) - \tilde{\mu}_i]^2}{\tilde{\sigma}_i^3} \tag{A.25}$$

$$\frac{\partial \tilde{\sigma}_i}{\partial \mu_i} = -\frac{v^2}{\tilde{\sigma}_i (\mu - a)(1 + v^2)} \tag{A.26}$$

$$\begin{aligned} \frac{\partial f(\mathbf{x})}{f(\mathbf{x}) \partial \mu_i} &= \frac{\ln(x_i) - \tilde{\mu}_i}{\tilde{\sigma}_i^2} \cdot \left(\frac{1}{\mu_i} + \frac{v_i^2}{(\mu_i - a)(1 + v_i^2)} \right) \\ &+ \frac{v^2}{\tilde{\sigma}_i (\mu - a)(1 + v^2)} \cdot \left(\frac{1}{\tilde{\sigma}_i} - \frac{[\ln(x_i) - \tilde{\mu}_i]^2}{\tilde{\sigma}_i^3} \right) \end{aligned} \tag{A.27}$$

$$\begin{aligned} \frac{\partial P_f}{\partial \mu_i} &= \int_{\Omega_{\mathbf{u}}} I(G(\mathbf{u}) \le 0) \cdot \left[\frac{\partial f(\mathbf{x})}{f(\mathbf{x}) \partial \mu_i} \right]_{\mathbf{x}=\mathbf{T}^{-1}(\mathbf{u})} \varphi(\mathbf{u}) d\mathbf{u} \\ &= \frac{1}{N} \sum_{j=1}^{N} \left[\begin{aligned} &\frac{\ln(x_i^j) - \tilde{\mu}_i}{\tilde{\sigma}_i^2} \cdot \left(\frac{1}{\mu_i} + \frac{v_i^2}{(\mu_i - a)(1 + v_i^2)} \right) \\ &+ \frac{v^2}{\tilde{\sigma}_i (\mu - a)(1 + v^2)} \cdot \left(\frac{1}{\tilde{\sigma}_i} - \frac{[\ln(x_i^j) - \tilde{\mu}_i]^2}{\tilde{\sigma}_i^3} \right) \end{aligned} \right]_{\mathbf{x}=\mathbf{T}^{-1}(\mathbf{u})} \end{aligned} \tag{A.28}$$

The correctness of the derivation is proved by comparing the sensitivity result of sampling based approach with that of FORM. Linear performance function in Eq.(A.6) is used as test function.

$$\begin{cases} G(x) = 1.6 - 3x \\ x \sim Log - Normal(0.5, 0.4^2) \end{cases} \tag{A.29}$$

Because of the simplicity of the performance function, the exact solution for probability of failure can be found by directly integrating the lognormal PDF from 1.6/3 to infinity(1.6-3x<0). As shown in Table A-3, the sampling-based approach with c=10,000 and 200,000 samples is more accurate than FORM.

Table A-3: Accuracy of proposed probability sensitivity method for Log-normal distribution using 200,000 sampling MCS

	FORM	Sampling based approach (c=10000,200,000 samples)	Exact
P_f	0.3287	0.3287	0.3287
$dP_f/d\,\mu_x$	1.1757	1.1763	1.1765

APPENDIX B
NATURAL FREQUENCY OF CANTILEVER COMPOSITE BEAM

Bending Moment

As indicated in Figure 7-2, the cantilever composite beam subjects to a bending moment (M_0) at the ends of the piezoceramic. This is caused by induced strain from applied voltage (Cattafesta et al. 2000). Figure A-1 replaces the mass of the composite beam as an equivalent uniform load (q) due to its weight. R and M_r are the reaction force and bending moment at the clamp.

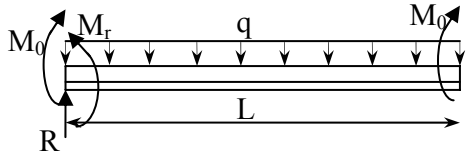

Figure B-1: Free body diagram of two-layer beam

Thus, the bending moment in the composite beam can be expressed as

$$M(x|0 \le x \le L) = M_r + Rx - M_0 - q\frac{x^2}{2} \tag{B.1}$$

where $R = qL$ and $M_r = qL^2/2$.

Geometric Properties of Composite Beam

Before we calculate the effective compliance and lumped mass, geometric properties such as location of neutral axis and flexural rigidity of the composite beam are required in static analysis of the beam.

If we define c_2 as the location of the neutral axis from the bottom of piezoceramic and $(EI)_c$ as equivalent flexural rigidity in composite beam, they can be calculated by the following two expressions:

$$c_2 = \frac{E_s t_s \left(t_p + \frac{t_s}{2} \right) + E_p \frac{t_p^{\,2}}{2}}{E_s t_s + E_p t_p}, \tag{B.2}$$

$$(EI)_c = E_s I_{sc} + E_p I_{pc} \tag{B.3}$$

where I_{sc} and I_{pc} are the moment of inertia of the shim and PZT layer with respect to its own neutral axis, respectively.

Effective Compliance for Composite Beam

To find the effective compliance for the composite beam in Eq. (7.13), we need to use total potential energy in the beam as shown Eq. (B.4):

$$PE = \frac{(EI)_c}{2} \int_0^L \left(\frac{d^2 w(x)}{dx^2} \right)^2 dx \tag{B.4}$$

where

$$w(x) = -\frac{q}{24(EI)_c} x^4 + \frac{qL}{6(EI)_c} x^3 - \frac{qL^2}{4(EI)_c} x^2 \tag{B.5}$$

Equation (B.5) is obtained by conventional Euler-Bernoulli beam theory. Thus, by lumping the overall potential strain energy at the tip, an effective short circuit mechanical compliance for the composite beam will be calculated as

$$C_e = \frac{(w_{tip_F})^2}{2PE} \tag{B.6}$$

Effective Mass for Composite Beam

In order to calculate the effective lumped mass in Eq. (7.13), total kinetic energy in the composite beam [Eq. (B.7)] will be used.

$$KE = \frac{\rho_{Lc}}{2} \int_0^L \dot{w}(x)^2 \, dx \tag{B.7}$$

where ρ_{Lc} is the equivalent mass density of the composite beam and $\dot{w}(x)$ is the velocity in the beam.

For a simple harmonic motion, the velocity of the beam are related to the displacement by

$$\dot{w}(x) = j\omega w(x) \tag{B.8}$$

$\dot{w}(x)$ is then expressed as

$$\dot{w}(x) = \frac{w(x)}{w_{tip_F}} \dot{w}_{tip_F} \tag{B.9}$$

Effective mass for the composite beam from its deflection shape is obtained by lumping the kinetic energy of the beam at its tip:

$$M_e = \frac{2KE}{(\dot{w}_{tip_F})^2} = \frac{\rho_{Lc}}{w_{tip_F}^2} \int_0^L w(x)^2 \, dx \tag{B.10}$$

LIST OF REFERENCES

Allen, J. K., Seepersad, C., Choi, H., and Mistree, F. (2006). "Robust Design for Multiscale and Multidisciplinary Applications." *Journal of Mechanical Design*, 128(4), 832-843.

Allgower, E. L., and Georg, K. (1990). *Numerical Continuation Methods: An Introduction*, Springer-Verlag, Berlin.

Ang, A. H.-S., and Tang, W. H. (1975). *Probability Concepts in Engineering Planning and Design, Basic Principles*, Wiley.

Arora, J. (2004). *Introduction to Optimum Design*, Academic Press.

Ayyub, B. M., Assakkaf, I. A., Kihl, D. P., and Siev, M. W. (2002). "Reliability-Based Design Guidelines for Fatigue of Ship Structures." *Naval Engineers Journal*, 114(2), 113-138.

Bannatine, J. A., Comer, J. J., and Handrock, J. L. (1990). *Fundamentals of Metal Fatigue Analysis*, Prentice-Hall, Englewood Cliffs, N. J.

Basquin, O. H. (1910). "The Exponential Law of Endurance Tests." *Proc Am Soc Test Mater*, 10, 625-630.

Breitung, K. (1984). "Asymptotic Approximations for Multinormal Integrals." *Journal of Engineering Mechanics*, 110(3), 357-366.

Brown, M. W., and Miller, K. J. (1973). "A Theory for Fatigue under Multiaxial Stress-strain Conditions." *Proceedings of the Institution of Mechanical Engineer*, 187, 745-756.

Cameron, R. H., and Martin, W. T. (1947). "The Orthogonal Development of Nonlinear Fuctionals in Series of Fouriers-Hermite Functionals." *Ann. Math.*, 48, 385-392.

Cattafesta, L., Mathew, J., and Kurdila, A. (2000). "Modeling and Design of Piezoelectric Actuators for Fluid Control," San Diego, CA.

Chandu, S. V. L., and Grandi, R. V. (1995). "General Purpose Procedure for Reliability Based Structural Optimization under Parametric Uncertainties." *Advances in Engineering Software*, 23, 7-14.

Chase, K. W., and Greenwood, W. H. (1988). "Design Issues in Mechanical Tolerance Analysis." *Manufacturing Review, ASME*, 1(1), 50-59.

Chen, C. J., and Choi, K. K. (1996). "Robust Design using Second-order Shape Design Sensitivity Analysis." Center for Computer-Aided Design, University of Iowa, Iowa City, IA.

Chen, W., Jin, R., and Sudjianto, A. (2005). "Analytical Variance-based Global Sensitivity Analysis in Simulation-based Design under Uncertainty." *Journal of Mechanical Design*, 127, 875-886.

Chen, X., Hasselman, T. K., and Neill, D. J. (1997). "Reliability Based Structural Design Optimization for Practical Application." *38th AIAA/ASME/ASCE/AHS/ASC Structure,Structural Dynamics,and Materials Conference*, Kissimmee,Florida.

Choi, K. K., and Kim, N. H. (2004a). *Structural Sensitivity Analysis and Optimization I: Linear Systems*, Springer.

Choi, K. K., and Kim, N. H. (2004b). *Structural Sensitivity Analysis and Optimization II: Nonlinear Systems and Applications*, Springer.

Choi, S. K., Grandhi, R. V., Canfield, R. A., and Pettit, C. L. (2003). "Polynomial Chaos Expansion with Latin Hypercube Sampling for Predicting Response Variability." *44th AIAA/ASME/ASCE/AHS Structures,Structural Dynamics,and Materials Conference*, Norfolk,Virginia.

Chopra, O. K., and Shack, W. J. (2003). "Review of the Margins for ASME Code Fatigue Design Curve - Effects of Surface Roughness and Material Variability." Argonne National Laboratory, Argonne, IL.

Coffin, L. F., Jr. (1954). "A Study of the Effects of Cyclic Thermal Stresses in a Ductile Metal." *ASME Transaction*, 16, 931-950.

De Rosa, M. A. (1994). "Free Vibrations of Stepped Beams with Elastic Ends." *Journal of Sound and Vibration*, 173(4), 563-567.

Devroye, L. (1986). *Noneuniform Random Variate Generation*, Springer-Verlag, New York.

Du, X., and Chen, W. (2002a). "Efficient Uncertainty Analysis Methods for Multidisciplinary Robust Design." *AIAA Journal*, 4(3), 545-552.

Du, X., and Chen, W. (2002). "Sequential Optimization and Reliability Assessment Method for Efficient Probabilistic Design." *ASME 2002 Design Engineering Technical Conferences and Computers and Information in Engineering Conference*, Montreal,Canada.

Enevoldsen, I., and Sorensen, J. D. (1994). "Reliability-Based Optimization in Structural Engineering." *Structural Safety*, 15, 169-196.

Fe-safe. (2004). "Software package, Version 5.1." Safe Technology, Sheffield, England.

Fuchs, H. O., and Stephens, R. I. (1980). *Metal Fatigue in Engineering*, John Whiley & Sons, New York.

Gautschi, W. (1996). "Orthogonal Polynomials: Applications and Computations." Acta Numerica, A. Iserles, ed., Cambridge University Press, Cambridge, 45-119.

Gerber, H. (1874). "Bestimmung der Zulassigen Spannungen in Eisen-konstruktionen." *Z Bayer Arch Ingenieur-Vereins*, 6, 101-110.

Ghanem, R., and Ghiocel, D. (1996). "A Comparative Analysis of FORM/SORM and Polynomial Chaos Expansions for Highly Nonlinear Systems." *11th ASCE Engineering Mechanics Conference*, Fort Lauderdale,Florida, 535-538.

Ghanem, R. G., and Spanos, P. D. (1991). *Stochastic Finite Elements: A Spectral Approach*, Springer-Verlag, New York.

Goodman, J. (1899). *Mechanics Applied to Engineering*, Longmans Green, London.

Grandhi, R. V., and L.P., W. (1998). "Reliability-Based Structural Optimization using Improved Two-Point Adaptive Nonlinear Approximations." *Finite Elements in Analysis And Design*, 29(1), 35-48.

Griffith, A. A. (1921). "The Phenomena of Rupture and Flow in Solids." *Phil. Trans. Roy. Soc. of London*, A221, 163-197.

Haftka, R. T., and Gurdal, Z. (1991). *Elements of Structural Optimization (Solid Mechanics and Its Applications)*, Springer.

Haldar, A., and Mahadevan, S. (2000). *Reliability Assessment using Stochastic Finite Element Analysis*, John Wiley & Sons Inc.

Hasofer, A. M., and Lind, N. C. (1974). "Exact and Invariant Second-Moment Code Format." *Journal of the Engineering Mechanics*, 100(EM1), 111-121.

Hoeppner, D. W., and Krupp, W. E. (1974). "Prediction of Component Life by Application of Fatigue Crack Growth Knowledge." *Engineering Fracture Mechanics*, 6, 47-70.

Inglis, C. E. (1913). "Stresses in A Plate due to the Presence of Cracks and Sharp Corners." *Transaction of the Institute of Naval Architects*, 55, 219-241.

Irwin, G. R. (1956). "Onset of Fast Crack Propagation in High Strength Steel and Aluminum Alloys." *Sagamore Research Conference Proceedings*, 289-305.

Isukapalli, S. S., Roy, A., and Georgopoulos, P. G. (1998). "Stochastic Response Surface Methods(SRSMs) for Uncertainty Propagation: Application to Environmental and Biological Systems." *Risk Analysis*, 18(3), 351-363.

Isukapalli, S. S., Roy, A., and Georgopoulos, P. G. (2000). "Efficient Sensitivity/Uncertainty Analysis Using the Combined Stochastic Response Surface Method and Automated Differentiation: Application to Environmental and Biological Systems." *Risk Analysis*, 20(5), 591-602.

Jang, S. K., and Bert, C. W. (1989a). "Free Vibration of Stepped Beams:exact and numerical solutions." *Journal of Sound and Vibration*, 130(2), 342-346.

Jang, S. K., and Bert, C. W. (1989b). "Free Vibration of Stepped Beams:higher mode frequencies and effects of steps on frequency." *Journal of Sound and Vibration*, 132(1), 164-168.

Karamchandani, A., and Cornell, C. A. (1992). "Sensitivity Estimation within First and Second Order Reliability Methods." *Structural Safety*, 11, 95-107.

Khuri, A. I., and Cornell, J. A. (1996). *Response Surface: Design and Analysis*, Marcel Dekker,Inc., New York.

Kim, N. H., Choi, K. K., and Botkin, M. E. (2003). "Numerical Method for Shape Optimization Using Meshfree Method." *Structure and Multidisciplinary Optimization*, 24, 418-429.

Kim, N. H., Choi, K. K., and Chen, J. S. (2000). "Shape Design Sensitivity Analysis and Optimization of Elasto-plasticity with Frictional Contact." *AIAA Journal*, 38(9), 1742-1753.

Kim, N. H., Wang, H., and Queipo, N. V. (2004). "Adaptive Reduction of Design Variables using Global Sensitivity Indices in Reliability-Based Optimization." *10th AIAA/ISSMO Multidisciplinary Analysis and Optimization Conference*, Albany, New York.

Kim, N. H., Wang, H., and Queipo, N. V. (2004). "Efficient Shape Optimization Technique using Stochastic Response Surfaces and Local Sensitivities." *ASCE Joint Specialty Conference on Probabilistic Mechanics and Structural Reliability*, Albuquerque, New Mexico.

Koch, P. N., Yang, R.-J., and Gu, L. (2004). "Design for Six Sigma through Robust Optimization." *Structural and Multidisciplinary Optimization*, 26, 235-248.

Krishmamurthy, T. (2003). "Response Surface Approximation with Augmented and Compactly Supported Radial Basis Functions." *44th AIAA/ASME/ASCE/AHS Structures,Structural Dynamics, and Materials Conference*, Norfolk,Virginia.

Kwak, B. M., and Kim, J. H. (2002). "Concept of Allowable Load Set and Its Application for Evaluation of Structural Integrity." *Mechanics of structures and machines*, 30(2).

Kwak, B. M., and Lee, T. W. (1987). "Sensitivity Analysis for Reliability-Based Optimization Using an AFOSM Method." *Computers & Structures*, 27(3), 399-406.

Lauridensen, S., Vitali, R., Van Keulen, F., Haftka, R. T., and Madsen, J. I. (2001). "Response Surface Approximation Using Gradient Information." *The Fourth World Congress of Structural and Multidisciplinary Optimization*, Dalian, China.

Li, Y., Papila, M., Nishida, T., Cattafesta, L., and Sheplak, M. (2006). "Modeling and Optimization of A Side-implanted Piezoresistive Shear Stress Sensor." San Diego, CA.

Liang, J., Mourelatos, Z. P., and Tu, J. (2004). "A Single-Loop Method for Reliability-Based Design Optimization." *Proceedings of DETC'04, ASME 2004 Design Engineering Technical Conferences and Computers and Information in Engineering Conference*, Salt Lake City, Utah.

Liu, H., Chen, W., and Sudjianto, A. (2004). "Probability Sensitivity Analysis Methods for Design under Uncertainty." *10th AIAA/ISSMO Multidisciplinary Analysis and Optimization Conference*, Albany, New York.

Liu, P. L., and Kiereghian, A. D. (1991). "Optimization Algorithms For Structural Reliability." *Structural Safety*, 9, 161-177.

Mahadevan, S., and Shi, P. (2001). "Multiple Linearization Method for Nonlinear Reliability Analysis." *Journal of Engineering Mechanics*, 127(11), 1165-1173.

Malkov, V. P., and Toropov, V. V. (1991). "Simulation Approach to Structural Optimization Using Design Sensitivity Analysis." *Engineering Optimization in Design Process, Proc. Int. Conf., Lecture Notes in Engineering*, Karlsruhe,Germany, 225-231.

Manson, S. S. (1954). "Behavior of Materials Under Conditions of Thermal Stress." National Advisory Comittee for Aeronautics, Cleveland.

Matsuishi, M., and Endo, T. (1968). "Fatigue of Metals Subjected to Varying Stress-Fatigue Lives Under Random Loading." *Proceedings of the Kyushu District Meeting*, 37-40.

Melchers, R. E. (2001). *Structural Reliability Analysis and Prediction*, John Wiley & Sons, New York.

Metropolis, N., and Ulam, S. (1949). "The Monte Carlo Method." *Journal of the American Statistical Association*, 44(247), 335-341.

Miller, W. R., Ohji, K., and Marin, J. (1966). "Rotating Principal Stress Axes in High Cycle Fatigue." *ASME Paper No. 66-WA/Met 9*, New York.

Miner. (1945). "Cumulative Damage in Fatigue." *Journal of Applied Mechancis*, 12, A159-A164.

Myers, R. H., and Montgomery, D. C. (1995). *Response Surface Methodology: Process and Product Optimization Using Designed Experiments*, John Wiley & Sons,Inc, New York.

Paris, P. C. (1964) "The Fracture Mechanics Approach to Fatigue." *Fatigue-An Interdisplinary Approach, Proceedings of the Tenth Sagamore Army Materials Research Conference*, Syracuse, N.Y., 107-132.

Paris, P. C., and Erdogan, F. (1963). "A Critical Analysis of Crack Propagation Laws." *Journal of Basic Engineering, ASME Transactions, Series D*, 85(4), 528-534.

Paris, P. C., Gomez, M. P., and Anderson, W. P. (1961). "A Rational Analytic Theory of Fatigue." *The Trend in Egineering*, 13, 9-14.

Park, G. J., Lee, T. H., Lee, K. H., and Hwang, K. H. (2006). "Robust Design: An Overview." *AIAA Journal*, 44(1), 181-191.

Qu, X., and Haftka, R. T. (2004). "Reliability-based Design Optimization using Probabilistic Sufficiency Factor." *Structural and Multidisciplinary Optimization*, 27(5), 314-325.

Qu, X., Venkataraman, S., and Haftka, R. T. (2000). "Response Surface Options for Reliability-Based Optimization of Composite Laminate." *8th ASCE Speciality Conference on Probabilistic Mechanics and Structural Reliability*, Notre Dame,Indiana.

Rackwitz, R.(2000). "Reliability Analysis-Past,Present and Future." *8th ASCE Specialty Conference on Probabilistic Mechanics and Structure Reliability*, Notre Dame,Indiana.

Rahman, S., and Xu, H. (2004). "A Univariate Dimension-reduction Method for Multi-dimensional Intergration in Stochastic Mechanics." *Probabilistic Engineering Mechanics*, Article in Press.

Rijpkema, J., Etman, L., and Schoofs, A. (2000). "Metamodel Based Design Optimization Including Design Sensitivities." *Proc. SMSMEO Workshop*, Lyngby,Denmark.

Rubinstein, R. Y. (1981). *Simulation and the Monte Carlo Method*, John Wiley & Sons,Inc.

Saltelli, A., Chan, K., and Scott, E. M. (2000). *Sensitivity Analysis*, John Wiley & Sons, Ltd.

Saltelli, A., Tarantola, S., and Chan, K. (1999). "Quantitative Model-independent Method for Global Sensitivity Analysis of Model Output." *Technometrics*, 41(1), 39-56.

Smarslok, B. P., and Haftka, R. T. (2006). "Taking Advantage of Separable Limit States in Sampling Procedures." *47th AIAA/ASME/ASCE/AHS/ASC Structures, Structural Dynamics, and Material Conference*, Newport, RI.

Smith, R. N., Watson, P., and Topper, T. H. (1970). "A Stress-Strain Function for the Fatigue of Metal." *Journal of Materials*, 5, 767-778.

Sobol, I. M. (1993). "Sensitivity Analysis for Nonlinear Mathematical Models." *Mathematical modeling and computational experiment*, 1, 407-144.

Sobol, I. M. (2001). "Global Sensitivity Indices for Nonlinear Mathematical Models and Their Monte Carlo estimates." *Mathematics and computers in simulation*, 55, 271-280.

Soderberg, C. R. (1939). "Factor of Safety and Working Stress." *Transaction of American Society Mechanical Engineers*, 52, 13-28.

Taguchi, G. (1986). *Introduction to Quality Engineering*, UNIPUB, White Plains,New York.

Taguchi, G. (1987). *System of Experimental Design:Engineering Methods to Optimize Quality and Minimize Cost*, UNIPUB/Kraus International, White Plains,New York.

Tu, J. (1999). "Design Potential Concept for Reliability-Based Design Optimization," PH.D, Univ. of Iowa, Iowa City,Iowa.

Tu, J., and Choi, K. K. (1997). "A Performance Measure Approach in Reliability Based Structural Optimization." *Techincal Report R97-02*, Center for Computer-Aided Design, University of Iowa, Iowa City,Iowa.

Tu, J., Choi, K. K., and Park, Y. H. (1999). "A New Study on Reliability-Based Design Optimization." *Journal of Mechanical Design*, 121(4), 557-564.

Tu, J., et al. (2001). "Design Potential Method for Robust System Parameter Design." *AIAA Journal*, 39(4), 667-677.

Van Keulen, F., Haftka, R. T., and Kim, N. H. (2004). "Review of Options for Structural Design Sensitivity Analysis. Part1: Linear Systems." *Computer methods in Applied Mechanics and Engineering*(to appear).

Van Keulen, F., Liu, B., and Haftka, R. T. (2000). "Noise and Discontinuity Issues in Response Surface Based on Functions and Derivatives." *Proceeding of the 41st AIAA/ASME/ASCE/AHS/ASC Structures, Structural Dynamics, and Materials Conference and Exhibit*, Atlanta, GA,USA.

Vanderplaats, G. N. (2001). *Numerical Optimization Techniques for Engineering Design*, Vanderplaats Research and Development, Inc.

Vervenne, K. (2005). "Gradient-based Approximate Design Optimization," Ph.D. Dissertation, Delft University of Technology.

Villadsen, J., and Michelsen, M. L. (1978). *Solution of Differential Equation Models by Polynomial Approximation*, Prentice Hall, Englewood Cliffs, New Jersey.

Wang, L., and Kodiyalam, S. (2002). "An Efficient Method for Probabilistic and Robust Design with Non-normal Distributions." *43rd AIAA/ASME/ASCE/AHS/ASC Structures,Structural Dynamics,and Materials Conference*, Denver,Colorado.

Wang, L. P., and Grandhi, R. V. (1995). "Improved 2-Point Function Approximations for Design Optimization." *AIAA Journal*, 33(9), 1720-1727.

Webster, M. D., Tatang, M. A., and McRae, G. J. (1996). "Application of the Probabilistic Collocation Method for an Uncertainty Analysis of a Simple Ocean Model." *4*, MIT Joint Program on the Science and Policy of Global Change.

Wohler, A. (1860). "Versuche uber die Festigkeit der Eisenbahnwagen-Achsen." *Zeitschrift fur Bauwesen*.

Wu, Y.-T. (1994). "Computational Methods for Efficient Structural Reliability and Reliability Sensitivity Analysis." *AIAA Journal*, 32(8), 1717-1723.

Wu, Y.-T., Shin, Y., Sues, R., and Cesare, M. (2001). "Safety-factor Based Approach for Probability-based Design Optimization." *42nd AIAA/ASME/ASCE/AHS/ASC Structure,Structural Dynamics,and Materials Conference*, Seattle,Washington.

Wu, Y. T., and Wang, W. (1996). "A New Method for Efficient Reliability-Based Design Optimization." *Probabilistic Mechanics & Structural Reliability: Proceedings of the 7th Special Conference*, 274-277.

Wyss, G. D., and Jorgensen, K. H. (1998). "A User's Guide to LHS: Sandia's Latin Hypercube Sampling Software." Sandia National Laboratories, Albuquerque,New Mexico.

Xiu, D., Lucor, D., Su, C.-H., and Karniadakis, G. E. (2002). "Stochastic Modeling of Flow-Structure Interactions Using Generalized Polynomial Chaos." *Journal of Fluids Engineering*, 124(1), 51-59.

Xu, H., and Rahman, S. (2004). "A Generalized Dimension-reduction Method for Multimensional Integration in Stochastic Mechanics." *International Journal for Numerical Methods in Engineering*, Article in Press.

Xu, S., and Grandhi, R. V. (1998). "Effective Two-Point Function Approximation for Design Optimization." *AIAA Journal*, 36(12), 2269-2275.

Yang, R. J., and Gu, L. (2004). "Experience with Approximate Reliability-Based Optimization Methods." *Structural and Multidisciplinary Optimization*, 26(1), 152-159.

Youn, B. D. (2001). "Advances in Reliability-Based Design Optimization and Probability Analysis," PH.D, Univ. of Iowa, Iowa City,Iowa.

Youn, B. D. (2001). "Advances in Reliability-Based Design Optimization and Probability Analysis," PH.D, Univ. of Iowa, Iowa City,Iowa.

Youn, B. D., and Choi, K. K. (2004). "A New Response Surface Methodology for Reliability-Based Design Optimization." *Computers & Structures*, 82, 241-256.

Youn, B. D., Choi, K. K., and Park, Y. H. (2003). "Hybrid Analysis Method for Reliability-based Design Optimization." *Journal of Mechanical Design*, 125, 221-223.

Yu, X., Choi, K. K., and Chang, K. H. (1997). "Reliability and Durability Based Design Sensitivity Analysis and Optimization." Center for Computer-Aided Design, University of Iowa, Iowa City,Iowa.

Yu, X. M., Chang, K. H., and Choi, K. K. (1998). "Probabilistic Structural Durability Prediction." *AIAA Journal*, 36(4), 628-637.

BIOGRAPHICAL SKETCH

Haoyu Wang was born in Jiangyin, China, on May 7th, 1976. He received his Bachelor of Science in mechanical design and manufacture in July 1998 from Nanjing University of Science and Technology, and a Master of Science in mechanical manufacture and automation from Southeast University in April 2002, both in China. His interest in conducting research motivated him to join the University of Florida in August 2002, to pursue his Ph.D. degree in mechanical engineering.